ASSESSMENT AND MODULATION OF ESSENTIAL TREMOR USING PERIPHERAL-NERVE STIMULATION

A Dissertation
Presented to
The Academic Faculty

by

Jeonghee Kim

In Partial Fulfillment
of the Requirements for the Degree
Doctor of Philosophy in the
School of Electrical and Computer Engineering

Georgia Institute of Technology
May 2018

ASSESSMENT AND MODULATION OF ESSENTIAL TREMOR USING PERIPHERAL-NERVE STIMULATION

Approved by:

Dr. Stephen P. DeWeerth, Advisor
School of Electrical and Computer Engineering & Department of Biomedical Engineering
Georgia Institute of Technology

Dr. Thomas Wichmann
Department of Neurology
Emory University

Dr. Omer T. Inan, Co-advisor
School of Electrical and Computer Engineering
Georgia Institute of Technology

Dr. J. Lucas McKay
School of Medicine
Emory University

Dr. Robert J. Butera
School of Electrical and Computer Engineering & Department of Biomedical Engineering
Georgia Institute of Technology

Dr. Martha A. Grover
School of Chemical & Biomolecular Engineering
Georgia Institute of Technology

Date Approved: [Dec. 08, 2017]

ACKNOWLEDGEMENTS

I would like to extend my deepest gratitude to my advisor, Dr. DeWeerth, who has supported my thesis project and offered tremendous insight into this project. I am also extremely grateful to my mentor, Dr. Wichmann, and my co-advisor, Dr. Inan, for taking so much of their valuable time to provide constructive input and guidance. I would like to extend my sincerest appreciation to the participants in our human subject trials, particularly the support group of the International Essential Tremor Foundation at Savannah Georgia. I would also like to extent special thanks my husband, Hangue, who, as a collaborator, a lab mate, and a friend, continuously encouraged me throughout this process. I am deeply indebted to my mother, my father, and my brother, without whose support I would not be here. I would like to thank my lovely son, William, and baby # 2 on the way, who have been extremely cooperative during the completion of my doctoral thesis.

TABLE OF CONTENTS

LIST OF TABLES

Page

LIST OF FIGURES

LIST OF SYMBOLS AND ABBREVIATIONS

ATs	Assistive Technologies
Botox	Botulinum Toxin
CNS	Central Nervous System
COT	Center-Out Tapping
DBS	Deep Brain Stimulation
EEG	Electroencephalography
EMG	Electromyography
ET	Essential Tremor
FES	Functional Electrical Stimulation
FFT	Fast-Fourier Transform
GM	Gyration Mouse
GUI	Graphical User Interface
HPF	High-Pass Filter
ID	Index of Difficulty
IMU	Inertial Measurement Unit
IRB	Institutional Review Board
ISO	International Standardization Organization
LPF	Low-Pass Filter
MEG	Magnetoencephalogram
MDT	Multi-directional Tapping/Click
MN	Median Nerve
PD	Parkinson's Disease

PSD	Power Spectral Density
RMS	Root Mean Square
RN	Radial Nerve
RTN	Rectangular Track Navigation
SDK	Software Development Kit
SPN	Spiral Navigation
TETRAS	The Essential Tremor Rating Assessment Scale
TRS	Tremor Rating Scale
UN	Ulnar Nerve
UPDRS	The Unified Parkinson's Disease Rating Scale
3D	Three Dimensional

SUMMARY

The research objective of this thesis is to quantitatively assess tremor movement and modulate/suppress tremor movement by changing the parameters of electrical stimulation on peripheral nerves using a custom-designed real-time system. We began by designing and evaluating standardized tasks based on Fitts' law to quantify the severity and frequency of tremor movement by tremor subjects controlling a three-dimensional gyration mouse on a computer. Then we determined performance metrics of the proposed computer-based assessment tasks and their correlations with tremor frequency and power and suggested a linear regression model of task performance that demonstrates the feasibility of quantitative tremor assessment for tremor frequency and severity. We expect that these techniques can be used in patient homes or clinics to easily track changes in symptoms by minimizing inter- and intra-rater variability.

After evaluating tremor frequency and severity, we designed a wireless wearable tremor monitor and stimulation system with a three-axis accelerometer that captures motion data and modulates tremor movement using peripheral-nerve electrical stimulation on patients with upper limb treatment-resistant tremor, particularly those with essential tremor. To evaluate the effects of the peripheral-nerve electrical stimulation on the radial nerve, we initially evaluated this system within a certain range of stimulation parameters. We found that this system significantly reduced the severity of tremor (i.e., tremor power), and more specifically, the analysis showed that kinetic, or essential tremor (ET) participants with a greater severity of tremor showed a higher rate of reduction.

Once we evaluated the effects of the system on ET patients, we analyzed their tremor movement by changing the stimulation parameters (i.e., amplitude, frequency, duty cycle, phase, and stimulation sites) to find an open-loop response to their tremor movement according to the stimulation parameters. Based on the response model of each ET participant and/or a group of ET participants, we expect to design a real-time tremor monitoring and parameter optimization algorithm that can play an important role in the long-term use of a tremor modulation system that uses peripheral-nerve electrical stimulation to minimize nerve fatigue and power consumption and maximizes the efficacy of electrical peripheral nerve stimulation.

CHAPTER 1

INTRODUCTION

Tremor is an abnormal oscillatory movement observed in patients with essential tremor (ET), Parkinson's disease (PD), and other neurological disorders. ET, which particularly affects movements that require a high degree of dexterity and precision, can severely disrupt the daily activities of patients. The ultimate goal of this doctoral thesis is to quantitatively assess tremor movement and monitor and modulate/attenuate tremor movement by providing a proper range of electrical stimulation on peripheral nerves using a custom-designed wearable real-time system. The objectives of this research are (1) to assess tremor movement with computer-based standardized tasks with quantitative performance metrics, (2) to develop a wireless wearable tremor monitor and modulation system that uses a motion sensor and electrical peripheral-nerve stimulation to modulate tremor movement, and (3) to analyze changes in tremor movement based on various stimulation parameters. Figure 1.1 presents an overview of the project objectives.

Current tremor evaluation methods primarily involve subjective and questionnaire-based approaches (Goetz et al. 2008; Elble et al. 2008; Tintner 2004). Even though researchers have used electronic devices to evaluate the severity and the characteristics of tremor (Bain et al. 1993; Giuffrida et al. 2009; Rigas et al. 2012), their analyses have mostly been limited to the dominant frequency and the maximum amplitude of tremor. We assign test subjects quantitative and standardized tasks based on Fitts' law (Soukoreff and MacKenzie, 2004; ISO 9241-9:2000 (E) 2002) to assess their functional performance while they move their arms with tremor as they control a three-dimensional (3D) gyration mouse

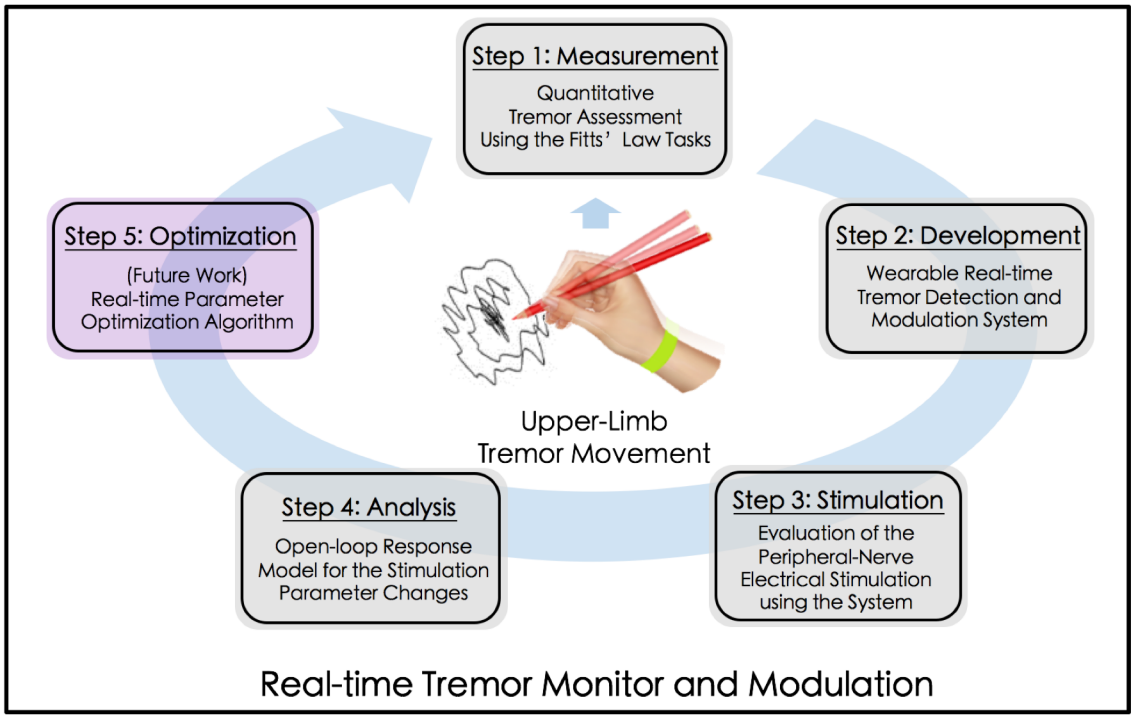

Figure 1.1 Overview of the real-time tremor monitor and modulation system.

on a computer. Ultimately, the results of this work should help both medical personnel and tremor patients evaluate the status of a patient's disease, track the progress of the disease, and analyze the effects of treatment.

Conventional clinical treatments for tremor patients are medications such as primidone or beta blockers (IETF, Essential Tremor (ET) Common Medications). However, many patients do not sufficiently respond to these treatments, or they experience intolerable side effects. A viable option in many patients is surgical treatment, such as thalamic deep brain stimulation (DBS). The DBS technique has shown the functional improvement of tremor for advanced PD patients based on the Unified Parkinson's Disease Rating Scale (UPDRS) (Kumar et al. 1998) with subthalamic nucleus (STN) stimulation in about 58% of overall PD symptom and 82% of tremor, for ET patients with significant

benefit in upper extremity, as well as head and voice tremor (Lyons and Pahwa 2008), and for the medication-resistant ET patients based on the subjective rating scale (Hubble et al. 1996), however the procedure of the electrode implantation is both costly and invasive. For patients with treatment-resistant tremor, several researchers have evaluated the efficacy of electrical stimulation (Prochazka et al. 1992; Javidan et al. 1992; Gillard et al. 1999; Hao et al. 2013) and muscle vibration (Jöbges et al. 2002; McAuley et al. 1997). Such techniques, however, have not been used extensively in patients because of the bulkiness of the systems or their lack of efficacy. Thus, using peripheral nerve stimulation to modulate tremor movement, this study examines an open-loop response to tremor movements within a proper range of stimulation parameters (i.e., amplitude, frequency, duty cycle, phase, and stimulation sites). It will also discuss a real-time closed-loop optimization method that can maximize the efficacy of tremor suppression.

1.1 Introduction to Essential Tremor

One of the most common, chronic, and progressive neurological movement disorders, tremor causes rhythmic shaking in frequencies between 4 and 12 Hz (Bain 2007; Bhidayasiri 2005; IETF, 12-Month Annual Report, 2006). Unlike tremor associated with Parkinsonism (i.e., resting tremor) which is usually unilateral and regular pattern of the tremor movement, ET is characterized by action tremor (Hess and Pullman 2012; Figure 1.2), which is usually bilateral and irregular pattern of the tremor movement. The action tremor can be classified into postural tremor and kinetic tremor occurring

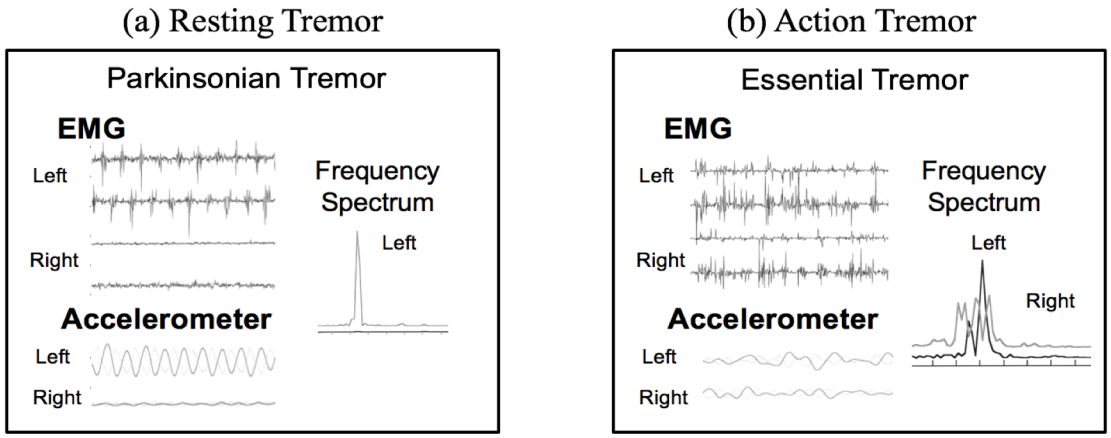

C.W. Hess and S.L. Pullman, *Tremor and Other Hyperkinetic Movements*, 2012.

Figure 1.2 Introduction to tremor movement: (a) resting tremor and (b) action tremor.

with a specific posture and tasks, respectively. ET affects about ten million people in the United States (IETF, 12-Month Annual Report, 2006). Even though this type of tremor can occur in any part of the body such as the hands, the head, the vocal chords, the legs, and the trunk, 90% of ET patients experience tremor in the upper limbs (Hess and Pullman 2012; IETF, 12-Month Annual Report, 2006). The onset of symptoms can occur at any age, but it most commonly manifests in people in their 40s and older, and about five percent of people over the age of 60 (Bhidayasiri 2005).

The origin of tremor and the physiological pathway of tremor generation remains unknown or controversial (Deuschl et al. 2001; Hellwig et al. 2001). However, possible origins of tremor generation can be categorized into mechanical resonances, reflex oscillations (stretch reflex or feedback resonance), or central oscillations (McAuley et al. 1997; Hess and Pullman 2012; Stein and Lee 1981) (Figure 1.3). Tremor, which can be influenced by mechanical resonance in the bones, the muscles, and other tissue, is related to physical properties such as the stiffness of structure and the moment of inertia (McAuley

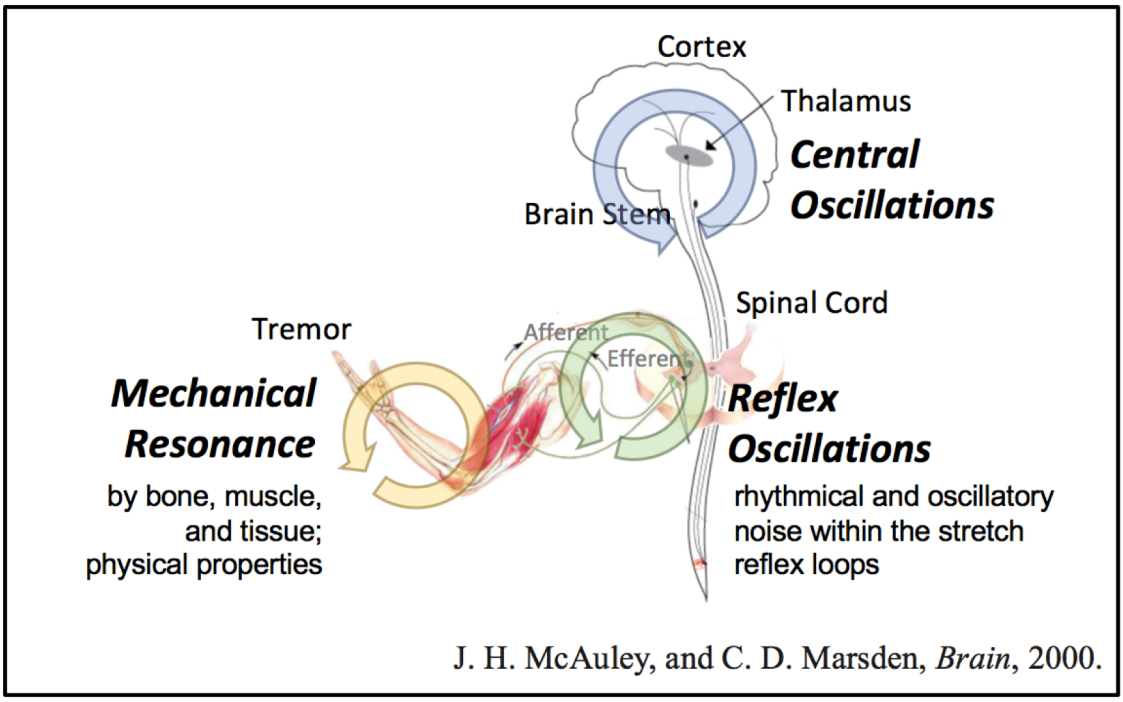

Figure 1.3 Origin of tremor and the physiological pathway.

et al. 1997; Joyce and Rank 1974; Stiles and Randall 1967; Walsh1992). The unstable feedback loop of a stretch reflex can lead to oscillatory movement (Marsden 1978; Matthews 1993). This rhythmical and oscillatory noise within stretch reflex loops (i.e., short or long latency reflex arcs from afferent receptors) connected to the spinal cord generates tremor in the 10-Hz range because of the feedback delays about 50 ms. Although a number of studies have examined the role of central cortical oscillations (Raethjen et al. 2007; Raethjen and Deuschl 2012; Schnitzler et al. 2009) and found the origin of tremor and the relationship between tremor frequency and brain activities, they have formed no consensus about cortical involvement in the generation of essential tremor. Some have observed brain activity using EEG (Raethjen et al. 2007; Raethjen et al. 2013; Schnitzler et al. 2009) and magnetoencephalography (Hellwig et al. 2001) to investigate the

relationship between tremor movement and brain activity in separate areas of the brain and the effects of various treatments.

1.2 Assessment and Measurement of Tremor

The most common methods of tremor assessment are subjective measurements by clinicians who score the severity of tremor in each body part through visual inspection (Goetz et al. 2008). To evaluate tremor severity, clinicians ask patients to perform tasks such as tapping the finger to the nose or writing a spiral (Elble et al. 1996; Elble et al. 2012; Elias and Shah 2014) (Table 1.1 and Figure 1.4). Several research groups have developed computerized methods of assessing tremor for PD or ET (Giuffrida et al. 2009; Rigas et al. 2012; Pulliam et al. 2014; González et al. 2014; Hellwig et al. 2009). They have typically used accelerometers and sensor modules on various body parts (e.g., legs, arms, hands, and

Table 1.1. Tremor Research Group evaluation guidelines of The Essential Tremor Rating Assessment Scale (TETRAS) for (a) writing an *Archimedes spiral*, (b) *handwriting*, and (c) vertically holding a pen (Elble et al. 2006 and 2008).

The Essential Tremor Rating Assessment Scale (TETRAS) by Tremor Research Group								
Archimedes Spiral (6.5 cm outer diameter)								
Score	0	1	2		3		4	
Upper Limb	No Tremor	Barely visible	Mild tremor < 1cm		Moderate tremor >1 cm		Unable to Complete	
Handwriting ("Today is a nice day")								
Score	0	1	2		3		4	
Upper Limb	No Tremor	Mildly abnormal	Moderately abnormal		Markedly abnormal; Illegible		Severely abnormal	
Hold pen vertically for 10 seconds								
Score	0	1	1.5	2	2.5	3	3.5	4
Upper Limb	No Tremor	Barely visible	Visible < 1 cm	1-3 cm	3-5 cm	5-10 cm	10-20 cm	> 20 cm

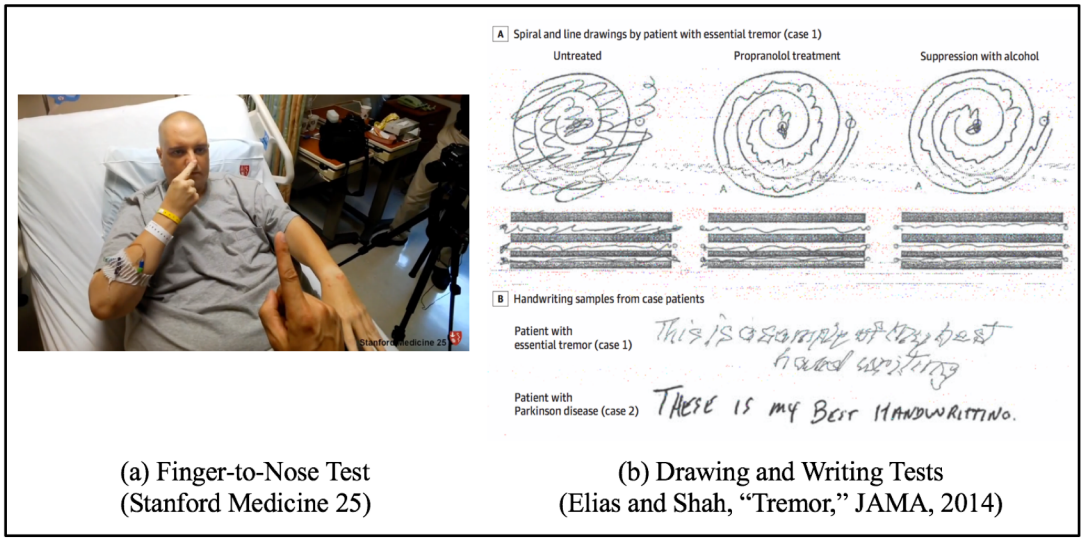

(a) Finger-to-Nose Test (Stanford Medicine 25)

(b) Drawing and Writing Tests (Elias and Shah, "Tremor," JAMA, 2014)

Figure 1.4 Tremor evaluation and assessment: examples of (a) the finger-to-nose task and (b) the drawing and writing tasks.

the head) to classify the severity of tremor (Rigas et al. 2012). Then they correlate quantitative assessments with clinical scores to enhance the accuracy of their diagnoses in the early stages of tremor (González et al. 2014) and to track its status over the long term (Pulliam et al. 2014; Hellwig et al. 2009).

To measure human activities, researchers and clinicians commonly use the inertial measurement unit (IMU) (Bao and Stephen 2004; Logan et al. 2007), which involves the use of an accelerometer and a gyroscope for sensing linear and angular motion. The development of sensing technology has led to a considerable reduction in the sizes of sensors and the amount of power consumption. Therefore, they are now embedded in most wearable devices such as smartphones, tablets, and smart watches. Sensor units have been used for classifying human activities such as health monitoring, exercise tracking, and entertainment. To assess tremor activity in human movement, researchers and clinicians apply IMUs for short-term use in a clinic or a laboratory (Giuffrida et al. 2009; Rigas et al.

2012; Pulliam et al. 2014) and for long-term use at home (Pulliam et al. 2014; González et al. 2014; Hellwig et al. 2009), and to increase the accuracy of tremor and activity detection, multiple sensor units are being mounted on various parts of the human body (Rigas et al. 2012; Bao and Stephen 2004). IMUs capture motion activity that is independent of neurological activity (e.g., activity measured by electromyography (EMG), or electroencephalography (EEG)). Therefore, sensor data collected by IMUs are rarely affected by electrical stimulation (i.e., nerve or muscle stimulation, DBS), so they can be analyzed without stimulation artifacts. EMG recordings also generate important information about muscle activity underlying tremor. Thus, to quantify tremor using IMUs and EMGs, several studies have analyzed the frequency and the amplitude of tremor movement. Some findings show that the sensorimotor cortex is involved in the generation of ET, because Hellwig's research team showed the significant corticomuscular coherences at the tremor frequency in ET using simultaneous Electroencephalography (EEG)-Electromyography (EMG) recordings (Hellwig et al. 2001); however, Halliday's research team showed a significant low-frequency component at the frequency of the tremor bursts and they insisted that there was no coherence between magnetoencephalogram (MEG) and EMG recordings at the tremor frequency (Halliday at el. 2000).

1.3 Treatments to Suppress Tremor

Once patients are diagnosed, the common and easiest treatment of their symptoms is pharmacotherapy. Common medications for the treatment of ET are primidone and beta blockers (e.g., propranolol, atenolol, metoprolol, and nadolol) (IETF, Essential Tremor (ET) Common Medications; Mayo Clinic, Essential Tremor: Treatment). However, these

Figure 1.5 Treatments for suppressing tremor: (a) medication, (b) Botulinum Toxin (Botox), (c) deep brain stimulation (DBS), and assistive technologies (ATs).

medications do not respond sufficiently, benefitting only about 60 percent of patients, and some cause intolerable side effects (e.g., fatigue, nausea, dizziness, ataxia, and sedation). Other possible therapies include the injection of botulinum toxin (Botox) into the muscle (Jankovic and Schwartz 1991; Pahwa et al. 1995) and the intake of alcohol (Growdon et al. 1975; Charles et al. 1999). Despite reports of the positive effects of these therapies at reducing tremor movement, their efficacy is short-lived, that is, only weeks (Botox) or even hours (alcohol). Patients with tremor also have a surgical option for DBS (Kumar et al. 1998; Lyons et al. 2008; Hubble et al. 1996). This option requires surgery in which a series of electrodes are implanted in the brain. However, such surgery is not only costly but also highly invasive, and it does not guarantee effective tremor suppression with stimulation (IEFF, Treatment Option: Surgical Treatment).

Other approaches to mitigating the effects of tremor are assistive devices. Even though they are not actual treatments, they can help individuals with tremor movement to smoothly perform daily activities. Devices such as weighted utensils, weighted universal holders for pens, and large keyboards are simple, easy to access, and relatively cheaper than the other treatments mentioned above. Another assistive device, Liftware (https://www.liftware.com/), is an active noise-cancelling device that automatically stabilizes an attached utensil. Researchers have reported 70% less tremor with Liftware than with a patient's bare hands (Pathak et al. 2014). Each device, however, is limited to a certain activity (i.e., eating, writing, typing), requiring users to purchase several devices and to change the device for each activity.

1.4 Use of Sensory Feedback in Tremor Suppression

Other than the currently available treatment options listed in the previous section, several techniques suppress tremor by providing sensory feedback. Several studies have investigated mechanical perturbations that reset the phase of tremor (Lee and Stein 1981; Britton et al. 1992) and hypothesize that such perturbations are able to generate changes within spinal reflex loops and torque pulses delivered to tremor movement and reset the phase of the tremor for ET, but not PD (Lee and Stein 1981). Another study used a small robotic arm with a haptic interface that provided force that suppressed tremor by controlling the impedance of the device (Pledgie et al. 2000).

Another technique that suppresses tremor is the wearable orthosis, or robotic tremor suppression system, equipped with active motor control and passive mechanical structures (Rocon et al. 2007; Figure 1.6 (a)). By dampening tremor with impedance and

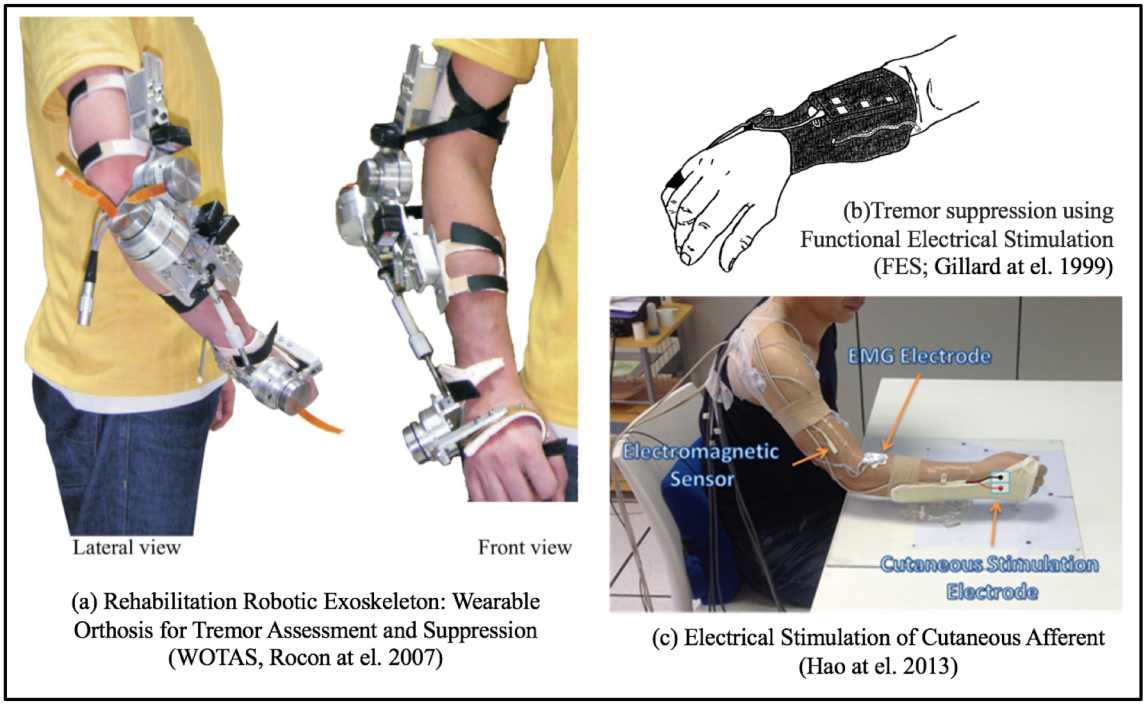

Figure 1.6 Examples of sensory feedback in tremor suppression: (a) rehabilitation robotic exoskeleton, (b) functional electrical stimulation (FES), and (c) cutaneous afferent electrical stimulation.

torque, these techniques can reduce the mechanical resonance of tremor movement. In addition, vibration feedback has been applied on the tendons of extensors and flexors to suppress tremor (Jöbges et al. 2002; McAuley et al. 1997), specifically PD resting tremor, and studies have found that vibratory feedback could modulate the frequency pattern of tremor movement by affecting reflex oscillations.

Also investigated as a technique for suppressing tremor is electrical stimulation. Researchers have explored how sensory stimulation affects the neurological pathway of tremor (Prochazka et al. 1992; Javidan et al. 1992; Gillard et al. 1999; Figure 1.6 (b); Hao at al. 2013). Several studies have found that functional electrical stimulation could attenuate tremor, particularly essential tremor, by about 73% (Prochazka et al. 1992;

Javidan et al. 1992). These studies showed that electrical stimulation activates flexor and extensor (biceps and triceps brachii, respectively) muscles out-of-phase, modulating the frequency of tremor, and the researchers have designed an open-loop response of upper-limb muscles to stimulation and used the collected data of tremor movement to modulate tremor frequency. Another study (Hao at al. 2013) applied cutaneous nerve stimulation to dorsal skin of the hand to suppress tremor movement (Figure 1.6 (c)). The authors of this study hypothesized that neurological commands from cutaneous afferents to the spinal cord can be modulated by transcutaneous nerve stimulation. Their preliminary results from one PD patient show the instant amplitude suppression of resting tremor, particularly tremor on shoulder. They believe that this finding support the role of propriospinal neurons in the spinal cord mediates cortical motor commands via cutaneous stimulation.

From the literature review, we hypothesize that tremor movement, particularly that in individuals with ET, is more likely related to the peripheral feedback loop than it is to central oscillations. Even if the generation of tremor and the origin of ET have not yet been identified, they may be the result of a combination of factors. Thus, we hypothesize that external feedback (i.e., electrical stimulation) to the peripheral nervous system affects the pathway of tremor, and real-time closed-loop stimulation with respect to one's current tremor status is capable of maximizing tremor suppression.

1.5 Specific Aims

To approach this doctoral thesis, we created a list of the specific aims, each accompanied by hypotheses for a quantitative assessment of tremor, the development of a wearable tremor modulation system, and an analysis of stimulation parameters.

Aim 1: Determine the effects of tremor movement on the performance of human subjects on computer-based standardized tasks and the relationship among currently available methods of tremor evaluation.

- **Hypothesis 1.1:** The tremor output metrics (i.e., dominant frequency and tremor power) using a three-axis accelerometer is highly correlated with the current method of tremor assessment.
- **Hypothesis 1.2:** Performance metrics from computer-based standardized tasks are strongly correlated with the current method of tremor assessment.
- **Hypothesis 1.3:** The relationship between performance metrics from computer-based standardized tasks and the tremor output metrics are highly correlated.

Aim 2: Determine the effects of peripheral-nerve electrical stimulation on tremor movement.

- **Hypothesis 2.1:** Electrical stimulation on the peripheral nerve can modulate the dominant frequency of tremor.
- **Hypothesis 2.2:** Electrical stimulation of the peripheral nerve can modulate tremor power (severity).

Aim 3: Determine the effects of various stimulation parameters for tremor movement.

- **Hypothesis 3.1:** The effects of stimulation parameters (i.e., amplitude, frequency, duty cycle, phase, and stimulation sites) can be modeled to find an open-loop response for tremor movement by various combinations of stimulation parameters.
- **Hypothesis 3.2:** A parameter optimization algorithm can maximize the efficacy of the electrical stimulation of the peripheral nerve and minimize nerve fatigue from the long-term stimulation and the power consumption of the system.

CHAPTER 2

QUANTITATIVE TREMOR ASSESSMENT

WITH COMPUTER-BASED STANDARDIZED TASKS

2.1 Introduction

Tremor movement can be observed in patients with neurological disorders such as essential tremor (ET) and Parkinson's disease (PD) (Hess and Pullman 2012). Even though the particular characteristics of tremor may vary by patient and etiology (Bain 2007; IETF, 12-Month Annual Report, 2006), tremor categorically affects movement and reduces the quality of life for all patients. For example, ET is a chronic and progressive neurological disorder with frequencies between 4-12 Hz (Hess and Pullman 2012; Bain 2007; IETF, 12-Month Annual Report, 2006). In the United States, about ten million ET patients, approximately 90% of whom experience arm tremor, live with ET (Bhidayasiri 2005). While tremor associated with Parkinsonism can be observed in patients who are resting, ET tremor is associated with actions (movements) and postures (Hess and Pullman 2012; IETF, 12-Month Annual Report, 2006). Despite differences in their characteristics, these two conditions are often misdiagnosed in their early stages (IETF, 12-Month Annual Report, 2006).

Currently available diagnostic methods consist of mostly subjective measurements (Goetz et al. 2008; Elble et al. 2008; Tintner 2004), and clinicians and researchers typically diagnose patients' symptoms with provocative maneuvers such as performing the nose-to-finger task, drawing a spiral, holding the arms still while holding a certain posture, and

writing a passage (Giuffrida et al. 2009; Miralles et al. 2006; Norman et al. 2011; Elble et al. 1996; Elble et al. 2012; Elble et al. 2006; Mostile et al. 2010; Elias and Shah 2014). While patients perform the tasks, a proctor formally scores their tremor movements and validates them on a rating scale such as the Unified Parkinson's Disease Rating Scale (UPDRS) (Goetz et al. 2008), The Essential Tremor Rating Assessment Scale (TETRAS) (Elble et al. 2008; Giuffrida et al. 2009; Elble et al. 2012; Elble et al. 2006), and the Tremor Rating Scale (Tintner 2004) with a 0-4 scale within a 1-point or 0.5-point range. The scoring methods mostly focus on the severity of one's tremor movement, but one important characteristic—the frequency of tremors—is often ignored, despite its importance in early intervention (Zeuner et al. 2003; Elble et al. 1994; Uhríková et al. 2011). Current diagnostic methods, particularly drawing and writing tasks, are also susceptible to inter- and intra-rater variability (Stacy et al. 2007).

To potentially both alleviate the concern about inter- and intra-rater variability and incorporate frequency measures into tremor assessment, we propose an automatic and quantitative method consisting of three computer-based tasks along with their performance metrics that assess the characteristics of tremor. We adapt a spiral navigation (SPN) task, a common tremor measurement task (Miralles et al. 2006; Elias and Shah 2014), but the proposed method uses a 3D mouse rather than a pen or a pencil on a piece of paper. We also adapted two additional tasks: a rectangular track navigation (RTN) task (Yousefi et al. 2012; Kim et al. 2016) and a multi-directional tapping/clicking (MDT) task (Soukoreff and MacKenzie 2004) (an International Standardization Organization (ISO) 9241-9 standard task; Soukoreff and MacKenzie 2004; ISO 9241-9:2000(E) 2002). The human motor performance of subjects on the MDT task is based on Fitts' law, which is applied to the

modeling of the tradeoff between velocity and accuracy (Soukoreff and MacKenzie 2004), and the movement can be quantified by a metric, *throughput* (in bits per second, bits/s). Fitts' law tasks are widely used in the evaluations of non-keyboard input devices (e.g., pointing devices) such as a computer mouse, a keyboard, a stylus, or a touchscreen, to design new ergonomic devices and user interfaces that achieve optimal performance and in assessments of motor performance within specific groups of users (Yousefi et al. 2012; Soukoreff and MacKenzie 2004; Natapov et al. 2009). This proof-of-concept study evaluates how task performance relates to the characteristics of pathological tremor in a small population of patients with ET. The goal of this work is to lay a foundation for larger studies that can then extensively validate the novel methods for objective and quantitative tremor assessment presented here in patients with ET.

2.2 Materials and Methods

2.2.1 Study Population

We recruited participants with diagnoses of ET and with present kinetic tremor in at least one arm. The ET participants were recruited from Atlanta, GA and Savannah, GA area via a recruitment flyer that was approved by Institutional Review Board (IRB) of the Georgia Institute of Technology (GT). Our research team had introduced this study at an ET Support Group (Savannah, GA) of International Essential Tremor Foundation (IETF), and recruited the participants from the meeting. As a baseline group, we also recruited a few participants with no tremor, who provided some baseline values expected for our measurements in healthy subjects. We collected arm movement data from eleven participants with ET, ranging in age from 19 to 82 (six females and five males whose

median age was 64) and three non-tremor participants ranging in age from 20 to 35 years old (two females and one male whose median age was 31). Detailed information about these participants is summarized in Table 2.1. We obtained approval for this study from the IRB of the GT and written informed consent from each participating subject. The participants were diagnosed by their own neurologists. Even though their first diagnosis were completed by different neurologists, nine of the eleven participants were recruited from a Savannah support group, which was overseen by a single neurologist.

2.2.2 Experimental Setting and Procedure

We first rated baseline tremor movement with TETRAS. We used the upper limb part of TETRAS, shown in Table 2.2 (modified version of TETRAS, Elble et al. 2006, 2008, and 2012) while the participants performed the *bean-transfer task,* shown in Figure 2.1 (a), which involved transferring a small object (a medium-sized lima bean) from one plate to another using a spoon for 7.5 seconds. We also analyzed tremor movement with a custom-designed wrist device to collect the motion information using a 3-axis accelerometer and a gyration mouse to quantitatively assess the subjects' performing computer-based tasks (SPN task: Figure 2.1 (b) and RTN task: Figure 2.1 (c)). Although we could not strictly control the speed of their arm movements, most participants were able to transfer three beans from one plate to another within 7.5 seconds. Thus, we analyzed baseline tremor movement during three 2.5-second-long segments of movement (Figure 2.2 (a)).

The quantitative tremor assessment system consists of a wireless 3D gyration mouse (GM; Air Mouse Go Plus, Gyration Inc.), a graphical user interface (GUI), and a custom-designed wrist device, shown in Figure 2.1 (b). The GM device converts 3D hand

Table 2.1 Participant Demographics.

ET Participant	Age, years	Sex	Year Since diagnosis	Dominant Hand	Medication	Tremor Frequency (Hz)	Tremor Power (g^2/Hz)	Tremor Presence (Dominant Side)	TETRAS Score (L /R)	Gyration Mouse (GM) Device Placement
Essential Tremor Participants										
ET 01	70	M	50	R	N/A	5.60 ± 0.69	9.66 ± 1.53	Both	2 / **3**	R
ET 02	76	F	8	R	Primidone	6.93 ± 1.29	9.10 ± 3.23	R	0 / **3**	R
ET 03	75	M	30	R	Propranolol, Primidone, Zonisamide	5.20 ± 1.39	13.65 ± 2.34	Both (L)	4 / **4**	R*
ET 04	58	F	10	R	Primidone	6.40 ± 0.80	12.80 ± 1.34	R	0 / **4**	R
ET 05	64	M	15	L	N/A	6.27 ± 2.54	22.68 ± 1.84	Both (L)	**4** / 1	L
ET 06	58	F	10	R	Trihexyphenidyl	5.60 ± 1.06	4.98 ± 1.20	Both (R)	1 / **1**	R
ET 07	82	F	10	L	Topiramate	5.33 ± 0.23	7.75 ± 1.98	Both (L)	**2** / 0	L
ET 08	79	M	10	R	N/A	6.27 ± 1.01	10.61 ± 1.71	Both (L)	4 / **3**	R*
ET 09	47	F	4	R	N/A	6.67 ± 1.01	7.29 ± 1.63	Both (L)	2 / **2**	R*
ET 10	20	F	10	R	N/A	8.93 ± 0.92	6.70 ± 0.40	Both	2 / **2**	R
ET 11	19	M	4	R	N/A	10.53 ± 1.22	3.95 ± 0.45	Both	1 / **1**	R
Non-Tremor Participants										
AB01	31	F	N/A	R	N/A	10.17 ± 2.93	1.59 ± 0.06	N/A	0 / 0	R
AB02	20	F	N/A	R	N/A	7.51 ± 0.47	2.37 ± 0.07	N/A	0 / 0	R
AB03	35	M	N/A	R	N/A	8.38 ± 2.13	1.69 ± 0.39	N/A	0 / 0	R

M: Male, F: Female, R: Right, L: Left, Freq.: Frequency, Amp.: Amplitude;
* indicates that the dominant hand side is not the same as tremor dominant side.

(a) Baseline Tremor Movement (Bean-transfer task)

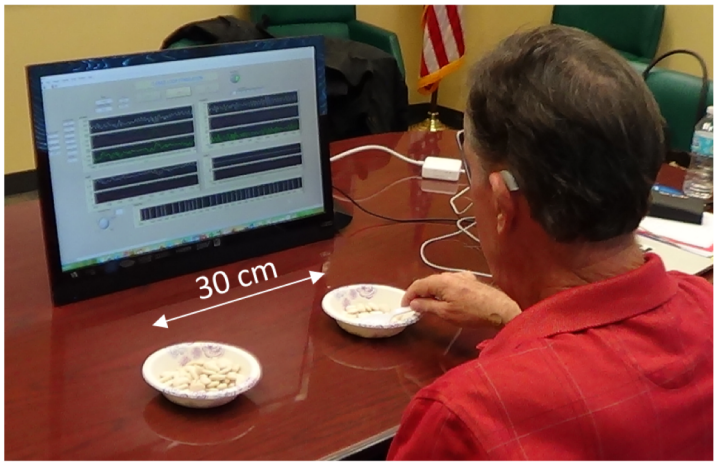

(b) Computer-based Task (Spiral Navigation Task)

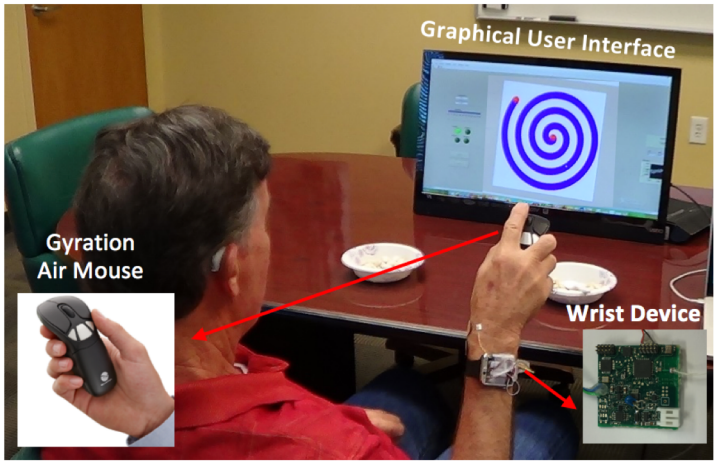

(c) Computer-based Task
(Rectangular Track Navigation Task)

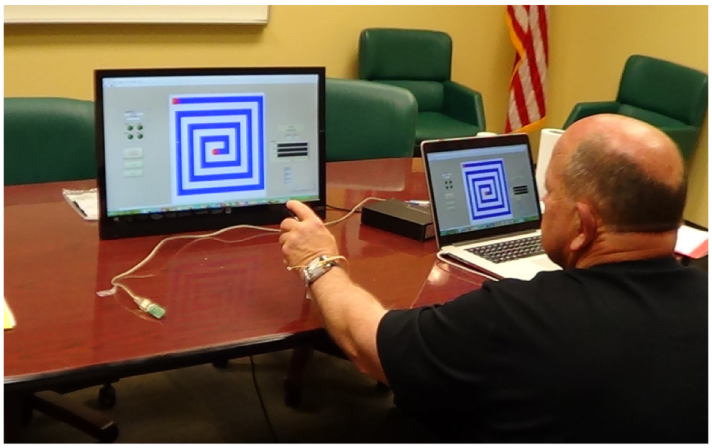

Figure 2.1 Experimental setup for quantitative tremor assessment tasks: (a) control (baseline) tremor movement, (b) spinal navigation (SPN), and (c) rectangular track navigation (RTN) tasks.

Table 2.2 Rating method for upper limb tremor based on The Essential Tremor Rating Assessment Scale (TETRAS).

Definition of TETRAS Score					
Score	0	1	2	3	4
Upper Limb	No Tremor	Barely visible < 1cm	1 to < 5cm	5 to < 20 cm	> 20 cm

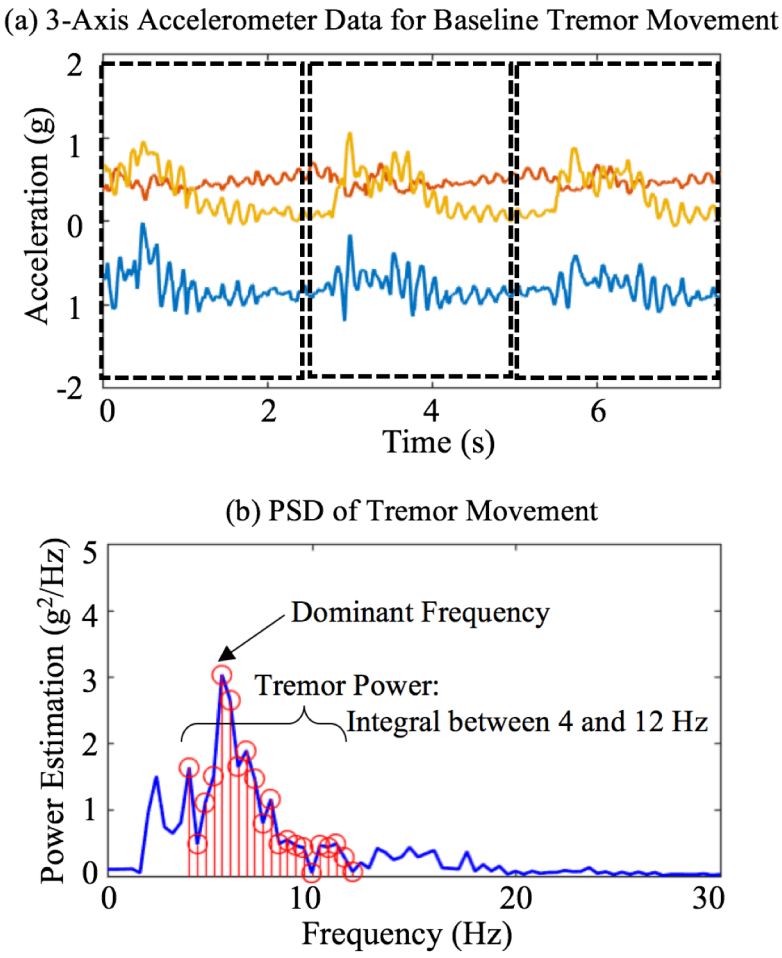

Figure 2.2 Data analysis for tremor movement: (a) raw three-axis accelerometer data of baseline tremor movement, and (b) an analysis of the power spectral density (PSD) for the tremor output metrics (i.e., dominant frequency and tremor power).

movement to 2D motion on a computer screen and captures the movement of the cursor at a 200 Hz sampling rate. The GUI of the computer-based tasks was implemented in a LabVIEW 2016 (National Instruments). The data from the wrist device, which contained a three-axis accelerometer at a 100Hz sampling rate, was wirelessly transmitted to a computer via a radio frequency of 2.4-GHz.

To evaluate upper limb tremor, we used the GM device to conduct the SPN, RTN, and MDT tasks on a laptop computer with a 22" LCD monitor, which was placed about 50 cm from the participants. This experiment was completed in the laboratory. The participants remained on their regular medication. We instructed the participants to hold and control the GM device to navigate with the mouse cursor without resting their elbows on the table or arm rest and then asked them to complete three tasks as quickly and as accurately as possible. The tracks of the SPN and RTN tasks or targets of the MDT task were displayed in an 800 × 800-square pixel field (225 mm × 225 mm).

To familiarize themselves with the task and to minimize the effect of learning, all participants had at least one practice trial before actual data collection and completion of three trials for each task. We collected and represented each data point for the trial of each SPN and RTN task. One trial for the MDT task consisted of 45 cursor clicks from one target to another, divided into three index of difficulty (ID) categories (ID_1: W = 57 pixels, D = 402 pixels, ID = 3.01; ID_2: W = 57 pixels, D = 705 pixels, ID_3 = 3.74; and condition 3: W = 76 pixels, D = 705 pixels, ID = 3.36). We represented the mean of the 15 data points for each ID category as a data point and analyzed three data points for one trial of the MDT task. The collection of all data from the baseline tremor movements and the three computer-based tasks for each participant took about 15 minutes.

2.2.2.1 Spiral Navigation and Rectangular Track Navigation Tasks

The tracks for the SPN and RTN tasks are shown in Figures 2.3 (a) and (b). We established one pattern for the spiral track, shown in Figure 2.3 (a), and four rectangular patterns for the RTN track. Each trial entailed the random selection of one of the four rectangular tracks, and the other three tracks were similar to that depicted in Figure 2.3 (b), yet with a different orientation for the starting path. We asked the subjects to use the GM device to navigate the mouse cursor to follow the tracks from the *start* in the center of the screen to the *end* as quickly and as accurately as possible.

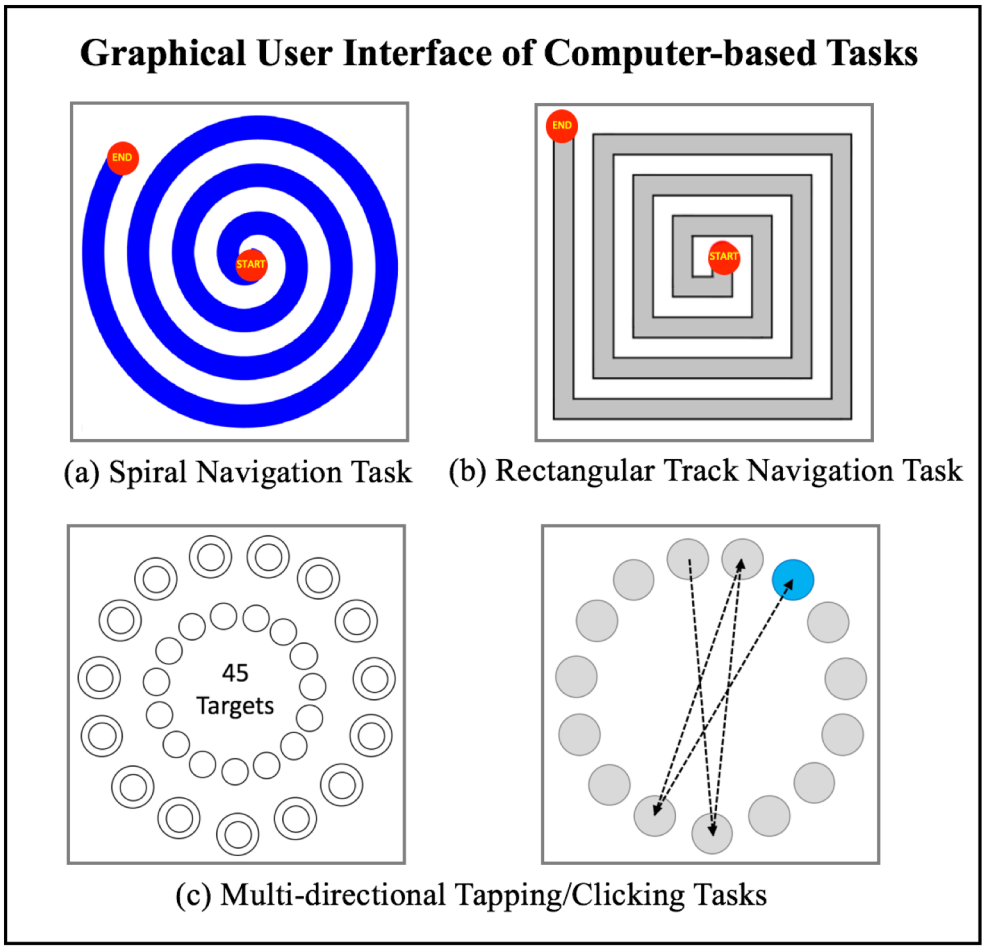

Figure 2.3 Graphical user interface (GUI) of the computer-based tasks: (a) SPN, (b) RTN, and (c) MDT tasks.

2.2.2.2 Multi-directional Tapping/Clicking Task

One round of the MDT task consisted of 45 circular targets that formed three conditions of the ID, each of which consisted of 15 circular targets (Figure 2.3 (c)). Three conditions of the targets were combinations of two target widths (W = 57 and 76 pixels) and two circumference distances (D = 402 and 705 pixels). The target width and the distance determine the ID for the targets, defined in Eq. (1) (Soukoreff and MacKenzie 2004).

$$ID = \log_2\left(\frac{D}{W} + 1\right) \quad (1)$$

Each condition had a unique ID (condition 1: W = 57 pixels, D = 402 pixels, ID = 3.01; condition 2: W = 57 pixels, D = 705 pixels, ID = 3.74; and condition 3: W = 76 pixels, D = 705 pixels, ID = 3.36). The calculated IDs for the three conditions ranged between 3.01 and 3.74 bits (mean: 3.37 bits). The targets were highlighted, one at a time, in a clockwise direction across the diameter of the outer circle, shown in Figure 2.3 (c). Then, using the GM device, the subjects moved the cursor as quickly and as accurately as possible to reach the target, and using the left-select button on the GM device, they clicked on the target.

2.2.2.3 Performance Metrics

Tremor Frequency and Power: To determine the performance metrics, we high-pass filtered the root-mean square (RMS) of the three-axis accelerometer data at a cutoff frequency of 3 Hz and then applied fast-Fourier transform (FFT) in the frequency analysis (sampling frequency (Fs) = 100 Hz, sampling period = 2.5 s, and length of signal = 250 samples). We defined the peak frequency of PSD as the tremor frequency (Figure 2.2 (b); Elble et al. 1996) and the integral of PSD between 4 and 12 Hz as tremor power (Eq. (2));

Figure 2.2 (b) (Dai et al. 2015). The * denotes the complex conjugate, N represents the sample points, and g^2/Hz (g equals 9.8 m/s^2) is the unit of the tremor power.

$$\text{Power} = \int_{f_a}^{f_b} \frac{FFT^*(tremor) \times FFT(tremor)}{N^2} df; \ \ f_a = 4\text{Hz}, \ f_b = 12\text{Hz} \quad (2)$$

After analyzing baseline tremor movement with the tremor frequency and power, we correlated them with TETRAS scores and the subject's performance on the mouse cursor for the computer-based tasks.

Completion Time: The completion time (CT) for the SPN and RTN tasks represents the total time it took subjects to move the cursor from the *start* position to the *end* position. The CT for the MDT task represents the time it took subjects to move the cursor from one target and click on the next (highlighted) target.

Outside Area: We defined the outside area (OA) of the SPN and RTN tasks as the total area traversed outside of the tracks (divided by 1,000; pixels squared). The actual cursor movements from ET and non-ET participants (between TETRAS=0 and 4) using the GM device for the SPN and RTN tasks are represented by blue lines in Figures 2.4 (a) and (b), and the OA between the actual cursor trajectory and closest track are represented by the red area.

Path Efficiency: The path efficiency (PE) for the SPN and RTN tasks was calculated as the ratio between the track length if the cursor strictly followed the center of the spiral or rectangular track and the length of the actual trace. The PE for the MDT task was the ratio of the length from the center of the previous target and the center of the current target to the length of the actual cursor trace. Because the superimposition of tremor added

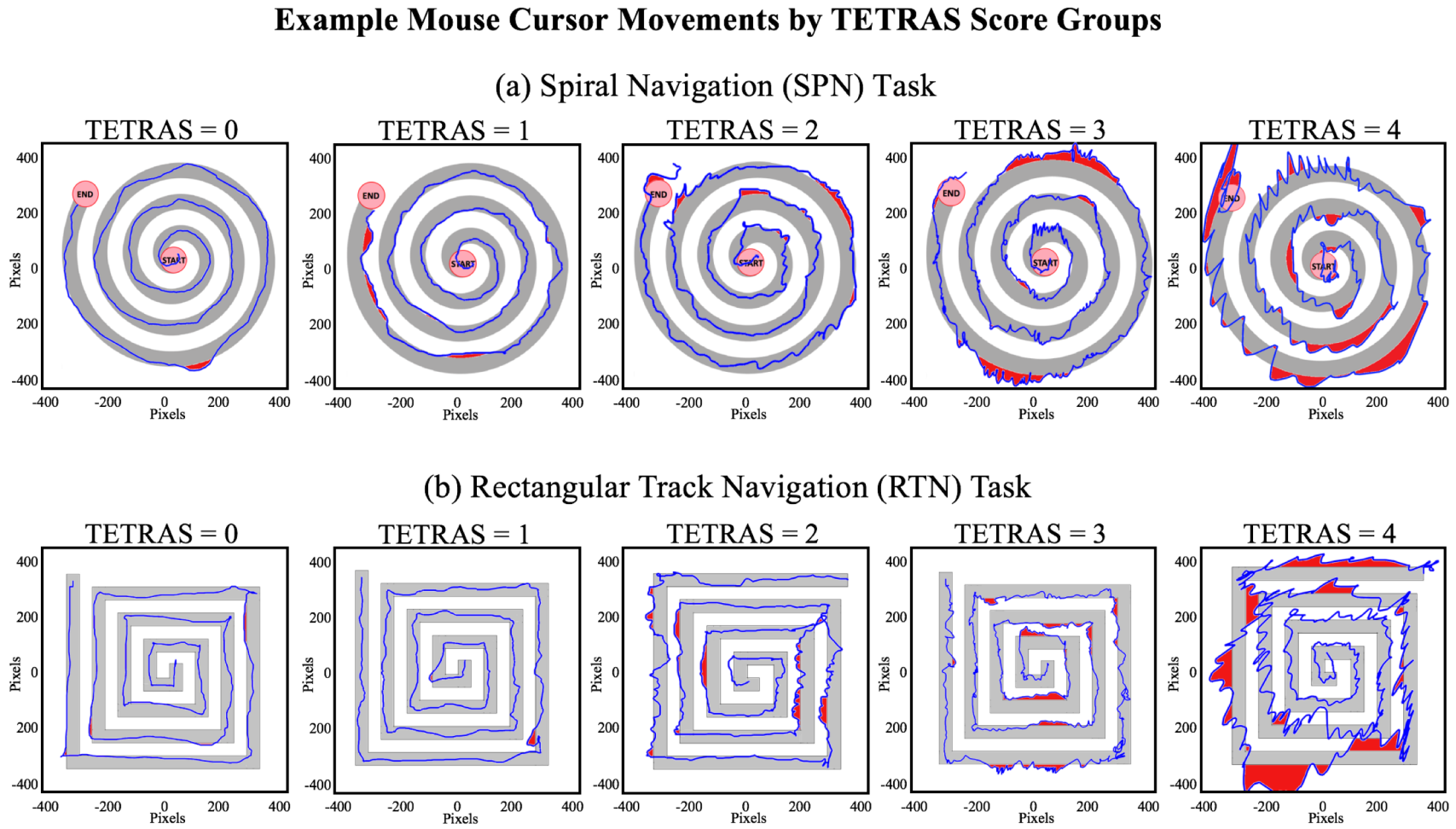

Figure 2.4 Example mouse cursor movements by TETRAS score groups: (a) SPN and (b) RTN tasks by TETRAS=0 to 4.

to the length of the cursor path, tremor lowered the path efficiency.

Throughput: The metric of the performance for MDT task was calculated as the throughput (TP) (Eq. (3)) (Soukoreff and MacKenzie 2004), defined as the ratio of the ID (Eq. (1)) (Soukoreff and MacKenzie 2004) to the CT.

$$Throughput\ (TP) = \frac{ID}{Completion\ Time} \quad (3)$$

2.2.3 Data and Statistical Analysis

To compare the tremor score group, we conducted a one-way analysis of variance (ANOVA) ($\alpha = 0.05$). We also conducted a linear regression analysis to correlate the two parameters of baseline tremor movement (e.g., tremor frequency vs. TETRAS score, tremor power vs. TETRAS score, etc.) and the two parameters of tremor output metrics (i.e., tremor frequency and power) and performance metrics (i.e., completion time, outside area, path efficiency, throughput, length of actual trace) for individual participants. The Statistical Package for the Social Sciences (SPSS) v. 24 was used for this statistical analysis.

2.3 Results

2.3.1 Baseline Tremor Movement

We first analyzed participants' baseline tremor movement on the bean-transfer task (Figure 2.1 (a)) using the three-axis accelerometer data and TETRAS scores. Using a linear regression analysis, we found a strong correlation between tremor power and TETRAS

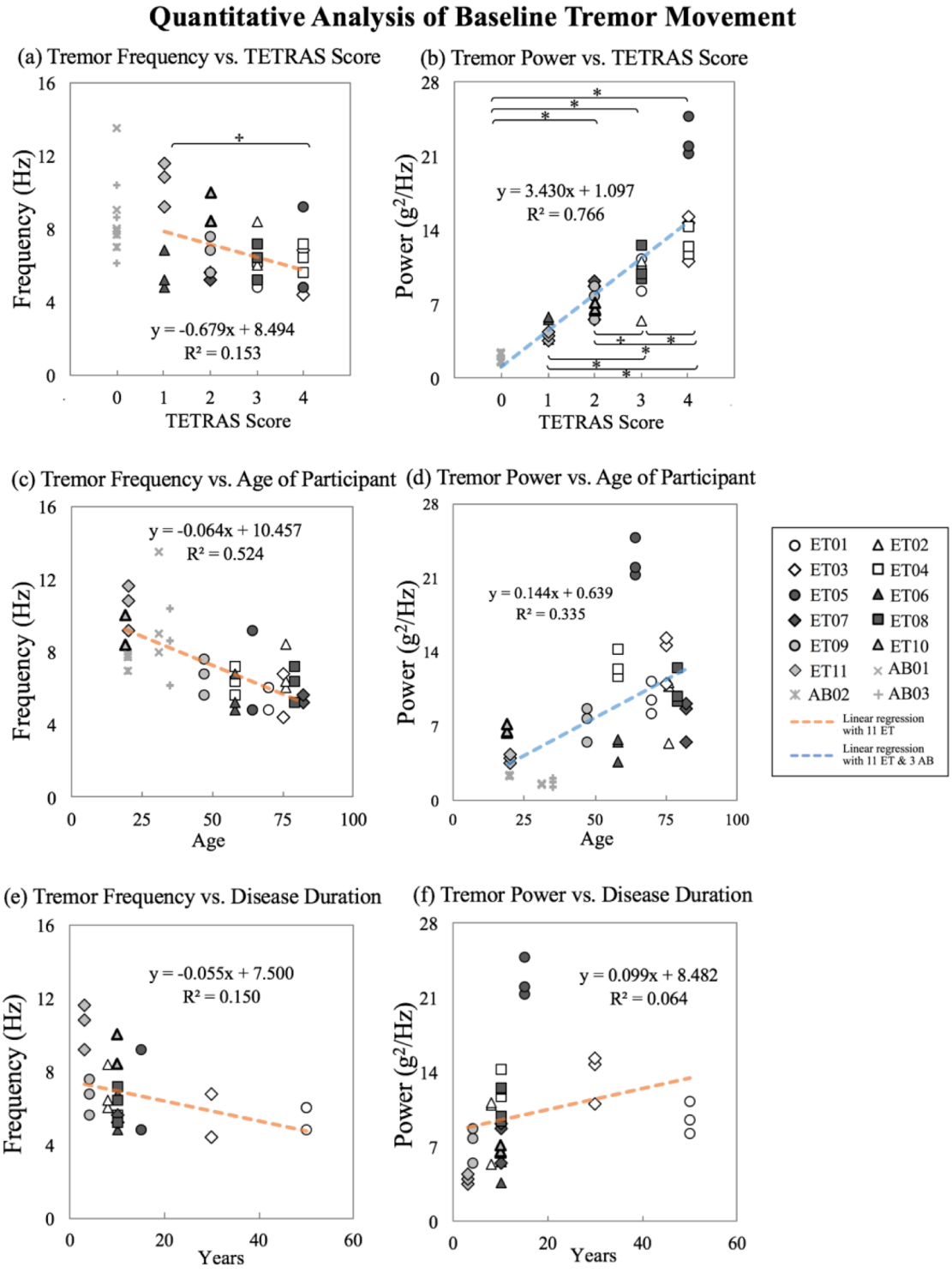

Figure 2.5 Quantitative analysis of baseline tremor movement for the relationship between the following parameters: (a) tremor frequency and TETRAS Score, (b) tremor power and the TETRAS score, (c) tremor frequency and subjects' age, (d) tremor power and subject' age, (e) tremor frequency and disease duration, and (f) tremor power and disease duration; ∗: $P < 0.005$, ∔: $P < 0.05$.

scores (R^2 = 0.766) (Figure 2.5 (b)). The dominant frequency of the baseline movement was less correlated with the TETRAS scores (R^2 = 0.153) (Figure 2.5 (a)), but it was correlated with the age of the subjects (R^2 = 0.524; β_1 = -0.064) (Figure 2.5 (c)), which is consistent with the finding in Elble (2000). However, neither the age of the participant (R^2 = 0.335) (Figure 2.5 (d)) nor the duration of the disease (R^2 = 0.064) (Figure 2.5 (f)) was significantly correlated with tremor power (Table 2.3). Therefore, we conclude that tremor power more precisely represents TETRAS score as an indicator of the severity of tremor movement.

Table 2.3 Summary of the coefficients of the linear regression analysis for the control trial and the computer-based standardized tasks.

	Parameters		**Score**			**Age**			**Disease Duration**		
Baseline		β_1	β_0	R^2	β_1	β_0	R^2	β_1	β_0	R^2
	Power	3.430	1.097	0.766	0.144	0.639	0.335	0.099	8.482	0.150
	Frequency	-0.679	8.494	0.153	-0.064	10.457	0.524	-0.055	7.500	0.064

	Parameters		**Power**			**Frequency**			**Score**			**Age**		
			β_1	β_0	R^2	β_1	β_0	R^2	β_1	β_0	R^2	β_1	β_0	R^2
SPN		CT	1.451	12.211	0.442	-1.972	39.941	0.063	4.284	15.236	0.251	0.220	12.403	0.165
		OA	6.345	24.650	0.641	-1.739	100.221	0.006	18.090	39.213	0.339	0.471	51.965	0.057
		PE	-0.026	0.890	0.654	0.052	0.278	0.280	-0.101	0.882	0.606	-0.006	0.963	0.456
RTN		CT	2.122	18.363	0.577	-3.297	62.636	0.154	6.564	22.124	0.356	0.297	20.345	0.183
		OA	2.588	-2.037	0.760	-5.272	59.319	0.324	8.098	2.354	0.480	0.423	-2.757	0.328
		PE	-0.033	0.986	0.628	0.086	0.056	0.528	-0.129	0.985	0.627	-0.007	1.098	0.508
MDT	All IDs	CT	0.113	1.605	0.234	-0.468	6.003	0.423	0.451	1.530	0.329	0.041	0.300	0.682
		TP	-0.087	2.465	0.368	0.186	0.132	0.459	-0.400	2.543	0.511	-0.028	3.201	0.636
		PE	-0.023	0.847	0.605	0.021	0.474	0.053	-0.071	0.805	0.373	-0.003	0.806	0.147
	ID= 3.01	CT				-0.281	4.656	0.272						
		TP				0.136	0.314	0.226						
		PE	-0.024	0.888	0.582									
	ID= 3.36	CT				-0.506	6.275	0.414						
		TP				0.215	-0.034	0.458						
		PE	-0.023	0.845	0.436									
	ID= 3.74	CT				-0.581	6.248	0.569						
		TP				0.310	-0.394	0.702						
		PE	-0.026	0.861	0.594									

2.3.2 Spiral Navigation and Rectangular Track Navigation Tasks

We evaluated the performance of the SPN and RTN tasks for all participants with the performance metrics, CT, OA, and PE, by comparing with tremor power, frequency, TETRAS score, and the age of participants. The analysis by the linear regression model was based on task performance vs. baseline tremor movement. The coefficient of the linear regression model (Eq. (4)) and the statistical analysis for each model are summarized in Table 2.3.

$$y = \beta_0 + \beta_1 x \quad (4)$$

Results of the analysis showed that OA ($R^2 = 0.641$) (Figure 2.6 (c)) and PE ($R^2 = 0.654$) (Figure 2.6 (e)) for SPN and OA ($R^2 = 0.760$) (Figure 2.7 (c)) and PE ($R^2 = 0.628$) (Figure 2.6 (c)) for the RTN tasks highly correlated with tremor power, and although CT also exhibited some linear correlation with tremor power for both SPN ($R^2 = 0.442$) (Figure 2.6 (a)) and RTN ($R^2 = 0.577$) (Figure 2.7 (a)), it was not as strongly correlated with OA and PE. Tremor frequency showed a very weak relationship with CT ($R^2 = 0.063$) (Figure 2.6 (b)) and OA ($R^2 = 0.006$) (Figure 2.6 (d)) for SPN and CT ($R^2 = 0.154$) (Figure 2.7 (b)) and OA (R^2=0.324) (Figure 2.7 (d)) for the RTN tasks, but it had a somewhat stronger linear correlation with PE ($R^2 = 0.280$) (Figure 2.6 (f)) for SPN and PE ($R^2 = 0.528$) (Figure 2.7 (f)) for the RTN tasks. Overall, the OA and PE for both tasks well represented tremor severity (power), and PE showed a linear correlation with tremor frequency. Moreover, we observed that the performance of RTN (Figures 2.7 (a)-(f)) showed a slightly closer fit with the linear regression analysis than that of SPN, shown in Figures 2.6 (a)-(f).

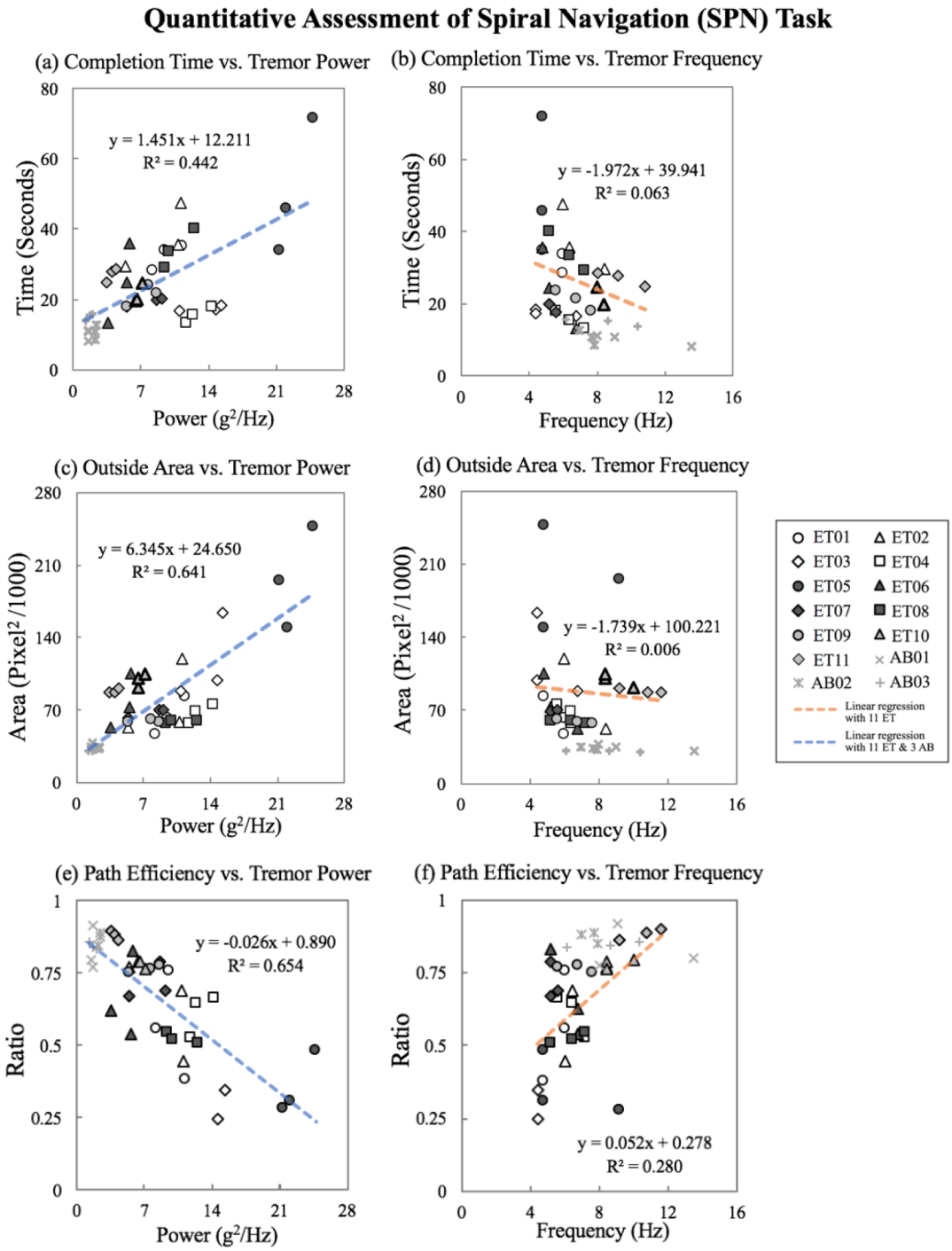

Figure 2.6 Quantitative assessment of the SPN task for the relationship between the following parameters: (a) completion time and tremor power, (b) completion time and tremor frequency, (c) outside area and tremor power, (d) outside area and tremor frequency, (e) path efficiency and tremor power, and (f) path efficiency and tremor frequency.

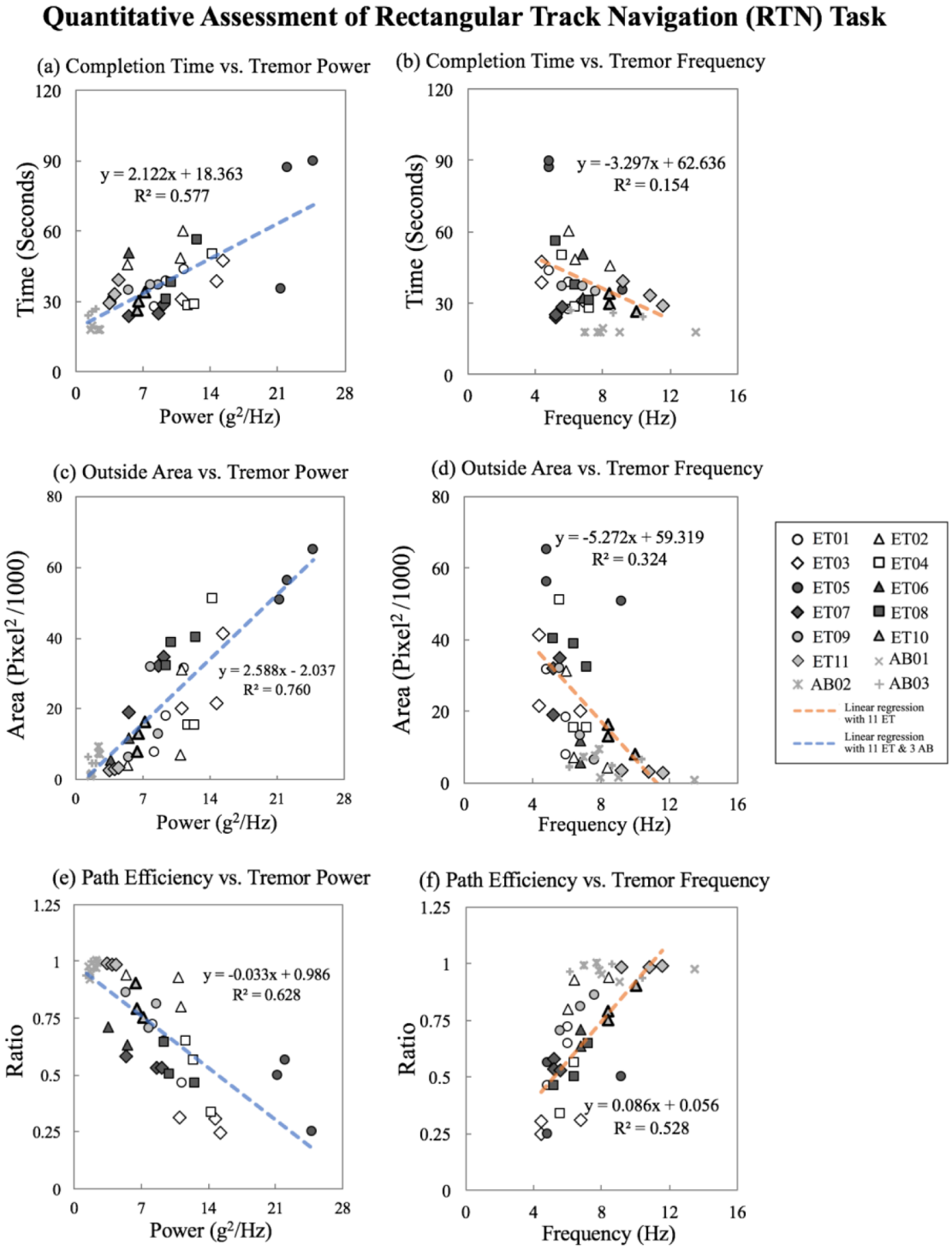

Figure 2.7 Quantitative assessment of the RTN task for the relationship between the following parameters: (a) completion time and tremor power, (b) completion time and tremor frequency, (c) outside area and tremor power, (d) outside area and tremor frequency, (e) path efficiency and tremor power, and (f) path efficiency and tremor frequency.

2.3.3 Multi-directional Tapping/Clicking Tasks

Similar to the relationship between the performance of the SPN and RTN tasks, the PE ($R^2 = 0.605$) (Figure 2.8 (e)) of the MDT task was highly correlated with tremor power. However, CT ($R^2 = 0.234$) (Figure 2.8 (a)) and TP ($R^2 = 0.368$) (Figure 2.8 (c)) of the MDT task was less correlated with tremor power. The relationship between CT ($R^2 = 0.423$) (Figure 2.8 (b)) and TP ($R^2 = 0.459$) (Figure 2.8 (d)) of the MDT task was more highly correlated with tremor frequency, but it was not as strong as the relationship between PE and actual trace (AT) with tremor power ($R^2 = 0.628$) (Figure 2.8 (g)).

When we analyzed the performance correlation of the CT and TP with tremor frequency by their IDs, however, we observed that higher IDs had a much higher correlation on CT (ID = 3.74: $R^2 = 0.569$) (Figure 2.9 (c)) and TP (ID = 3.74: $R^2 = 0.702$) (Figure 2.9 (d)) than the lower IDs for CT (ID = 3.01: $R^2 = 0.272$) (Figure 2.9 (c)) and TP (ID = 3.01: $R^2 = 0.226$) (Figure 2.9 (d)). Therefore, we found that the performance metrics of the MDT task were highly correlated with the frequency and tremor power.

In terms of the slopes (β_1) of the linear regression models between the CT and tremor frequency, we found that the lower IDs showed the higher magnitudes of the slopes (Figure 2.9 (c)). In contrast, we found that the slopes of the linear regression models for the relationship between the TP and tremor frequency showed that the higher IDs showed the higher amplitudes of the slopes (Figure 2.9 (d)). When we analyzed the linear regression models of the PE vs. tremor power by IDs, we found that the three models had similar coefficients (i.e., β_0 and β_1) (Figures 2.9 (a) and Table 2.3).

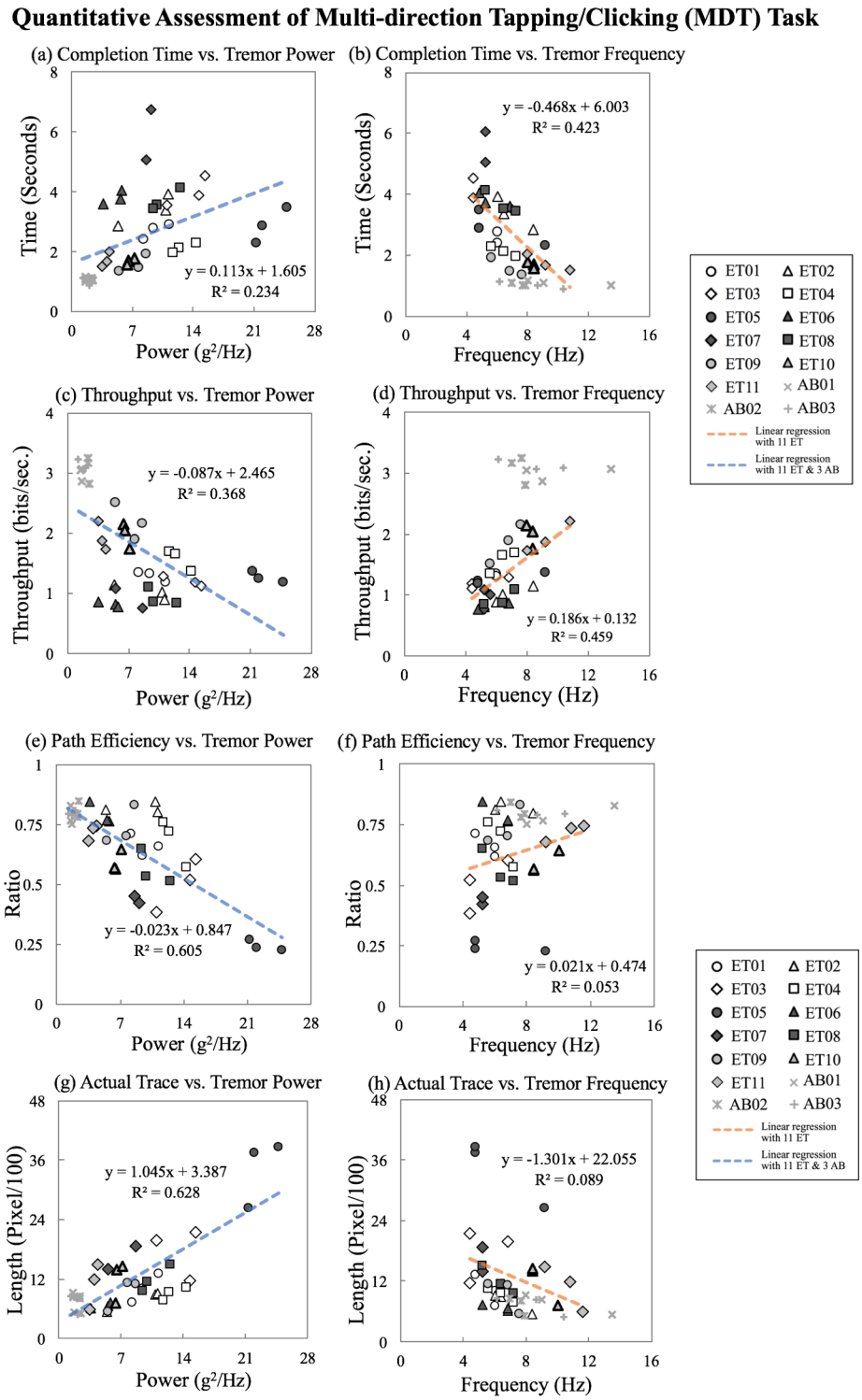

Figure 2.8 Quantitative assessment of the MDT task for the relationship between the following parameters: (a) completion time and tremor power, (b) completion time and tremor frequency, (c) throughput and tremor power, (d) throughput and tremor frequency, (e) path efficiency and tremor power, (f) path efficiency and tremor frequency, (g) actual trace and tremor power, and (h) actual trace and tremor frequency.

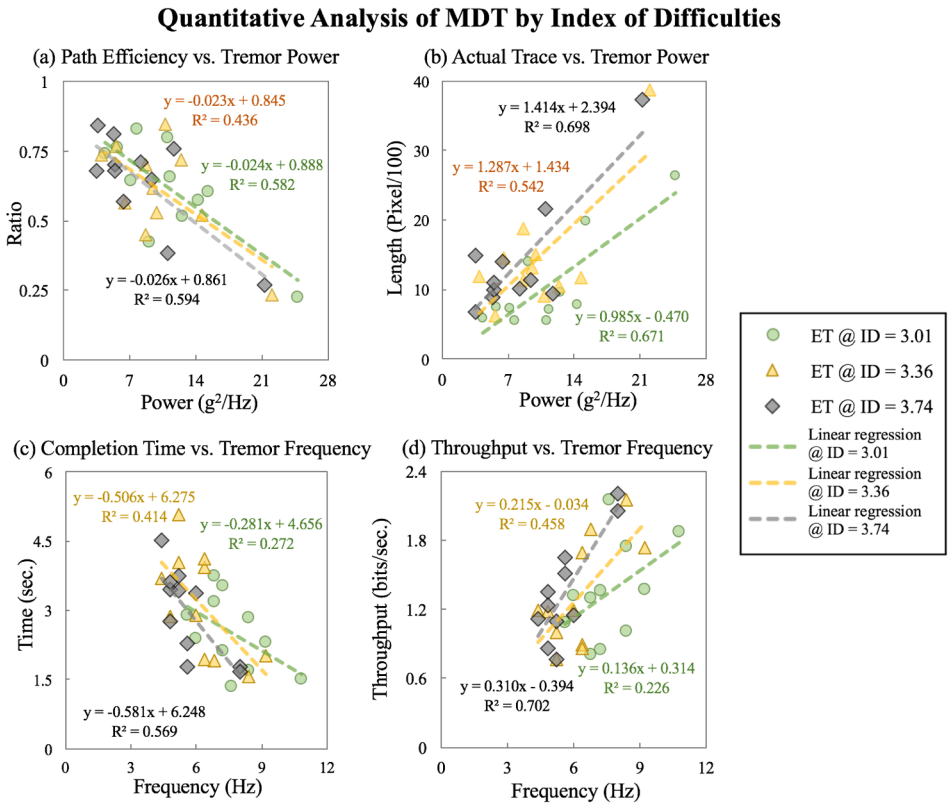

Figure 2.9 Quantitative analysis of the MDT task by IDs for the relationship between (a) path efficiency and tremor power, (b) actual trace and tremor power, (c) completion time and tremor frequency, and (d) throughput and tremor frequency.

2.4 Discussion

This study involved the data collection and analysis from eleven participants, all of whom were diagnosed with essential tremor at least four years ago or longer, and five of the eleven ET participants had taken at least one or more medications for their tremor symptoms. Even with medication, they exhibited upper limb tremor. As they were all taking their regular medication while data collection was taking place, their tremor movement deviated somewhat from their original tremor characteristics. However, during all of the data collection of baseline movements using a motion sensor, the subjective

tremor evaluation (TETRAS), and the three computer-based tasks completed within 10 to 15 minutes, we assumed consistent effects of medications. In addition, nine of the ET participants experienced upper limb tremor on both sides, and the dominant hands (for use of the mouse) of three participants differed from their dominant tremor sides. However, we collected data of baseline movement and computer-based tasks from the same side and conducted the evaluation of the baseline tremor characteristics and the performance of the computer-based tasks under the same conditions.

Our tremor scoring method for this study was based on the 0 - 4 scale of TETRAS. Despite carefully following the guidelines in the studied conducted by Elble's research team (Elble et al. 2008; Elble et al. 2006), a non-medical person conducted the tremor scoring method, which could be a limitation of this study. To maintain consistency, however, one person determined all TETRAS scores in this study. Moreover, this study focused only on the kinetic tremor movement of the subjects who performed the bean transfer task; it did not assess resting tremor or posture tremor tasks.

For the non-tremor participants, we found a wide range in the peak frequency of the FFT, an extremely small peak amplitude of the FFT, and a small difference between the first and second dominant peaks from the analysis of baseline movement. Therefore, the average dominant frequency, although not representative of the actual tremor frequency of the subjects, might have been within the sensor variability. Therefore, for the linear regression analysis, we excluded the tremor frequency data of the non-tremor participants. We also found a negative linear correlation between the age of the participants and tremor frequency for the baseline movement, which is consistent with the findings of a previous study (Elble 2000). Thus, the strong relationship between participants' ages and TP, as well

as the tremor frequency and the TP for the MDT task, was not surprising. In this study, we collected performance data only from the ET participants, so we found a coefficient for the linear regression model of the TP vs. age and TP vs. tremor frequency based on ET patients. Thus, we cannot conclude that a particular level of TP was a representative value of the tremor frequency. To distinguish among the frequency characteristics of tremor diseases such as PD, we need to collect performance data from and analyze a performance model for another pathological tremor group. Therefore, in future research, we plan to recruit other types of tremor patients, and since we had only three IDs in this study, we also plan to expand the levels of IDs to find the performance model that best fits tremor characteristics.

2.5 Conclusion

This study evaluated the feasibility of a new quantitative assessment method capable of accurately predicting metrics based on the characteristics of tremor movement. The performance metrics of computer-based assessment tasks showed highly correlated linear regression models with tremor frequency and power. We also observed subjects with tremor characteristics and quantified their performance on these tasks. This quantitative assessment method, which entails the use of a personal computer, a tablet, a smartphone, or a smart TV and a commercially available 3D mouse, can easily be performed at either a clinic or a patient's home. In future work, we expect to expand longer-term tremor tracking for more accurate diagnosis and evaluation of the effects of current medications or treatment. Moreover, this quantitative tremor assessment method can minimize inter-rater variability inherent in subjective approaches.

CHAPTER 3

PERIPHERAL-NERVE ELECTRICAL STIMULATION FOR MODULATION OF ESSENTIAL TREMOR

3.1 Introduction

Tremor, an abnormal oscillatory movement, can be observed in patients with neurological disorders such as essential tremor (ET) and Parkinson's disease (PD) (Hess and Pullman 2012). Tremor frequency, typically ranging between 4 and 12 Hz, varies among patients and among tremor etiologies (Hess and Pullman 2012; Bain 2007; IETF, 12-Month Annual Report, 2006; Bhidayasiri 2005). More than 90 percent of ET patients experience upper limb tremor (Bhidayasiri 2005), which can be characterized as kinetic tremor, or postural tremor (Hess and Pullman 2012; IETF, 12-Month Annual Report, 2006). Tremor associated with PD is referred to as *resting tremor,* which can initiate rhythmical shaking when the arms are at rest. Tremor associated with ET is referred to as *action tremor*, which can be particularly debilitating because it prevents patients from performing movements that require high degrees of dexterity and precision.

The most common tremor treatments are medications such as primidone or beta blockers (IETF, ET Common Medications). These medications demonstrate benefits in approximately 60 percent of patients who use them. They do not respond to tremor sufficiently, and they often have intolerable side effects (e.g., fatigue, nausea, dizziness, ataxia, sedation) (IETF, ET Common Medications). Other possible therapies are botulinum toxin (Botox) injection into the muscle (Mayo Clinic, Essential Tremor: Treatment;

Jankovic and Schwartz 1991; Pahwa et al. 1995) and alcohol consumption (Growdon et al. 1975; Charles et al. 1999). Although Botulinum toxin has been reported to reduce tremor movement, its efficacy is temporary, lasting for days or weeks.

Deep-brain stimulation (DBS) is a surgical treatment that entails the implantation of a series of electrodes in the brain (Kumar et al. 1998; Hubble et al. 1996; Lyons and Pahwa 2008). It is, however, expensive and highly invasive, and it does not effective for every tremor patients to suppress tremor (IEFT, Treatment Option: Surgical Treatment). Several research teams have also evaluated the efficacy of external feedback with functional electrical stimulation (FES) (Prochazka et al. 1992; Javidan et al. 1992; Gillard et al. 1999) and muscle vibration (Jöbges et al. 2002; McAuley et al. 1997) for PD and ET patients. The bulkiness of these systems and their lack of efficacy limit their use as a viable treatment for tremor.

We have developed an easy-to-use, non-invasive, wearable tremor modulation system that uses peripheral nerve stimulation (Figure 3.1) and quantitatively evaluated the efficacy of the system. Although the neurological pathways that underlie the origin and the generation of ET are not clearly understood (Deuschl et al. 2001; Hellwig et al. 2001; McAuley and Marsden 2000) and the effects of external stimulation of peripheral nerves within this pathway are also unclear (Hao et al. 2013; Xu et al. 2016), we hypothesized that the stimulation of peripheral nerves can modulate tremor, ultimately reducing tremor activity. In this study, we demonstrated the effects of the electrical stimulation of peripheral nerves using a selected set of stimulation parameters, and analyzed the tremor frequency and power in ET participants during sustained active arm movement with and without stimulation.

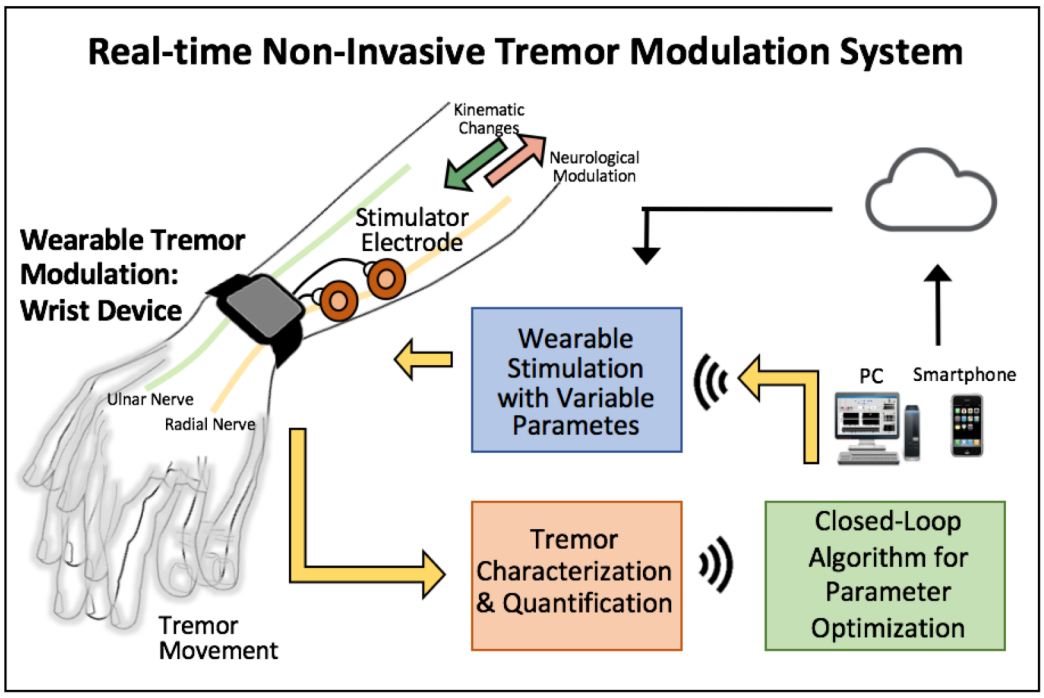

Figure 3.1 Overview of the real-time non-invasive tremor modulation system for essential tremor.

3.2 Wearable Tremor Modulation System

We developed a wireless wearable stimulation system that analyzes upper limb tremor using a three-axis accelerometer and that modulates/attenuates tremor using a peripheral-nerve electrical stimulation system with adjustable stimulation parameters. We designed hardware and software that facilitate the setting of stimulation parameters and the analysis of tremor performance metrics.

3.2.1 System Hardware and Software

The wireless wearable tremor modulation system consists of four components: (1) a wireless wrist device (Figures 3.2 (a), (b), and (d)) that consists of a sensor interface and a constant voltage stimulator (Figure 3.2 (c)), (2) a wireless transceiver (Figure 3.2 (e)), (3)

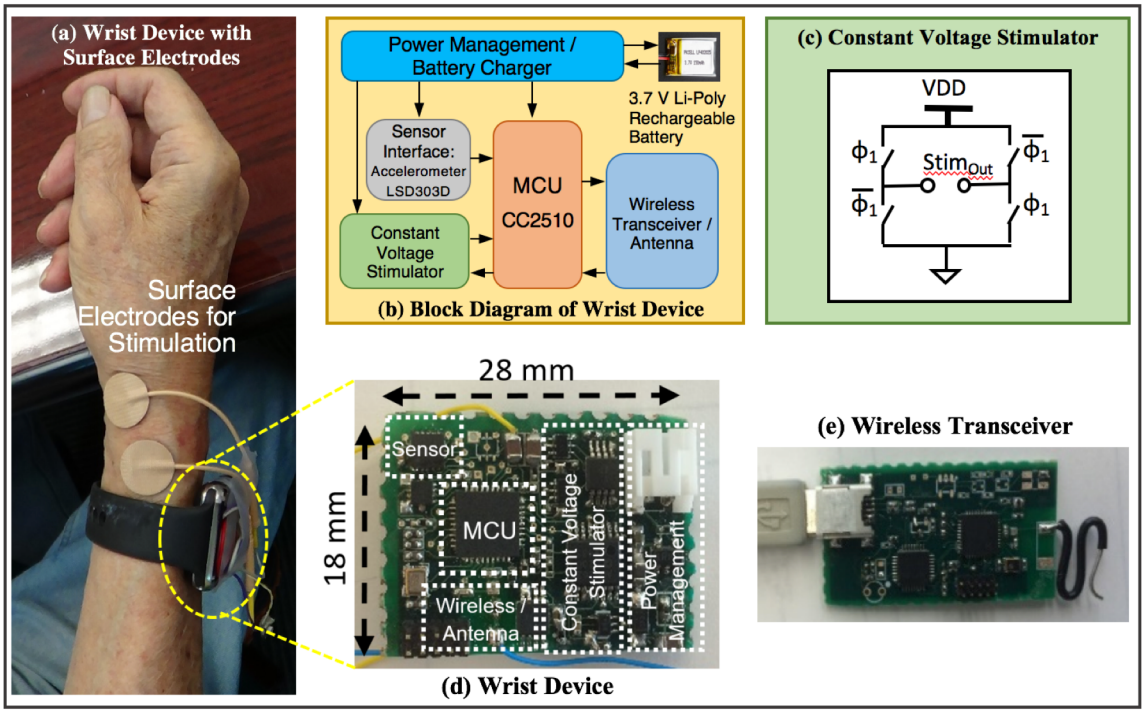

Figure 3.2 Block diagram of the wireless wearable stimulation system for essential tremor. (a) Experimental setup for the wrist device with a pair of surface electrodes, (b) a block diagram of the wrist device for wireless tremor modulation, (c) a block diagram of the constant voltage mode stimulator, (d) a custom-designed printed circuit board for the wrist device, and (e) a custom-designed wireless transceiver for the wrist device.

a pair of gel-based surface electrodes (Figure 3.2 (a)), and (4) a graphical user interface (GUI) (Figure 3.3 (b)) with a signal-processing algorithm (Figure 3.3 (c)). The wrist device consists of a three-axis motion sensor (LSM303D, STMicroelectronics), a microcontroller (CC2510, Texas Instruments), a wireless transceiver (2.4-GHz radio frequency), custom-built constant voltage mode stimulator circuitry (Figure 3.2 (c)), and a rechargeable 3.7 V lithium ion battery. All custom-designed electronics (18 x 28 mm^2) are enclosed in the commercially available wrist band (Figure 3.2 (a)). The battery is charged by a standard linear lithium-ion battery component (LTC4054, Linear Technology) connected to a 5 V mini-USB adapter. A full charge takes about three hours.

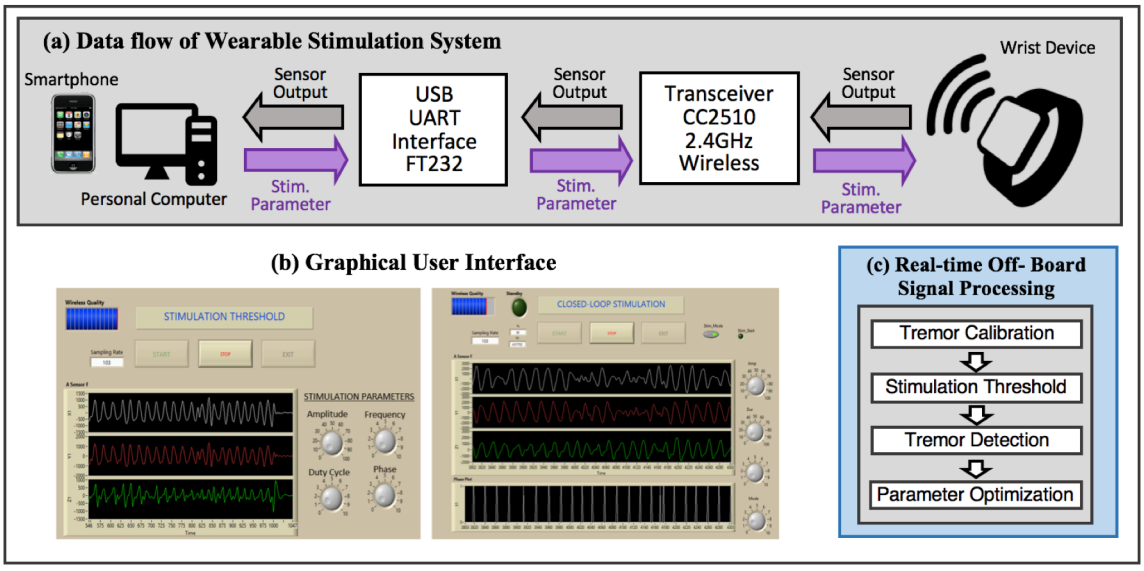

Figure 3.3 (a) Overall data flow of the wearable stimulation system from a PC or a smartphone to the wrist device, (b) the graphical user interface (GUI) for the experimental setup (i.e., tremor calibration, stimulation threshold setting, and closed-loop stimulation session), and (a) real-time off-board signal processing for the tremor detection and parameter optimization algorithm.

The peripheral-nerve stimulation is generated by a voltage-mode stimulator, which was selected (over the current mode) to prevent skin burns on the subjects if the resistance between the surface electrode and the skin abnormally increases because of a loss of adhesion (Forst et al. 2015). We use a boost converter (LM27313, Texas Instruments) to step up the voltage level of the supply (3.7 V battery) to as high as 20 V. We alternatively turn on the pair of electronic switches ($\emptyset_1$ and $\overline{\emptyset_1}$ in Figure 3.2 (c)) for biphasic stimuli (up to ± 20 V), the amplitude of which varies according to the output voltage of the boost converter. The reference voltage is controlled by a voltage divider circuit consisting of a variable resistor (AD5162, Analog Device), which is controlled by the MCU via a serial peripheral interface (SPI). We are also able to vary the duration of each stimulus (set at

200 μs for this study), the duration between the stimuli (frequency), the number of stimuli (duty cycle), and the onset of the stimulus (phase).

The motion-sensor data are wirelessly transmitted to a computer that uses off-board signal processing (Figure 3.3 (c)) to detect *active tremor*, defined as >60% of the maximum amplitude and ±30% range of the dominant frequency of baseline tremor. At the onset of the tremor, the computer sends the signal for stimulus onset to the wrist device via the wireless transceiver. The stimulation voltage generated by the wrist device is conveyed to the peripheral nerve via a pair of surface electrodes (0.8" round transcutaneous electrical nerve stimulation unit electrodes, Syrtenty).

The GUI is implemented on the computer using LabVIEW 2016 (National Instruments). The interface has two experimental modes, (1) a calibration mode, in which tremor is measured in the absence of stimulation, and (2) an experimental mode, in which phase-locked stimulation is used to modulate tremor. The GUI also controls the stimulation parameters, including amplitude, duty cycle, frequency, and phase. In the current study, the parameters are controlled manually. In future studies, we will use a real-time optimization algorithm that automatically sets the parameters. Detailed specifications of the wearable peripheral-nerve electrical stimulation system are summarized in Table 3.1.

3.2.2 Experimental Configuration

For the experiments performed in this study, one stimulation electrode was placed on the radial nerve near the wrist and the other electrode on the skin of the upper limb, about 2 cm apart from the stimulation electrode (see Figures 3.2 (a) and 3.4 (b)). The stimulation parameters were set as follows: amplitude = 1T (sensory thresholds), frequency = 100 Hz, duration = 200 μs, duty cycle = 12.5%, and phase = 0 (Figure 3.4 (a)).

Table 3.1 Wearable peripheral-nerve electrical stimulation system specifications.

Specification	Value
Control Unit (Wrist Device)	
Microcontroller	CC2510 2.4-GHz RF
Control Unit Dimensions	28 x 18 mm^2
Power Source	3.7 V 300 mAh Li-ion battery
Board Weight (with Battery)	5 grams (11 gram)
Total System with Enclosure	36 grams
Sampling Rate	100 Hz
Operating Hours	~ 20 Hours
Accelerometer Sensor Module	
Accelerometer	LSM303D
Sensitivity	0.061 mg/LSB (± 2g)
Stimulator	
Stimulation Voltage Range	± 20 V
Channel	1
Adjustable Parameters	Amplitude, frequency, duty cycle, phase
Electrode	
Size	0.8" Round
Material	Silver Tan Tricot Electrodes

We analyzed tremor movement using three output metrics: (1) the dominant frequency of the tremor, (2) power of the tremor between 4 and 12 Hz, and (3) the frequency deviation for the overall tremor movement. Dominant frequency (Elble et al. 1996; Miralles et al. 2006) and power (Dai et al. 2015) have been used previously by several researchers; frequency deviation was a novel to this study.

In order to calculate the metrics, we high-pass filtered the RMS value of the three-axis accelerometer data (Mostile et al. 2010), defined in Eq. (1), with a cutoff frequency of 3 Hz and applied a spectral analysis using fast-Fourier transform (FFT) for a frequency analysis (sampling frequency (Fs) =100 Hz, sampling period =2.5 s, and length of signal = 250 samples).

$$\text{RMS} = \sqrt{\frac{1}{3}(A_x{}^2 + A_y{}^2 + A_z{}^2)} \qquad (1)$$

We defined the dominant tremor frequency as the peak frequency of the power spectral density (PSD) (Figure 3.5). We defined the tremor power as the integral of the

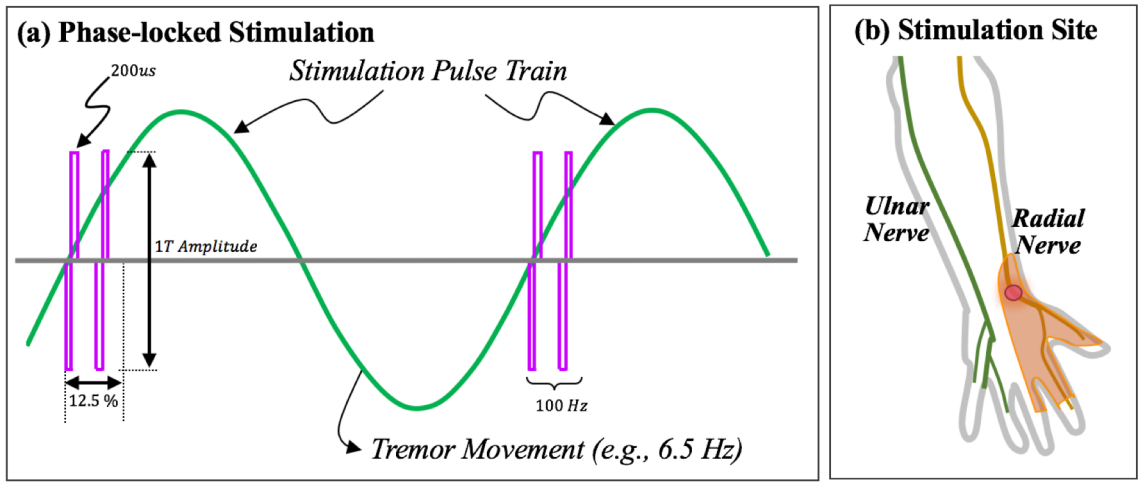

(e) The Essential Tremor Rating Assessment Scale (TETRAS) for upper limb

Definition of TETRAS Score					
Score	0	1	2	3	4
Upper Limb	No Tremor	Barely visible < 1cm	1 to < 5cm	5 to < 20 cm	> 20 cm

Figure 3.4 Electrical stimulation with parameters for tremor modulation on the peripheral nerve. (a) Example phase-locked stimulation with a T amplitude (sensory threshold), a 100 Hz frequency, and a 12.5% duty cycle with a 200 μs bi-phasic stimulus. (b) The site of the stimulation (radial nerve) and the desired location of sensation by the stimulation. (c) The data segment of the control and stimulation trials. (d) Example phase-locked stimulations based on the high-pass filtered (HPF), root-mean squared (RMS) 3-axis accelerometer for tremor movements. (e) Modified definition of the TETRAS score for this study.

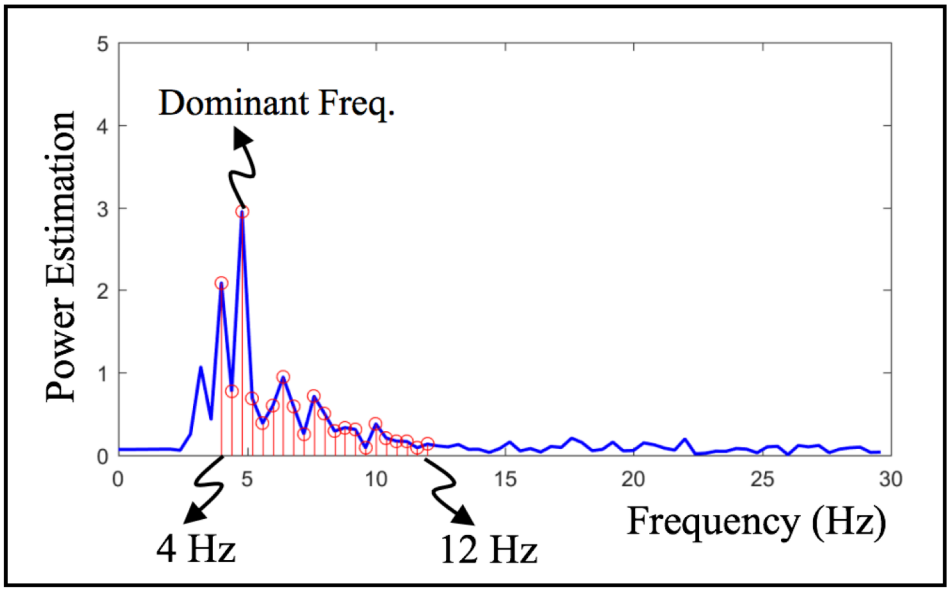

Figure 3.5 Dominant tremor frequency and tremor power in a power spectral density (PSD) of tremor movement in the frequency domain.

PSD output between 4 and 12 Hz (Figure 3.5) (Eq. (2)) (Dai et al. 2015); the * denotes the complex conjugate, N represents the sample points, and g^2/Hz (g equals 9.8 m/s^2) is the unit of tremor power.

$$\text{Power} = \int_{f_a}^{f_b} \frac{FFT^*(tremor) \times FFT(tremor)}{N^2} df; \quad f_a = 4\text{Hz}, f_b = 12\text{Hz} \quad (2)$$

We defined frequency deviation as the interquartile range (IRQ) of all tremor frequencies. Even though the average dominant frequency remained relatively constant across sessions, there was clearly cycle-to-cycle variability across each session. Thus, we calculated the timing of every tremor cycle (frequency), and the IQR of all tremor frequencies as the frequency deviation. The IQR was the difference between the 75th (3rd quartile) and 25th (1st quartile) percentiles of all components of the tremor frequencies.

Figure 3.6 Experimental setups for the baseline trial and stimulation trial during the bean-transfer task using the wrist device with ET participants.

3.3 Performance Evaluation

To evaluate the effect of nerve stimulation using the wrist device, we collected data without and with stimulation while the subjects performed a prescribed task (Figure 3.6) and analyzed the tremor movement using three output metrics: dominant frequency, tremor power, and frequency deviation. We also evaluated the system with the responses of the self-evaluation questionnaire.

3.3.1 Human Subjects

To evaluate the effect of the wearable tremor modulation system, we conducted experiments with the nine ET participants, one of whom participated in two sessions on different days). Detailed information about these participants is summarized in Table 3.2. After the study was approved by the Institutional Review Board (IRB) of the Georgia Institute of Technology, each participant signed a written informed consent prior to the experiment. We collected tremor movement data with and without peripheral-nerve electrical stimulation from our wearable tremor modulation device worn by nine ET participants between the ages of 47 and 82 (five females and four males whose median age was 70) with kinetic tremor in at least one arm. To determine the dominant hand for the movement experiment, we asked the subjects to answer the Edinburgh Handedness Inventory (EHI) questions (Oldfield 1971). The questions are summarized in Table 3.3 and the scores in 3.2.

From a subjective evaluation of the participants, we determined the presence of tremor. Based on their experience, they reported the dominant side on which they experienced tremor movement, summarized in Table 3.2. We also evaluated the tremor scores from The Essential Tremor Rating Assessment Scale (TETRAS). Figure 3.4 (e)

Table 3.2 Participant Demographics.

Participant	Age, years	Sex	Year Since diagnosis	Dominant Hand	Edinburgh Handedness Inventory Score	Tremor Presence (Dominant Side)	TETRAS Score (L /R)	Voltage of 1T of Electrical Stimulation (± V)	Wrist Device Placement
ET 01	70	M	50	R	4.00 ± 0.00	Both	2 / **3**	15.39	R
ET 02	76	F	8	R	4.45 ± 0.52	R	0 / **3**	9.80	R
ET 03	75	M	30	R	4.82 ± 0.40	Both (L)	4 / **4**	17.33	R*
ET 03**							3 / **2**	11.74	
ET 04	58	F	10	R	5.00 ± 0.00	R	0 / **4**	5.67	R
ET 05	64	M	15	L	1.00 ± 0.00	Both (L)	**4** / 1	12.96	L
ET 06	58	F	10	R	5.00 ± 0.00	Both (R)	1 / **1**	4.30	R
ET 07	82	F	10	L	2.18 ± 0.60	Both (L)	**2** / 1	15.63	L
ET 08	79	M	10	R	5.00 ± 0.00	Both (L)	4 / **3**	14.17	R*
ET 09	47	F	4	R	5.00 ± 0.00	Both (L)	2 / **2**	3.57	R*

M: Male, F: Female, R: Right, L: Left, Freq.: Frequency, Amp.: Amplitude;
* indicates that the dominant hand side is not the same as tremor dominant side; ** represents the second session.

Table 3.3 Edinburgh Handedness Inventory.

Which hand do you prefer to use for each activity?	
Q1. Writing	**Q7.** Spoon
Q2. Drawing	**Q8.** Broom (upper hand)
Q3. Throwing	**Q9.** Striking Match (match)
Q4. Scissors	**Q10.** Opening box (holding the lid)
Q5. Toothbrush	**Q11.** Holding a Computer Mouse
Q6. Knife (without fork)	
Always Left - Usually Left - No Preference - Usually Right - Always Right	
1 2 3 4 5	

shows how we defined and followed the TETRAS for this study (Elble et al. 2006 and 2008). While the participants performed the prescribed task (explained in *Section 3.3.2*), the research team measured tremor movement using a motion sensor and used the TETRAS upper limb score to rate the kinetic tremor of the participants.

Results of the evaluation showed that seven participants had tremor on both sides. Even though they had tremor on both sides, five of the subjects had left-side dominant tremor. Two participants had tremor only on the right side. Each participant wore the wrist device on the dominant hand: seven on their right and two on their left. Although three of the right-handed subjects had left-side dominant tremor, they also experienced tremor on the right side.

3.3.2 Experimental Design and Procedure

Once the participants signed the consent form, they were asked to a questionnaire regarding their tremor history, the presence of their tremor, and their dominant hand using EHI questions. The information from the questionnaire is summarized in Table 3.2.

To evaluate the effect of stimulation on tremor movement, the subjects performed

the *bean-transfer task*, transferring a small object (a medium-sized lima bean) from one plate to another using a spoon. Before this experiment trial, we first performed a control trial, collecting data for ten seconds in the absence of stimulation (Figure 3.4 (c)). We analyzed the characteristics of the control movement using three output metrics—dominant frequency, tremor power, and frequency deviation (IQR)—as shown in Table 3.4 and Figures 3.8 (a)-(f).

In order to determine the stimulus amplitude, we placed a pair of electrodes on a branch of the radial nerve on the wrist (Figures 3.2 (a) and 3.4 (b)), and gradually increased the amplitude until the participant could sense the stimulation. We adjusted the placement of the electrodes so that the subjects sensed the stimulus in the desired location (see Figure 3.4 (b), highlighted). We defined this sensation threshold as T, and we measured T for each participant. The thresholds ranged from 3.57 V to 17.33 V (mean: 11.06 ± 5.00 V) with a pair of bi-phasic stimuli, as summarized in Table 3.3. This process took less than two minutes, during which period the stimulation was not activated intermittently. Subsequently, no stimulation was applied for five minutes to minimize any carry-over effects.

We next performed the stimulation trial, applying a ten-second stimulation during the active tremor, and phase locking the stimulation to the tremor cycle (Figure 3.4 (d)). We analyzed the ten-second stimulation period in four 2.5-second segments. Although we could not control the speed of all arm movements, most of the participants were able to transfer approximately four beans during the stimulus period.

After completing the stimulation trial, the participants responded to a five-point Likert-scale questionnaire consisting of eight questions about the system, the stimulation,

and their tremor condition. The eight questions of the questionnaire are summarized in Table 3.5, and the responses of the nine participants are summarized in Figure 3.10.

3.3.3 Statistical Analysis

To statistically analyze the effects of electrical stimulation on the tremor movements, we conducted one-way ANOVA tests ($\alpha = 0.05$) to determine the differences with and without stimulation for individual subjects and across all subjects. We also conducted a pairwise linear regression analysis to determine the correlation between each pair of output metrics: frequency, power, deviation, and TETRAS score.

3.4 Results

In order to assess the effects of stimulation on tremor movements, we analyzed the movements for all participants using the three output metrics, both without stimulation and with stimulation. We also included the TETRAS scores in our analyses. Figures 3.7 (a)-(f) illustrate an example data set for a single participant (ET04) from TETRAS=4 group. The analyses show that the stimulation reduces the tremor for this participant.

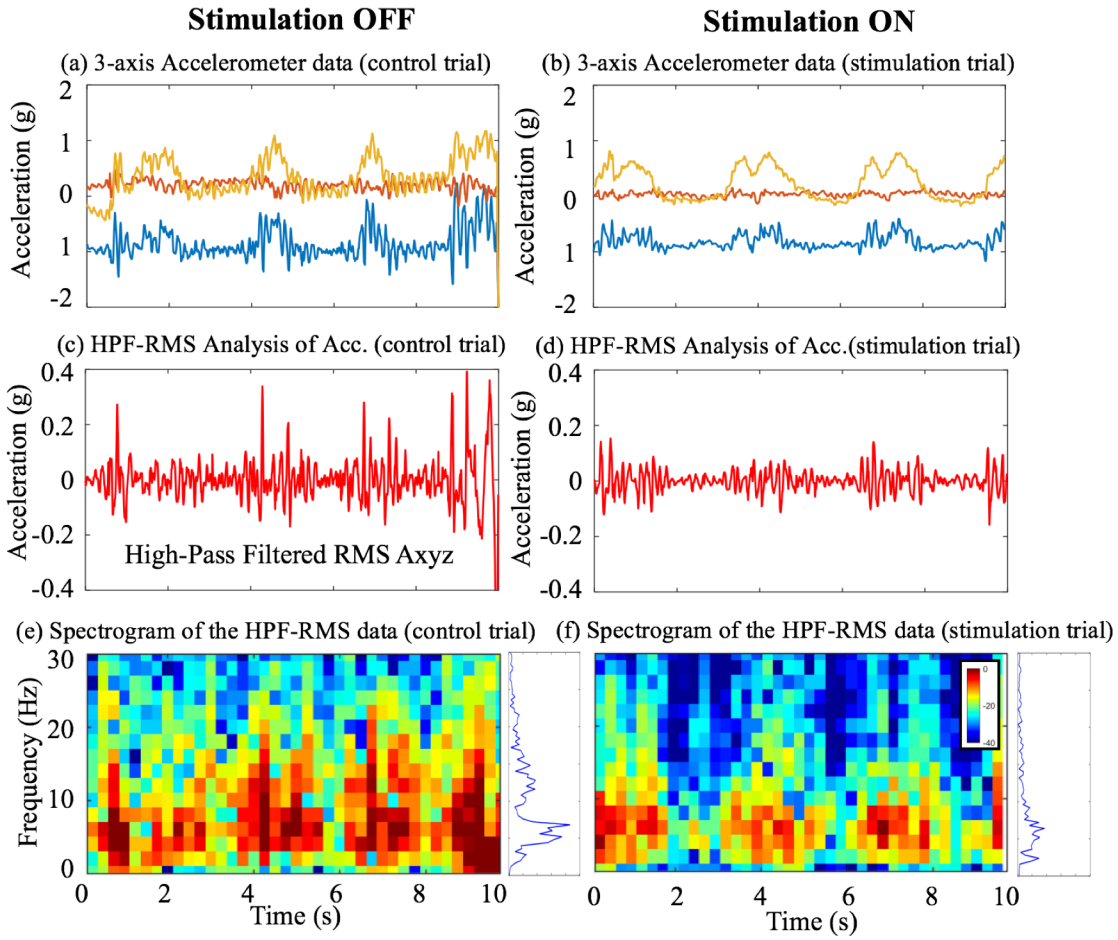

Figure 3.7 Tremor movements during a control trial (stimulation OFF) and a stimulation trial (stimulation ON) for participant ET04. Raw three-axis accelerometer data with tremor movements during the bean-transfer task for (a) the control trial and (b) the stimulation trial. A HPF RMS analysis of the three-axis data for (c) the control trial and (d) the stimulation trial. A spectrogram of the HPF RMS data (window: ½ sampling frequency (Fs), overlap: Fs) and the averaged power density for (e) the control trial and (f) the

3.4.1 Movements During the Control Trials

Table 3.4 shows the output metrics for all of the subjects during the control trials for the bean-transfer task. The dominant frequencies of the baseline tremor movements were between 4.80 and 6.80 Hz (mean: 5.71 ± 0.79Hz). The tremor power was between 4.47 and 23.46 g^2/Hz (mean: 10.27 ± 5.51 g^2/Hz), and the IQR of tremor frequencies were

Table 3.4 Summary of tremor output metrics during the control trial.

PT #	Tremor Frequency (Hz)	Tremor Power (g^2/Hz)	IQR of Frequency (Hz)
ET01	6.00 ± 0.33	8.44 ± 0.93	2.58 ± 0.54
ET02	5.60 ± 0.01	9.10 ± 3.23	3.91 ± 1.28
ET03	4.80 ± 0.33	13.65 ± 2.34	3.24 ± 1.26
ET04	5.90 ± 0.50	12.80 ± 1.34	1.82 ± 0.45
ET05	4.93 ± 0.23	23.46 ± 1.73	2.78 ± 0.47
ET06	6.80 ± 1.31	4.97 ± 1.20	2.61 ± 0.76
ET07	5.10 ± 0.38	4.47 ± 1.12	2.93 ± 0.46
ET08	6.50 ± 0.38	10.61 ± 1.71	2.47 ± 1.21
ET09	6.70 ± 0.95	7.75 ± 1.98	4.73 ± 1.09
ET03**	4.80 ± 0.65	7.43 ± 1.74	3.11 ± 0.67

** represents the second session.

between 1.82 and 4.73 Hz (mean: 3.02 ± 0.81 Hz). Figures 3.8 (a), (c), and (e) show the correlation between each tremor output metric and TETRAS score (Mostile et al. 2010). Although TETRAS is a subjective method, it is the clinical standard, and we consistently followed the guidelines from the literature (Elble et al. 2006 and 2008). We found a high correlation (using a linear regression analysis) between tremor power and TETRAS scores in ten experimental sessions (Figure 3.8 (c)) (R^2=0.603). The dominant frequency and the IQR of the tremor frequencies were independent of TETRAS score (Figure 3.8 (a); R^2 = 0.110 and Figure 3.8 (c); R^2 = 0.003, respectively). Figures 3.8 (b), (d), and (f) show the correlations between each pair of tremor output metrics. All three pairs—tremor frequency vs. power (R^2 = 0.151) (Figure 3.8 (b)), IQR vs. frequency (R^2 = 0.265) (Figure 3.8 (d)), and IQR vs. power (R^2 = 0.016) (Figure 3.8 (f))—were uncorrelated.

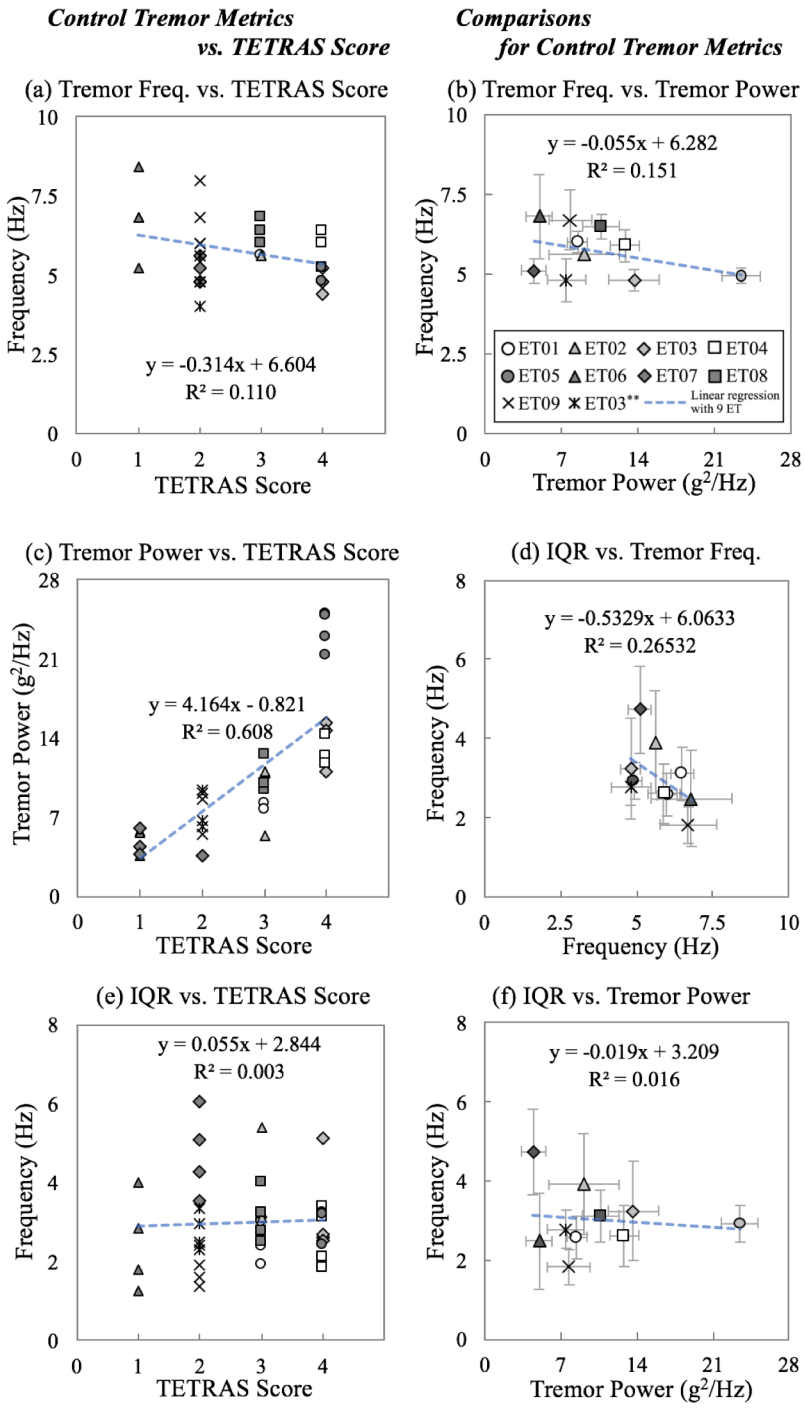

Figure 3.8 Summary of the tremor movements (control trials) that were quantitatively analyzed with three tremor metrics: dominant tremor frequency, tremor power, and frequency deviation (IQR). These metrics and TETRAS scores were compared: (a) the dominant frequency and TETRAS, (c) tremor power and TETRAS, and (e) IQR and TETRAS. The tremor metrics were also correlated: (b) tremor frequency and tremor power, (d) IQR and tremor frequency, and (f) IQR and tremor power.

3.4.2 Effects of Stimulation on Tremor

To evaluate the effect of the nerve stimulation, we compared changes in tremor movements without and with stimulation during the bean-transfer task, and the results are plotted in Figures 3.9 (a), (c), (e). With regard to the dominant frequency, all of the subjects remained in same range or decrease with the stimulation. The analysis of the dominant frequency showed that four significantly decrease, four others slightly decrease, but the decrease was statistically insignificant, and two showed no measureable changes (Figure 3.9 (a)). Tremor power for all subjects decreased with stimulation. In six of the ten sessions, the analysis of tremor power showed a statistically significant reduction in tremor power, but the other four showed a slight, insignificant decrease (Figure 3.9 (c)). Given that TETRAS score was highly correlated to the tremor power, we expected that the power decreases from the stimulation were clinically relevant effects that reduce the tremor. Finally, the frequency deviation (IQR) in all subjects stayed in the same range or increased by stimulation. The analysis of IQR showed that two exhibited a significant increase, three an insignificant increase, four no measureable changes, and one a decrease (Figure 3.9 (e)).

In order to assess the relative changes of the tremor output metrics, we defined each normalized metric as a ratio of the output metric of the control trial to that of the stimulation trial ($\frac{stimulation\ trial\ metric}{control\ trial\ metric}$) for each participant. We then plotted these normalize metrics against the raw metrics (Figures. 3.9 (b), (d), (f)). The frequency data showed no statistically significant relationship between the normalized and raw frequencies across all of the subjects (the blue line in Figure 3.9 (b)) (R^2=0.001).

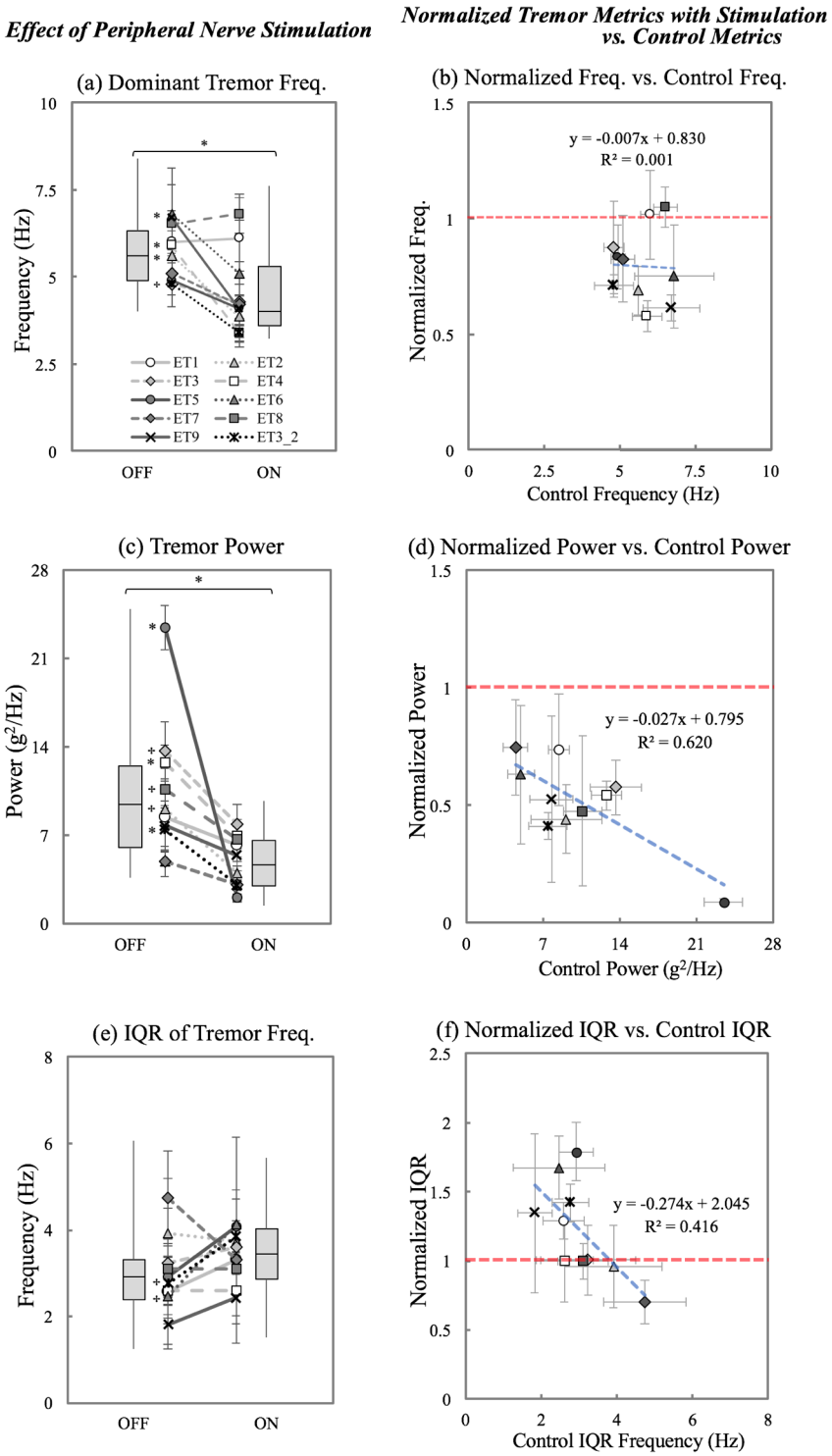

Figure 3.9 Effects of peripheral nerve stimulation. Overall tremor movement changes without and with stimulation for three tremor metrics: (a) dominant frequency, (c) tremor power, and (e) frequency deviation (IQR). The normalized metrics were compared with each control trial metric: (b) normalized frequency and control frequency, (d) normalized power and tremor power, and (f) normalized IQR and control IQR. The error bar represents the standard deviation; ⁎: $P < 0.005$, ÷: $P < 0.05$.

The power data demonstrate a significant decrease in normalized tremor power as a function of raw tremor power via linear regression (Figure 3.9 (d)) (mean: 0.52 ± 0.26). In other words, the participants exhibiting higher tremor power in the control trial experienced a higher relative reduction (lower normalized tremor power) with stimulation. The IQR data demonstrated a significant decrease in normalized IQR as a function of raw IQR via linear regression (Figure 3.9 (f)) (R^2=0.416). Except for one outlier participant who showed an opposite trend in IQR (reduced frequency deviation), most frequency deviation fell within a similar range and increased with stimulation, and the participants who showed lower IQR exhibited a higher increase in IQR.

3.4.3 Self-evaluation

After the experiment, the participants responded to a self-evaluation questionnaire, based on a five-point Likert scale, consisting of eight questions (Table 3.5). They answered

Table 3.5 Questionnaire of the self-evaluation of the wearable tremor modulation system.

Questionnaire after the experiment:	
Q1.	Comfort of the wearable tremor modulation system: 1-Very uncomfortable, 3-Normal, 5-Very comfortable
Q2.	Fatigue during the experiment: 1-Very tired, 3- Normal, 5- Not at all tired
Q3.	The tremor condition compared to the normal condition: 1-More severe, 3- the same as the normal condition., 5- Less severe
Q4.	Comfort of electrical stimulation: 1-Very uncomfortable, 3-Normal, 5-Very comfortable
Q5.	Pain from electrical stimulation: 1-Very painful, 3-Normal, 5-Not painful at all
Q6.	Tingling from electrical stimulation: 1-A large amount of tingling, 3-Normal, 5-No tingling at all
Q7.	Strength of electrical stimulation: 1-Very strong, 3-Normal, 5-Not strong at all
Q8.	Willingness to use this system for potential treatment: 1-Very negative, 3-Normal, 5-Very positive

questions, which asked them about the comfort of the system, fatigue from the experiment, the feeling of electrical stimulation, and the qualitative effects of stimulation. The averaged values of the responses of the nine subjects (one of whom participated in two sessions; total n=10) for all questions are summarized in Fig. 3.10. The responses indicated that the system and stimulation were comfortable (Q1: 4.50 ± 0.85 and Q4: 4.30 ± 0.82, respectively). They also indicated experiencing no feeling of pain from stimulation (Q5: 4.90 ± 0.32) but feeling normal tingling and strength (Q6: 3.00 ± 0.67, and Q7: 3.50 ± 1.18, respectively). Except for the response of one participant who experienced minor fatigue (2), the participants experienced normal fatigue or no fatigue (3 or higher; Q2: 3.60 ± 1.07). Six of the ten responded that their tremor was less severe during the stimulation trials than in their normal condition (Q3: 3.70 ± 0.67), and six of them were positive or very positive about potential use of the wearable tremor modulation system for treatment of their tremor (Q8: 3.80 ± 0.79).

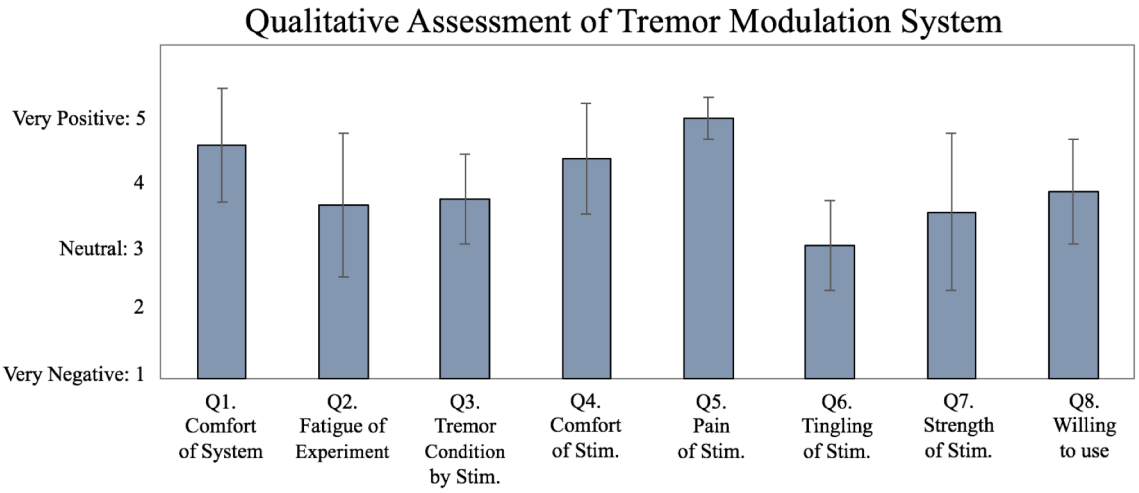

Figure 3.10 Summarized results of the self-evaluation of nine ET participants after the experimental trials. The error bar represents the standard deviation.

3.5 Discussion and Conclusion

The purpose of this study was to present a wearable on-wrist tremor modulation system that provides constant-voltage peripheral-nerve stimulation, and to quantitatively assess the effects of this stimulation on essential tremor (ET). The study included subjects who had been diagnosed with ET for at least four years or longer. The participants were diagnosed by their own neurologists. Even though their first diagnosis were completed by different neurologists, nine of the eleven participants were recruited from a Savannah support group, which was overseen by a single neurologist. All participants experienced tremor during movements of their upper limbs, with a range of amplitudes that varied dependent upon the task being performed. We administered a specific task, the bean-transfer task, that mimicked utensil movements during eating (one of the most common and important daily activities). Although this study focused on only one task, we plan to include other tasks in our future studies.

In this study, we did not control the medications of the subjects. Five of the nine took a typical medication, such as primidone, propranolol, zonisamide, trihexyphenidyl, or topiramate, to treat their tremor symptoms. All of the participants reported that they experienced tremor while taking medication, although their non-medicated tremor movements were typically more severe. In order to best control for changes due to medication, we ran both the control session and the stimulation session for each participant sequentially during a period shorter than the expected pharmacological time constants.

The study carefully followed the definition of TETRAS scores in Figure 3.6 (e), which was based on guidelines from Elble's research team (Elble et al. 2006 and 2008), and to maintain consistency, only one researcher conducted the scoring for all participants.

However, the researcher was not a medically trained individual, which may have affected the accuracy of the scoring. Moreover, the researcher who completed the scoring also knew the patients' medical history and tremor symptom; thus, the scoring might be affected by the prior information.

To evaluate the effects of peripheral-nerve stimulation, we collected data for tremor movement without and with the stimulation and analyzed the movement changes using three quantitative tremor parameters: the dominant tremor frequency, tremor power, and the frequency deviation (IQR). We provided phase-locked stimulation at 0π with a $200\mu s$ bi-phatic stimulus, a 100Hz frequency, a 12.5% duty cycle, and a *T* amplitude (sensation threshold). The results from the experiment involving nine ET participants showed that this system significantly reduced tremor frequency (mean normalized frequency: 0.79 ± 0.20) and tremor power (mean normalized power: 0.52 ± 0.26) during the bean-transfer task. In addition, ET patients who experienced higher tremor power showed a greater reduction in normalized tremor power reduction. These results demonstrate the potential of peripheral-nerve stimulation as a potential treatment to reduce tremor in ET patients.

In future studies, we aim to determine the optimal range of stimulation parameters for individual participants in real time and provide stimulation when it is needed (e.g., above a certain level of tremor amplitude) to minimize nerve fatigue by electrical stimulation and power consumption. We intend to determine the effects of various combinations of stimulation parameters and develop an open-loop response model for the stimulation parameters. We will also pursue real-time parameter optimization to maximize the effects of stimulation and to adapt to physiological changes.

CHAPTER 4

ANALYZING THE EFFECTS OF STIMULATION PARAMETERS FOR TREMOR MODULATION VIA PERIPHERAL-NERVE ELECTRICAL STIMULATION

4.1 Introduction

Essential tremor (ET) is a common, chronic, and progressive neurological disorder that causes rhythmic shaking between 4 – 12 Hz frequencies (Bain 2007; Bhidayasiri 2005; IEFT, 12-Month Annual Report 2006). Unlike the tremor that occurs in individuals with Parkinsonism (i.e., resting tremor), ET, also referred to as *action tremor* (Hess and Pullman 2012; IETF, 12-Month Annual Report, 2006), is associated with both postural and kinetic tremor that accompanies specific postures and tasks, respectively. ET affects about ten million people in the United States (IEFT, 12-Month Annual Report 2006). Although tremor movements can be observed in all parts of the body such as the hands, the head, the voice, the legs, and the trunk, 90% of ET patients experience upper limb tremor (Hess and Pullman 2012; IEFT, 12-Month Annual Report 2006). The symptoms of ET can occur at any age, but they most commonly appear in people in their 40s and older. Nine percent of people over the age of 60 experience tremor (Elble et al. 2008; Tintner 2004).

Possible sources of tremor generation can be categorized into mechanical resonances, reflex oscillations (i.e., stretch reflex or feedback resonance), and central oscillations (McAuley et al. 1997; Hess and Pullman 2012; Stein and Lee 1981). Mechanical resonance, which prompts the onset of tremor, can originate in the bones, the muscles, and other tissue. Such tremor is related to physical properties such as the stiffness of the

structure and the moment of inertia oscillations (McAuley et al. 1997; Joyce and Rank 1974; Stiles and Randall 1967; Walsh 1992), and an unstable feedback loop of the stretch reflex can cause oscillatory movement (Marsden 1978). The rhythmical and oscillatory noise within the stretch reflex loops (i.e., short- or long-latency reflex arcs from afferent receptors) connected to the spinal cord generate tremor in a range of about ±10 Hz. In an effort to determine the origin of tremor and the relationship between tremor frequency and brain activity, Hellwig's research team showed the significant corticomuscular coherences at the tremor frequency in ET using simultaneous electroencephalography (EEG) and electromyography (EMG) recordings (Hellwig et al. 2001); however, Halliday's research team showed a significant low-frequency component at the frequency of the tremor bursts and they insisted that there was no coherence between magnetoencephalogram (MEG) and EMG recordings at the tremor frequency (Halliday at el. 2000).

However, these studies do not agree that cortical activity is involved in the generation of essential tremor. While some have found evidence that the sensorimotor cortex is involved in the generation of essential tremor (Hellwig et al. 2001), others have hypothesized that cortical activity has no correlation with tremor movement in the range of around 10 Hz (Raethjen et al. 2007; Raethjen and Deuschl 2012).

Despite the absence of consensus on the origin of tremor and the physiological pathway of tremor generation (Deuschl et al. 2001; Hellwig et al. 2001; Halliday at el. 2000), we hypothesize that proper electrical stimulation of the peripheral nervous system affects the pathway in tremor generation. Therefore, for patients with treatment-resistant tremor, we have developed a wearable tremor modulation system that provides peripheral-nerve electrical stimulation that modulates tremor movement. By significantly reducing the

frequency and the power of tremor in ET participants while they experience kinetic tremor (Chapter 3), we have shown the efficacy of both the phase-locked stimulation of the peripheral nerve and stimulation of the radial nerve in the suppression of tremor. Moreover, the ultimate goal of this wearable tremor modulation system is to use a custom-designed, real-time closed-loop system that optimizes the parameters of the electrical stimulation of peripheral nerves and to maximize the efficacy of tremor suppression. Therefore, in this study, we examine an open-loop response for tremor modulation with a different range of stimulation parameters (i.e., amplitude, frequency, duty cycle, phase, stimulation sites) using various combinations of stimulation. We expect that the findings from this study will suggest a proper range of stimulation parameters and the development of an optimization algorithm in real time.

4.2 Wearable Tremor Modulation System

We developed a wearable tremor monitor and modulation system that includes custom-designed hardware and software (see Figure 4.1). We also implemented our tremor detection algorithm so that it provides electrical stimulation when it is synchronized with the tremor cycle (phase-locked stimulation) of the subjects.

4.2.1 Tremor Modulation Hardware and Software

The wearable wireless real-time closed-loop stimulation system collects/analyzes tremor movement and provides voltage-mode stimulation on peripheral nerves that modulate/attenuate tremor movement. The overall system consists of a wrist device, a 2.4-GHz radio-frequency wireless transceiver, a pair of surface electrodes (0.8” round TENS Unit Electrodes, Syrtenty), and a graphical user interface (GUI) implemented on LabVIEW

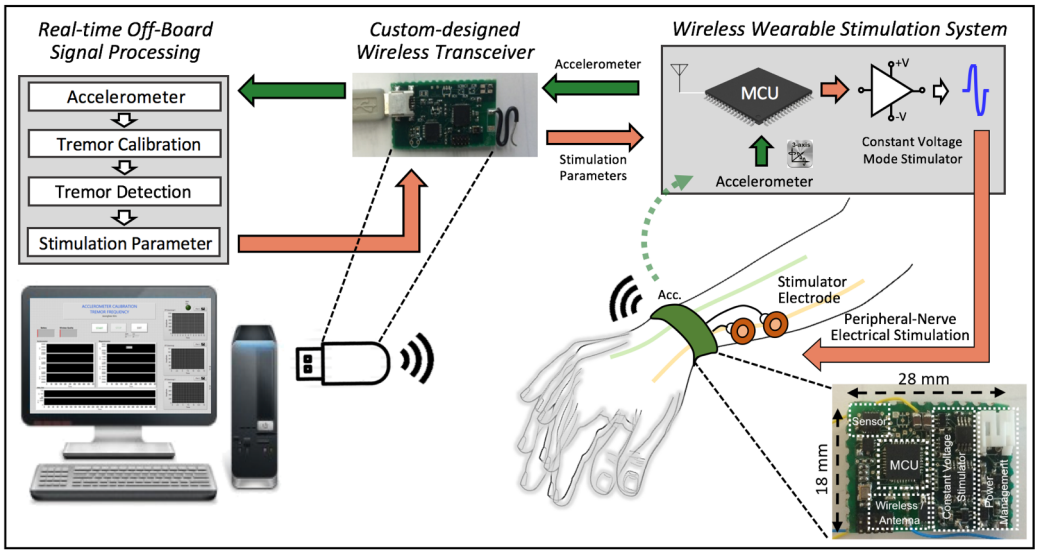

Figure 4.1 Overview of the real-time non-invasive tremor modulation system for essential tremor.

2016 with the tremor detection algorithm. The wrist device consists of a motion sensor interface and custom-designed voltage mode stimulation circuitry controlled by a microcontroller (CC2510, Texas Instruments) with a built-in 2.4-GHz RF transceiver powered by a rechargeable 3.7V lithium-ion (Li-Ion) battery (300 mAh).

The electronics of the wrist device set on an 18 x 28 mm^2 custom-designed printed circuit board (PCB) enclosed by a commercially available wrist band. The weight of the wrist device, including the battery and enclosure, is about 36 grams. The sampling rate of the motion sensor is 100 Hz, and the device can run up to 20 hours with minimal stimulation. The battery of the wrist device is charged with a 5 V mini-USB with a custom-designed circuit, which takes about three hours to charge. A detailed description of the hardware and software of the system appears in *Section 3.2.1.*

Every 10ms, the wrist device conveys motion sensor data to a computer/smartphone that runs the tremor detection algorithm and receives updated

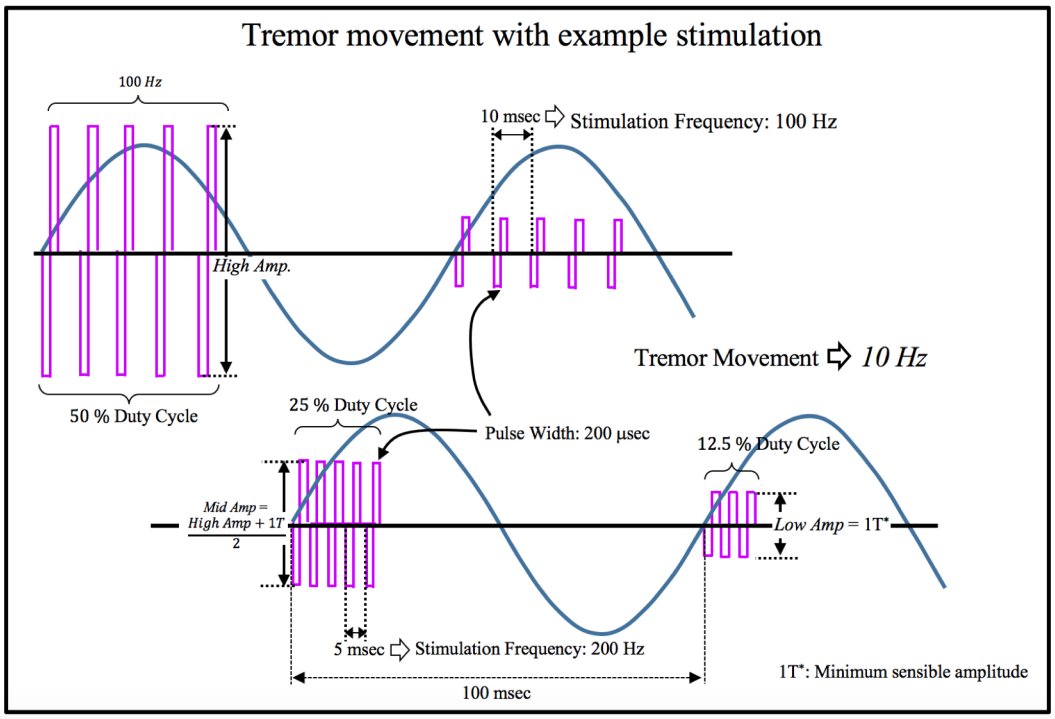

Figure 4.2 Example electrical stimulation with tremor movement for various combinations of stimulation parameters.

stimulation parameter information that includes the stimulation amplitude, the pulse width, the frequency, the duty cycle, the phase, and the stimulation onset. We select stimulation parameters using either a manual mode or an automatic tremor detection mode. In the manual mode, we can adjust the amplitude of the bi-phasic stimulus up to ± 20V to set the threshold of the amplitudes for each subject and select the rest of the parameter settings on the GUI. A detailed explanation of the stimulation parameters can be found in *Section 4.3.3* (Figures 4.2-4.4), and the ranges of the parameters are summarized in Table 4.1.

4.2.2 Stimulation Detection Algorithm

We initiated the stimulation detection algorithm by measuring the subjects' baseline tremor movement, or *tremor calibration*, with the dominant tremor frequency and

Table 4.1 Stimulation parameters and their ranges.

Stimulation Parameters	Range
Amplitude	Low = *1T*, Medium = $\frac{1+Max}{2}T$, High = *Max T*
Pulse Width	200μs
Frequency	50Hz, 100Hz, 200Hz
Duty Cycle	~5%, 12.5%, 25%, 37.5%, 50%
Phase	Phase-locked to the tremor cycle at 0 π, ½ π, 1 π, 1½ π; and Continuous Random Phase Stimulation of the tremor cycle
Stimulation Sites	Radial, Ulnar, Median Nerves

the peak tremor amplitude. When we provided constant random stimulation, the stimulator in the wrist device generated a combination of stimulation parameters at a constant frequency measured at a tremor calibration for each subject, regardless of his or her current tremor status. Since the tremor frequency varied according to their movements, the stimulation phase was not constant during the trial. For phase-locked stimulation (phase 1-4), we provided stimulation when the tremor was in the *active tremor range* with the selected phase. We defined the *active tremor range* as >60% of the maximum amplitude of the tremor and a ±30% range of the dominant frequency. Thus, when the tremor was within the active tremor range, we activated stimulation with the selected setting, including the selected phase.

4.3 Performance Evaluation

To evaluate the effect of stimulation parameters using the wrist device, we changed the range of the stimulation parameters: amplitude, frequency, duty cycle, phase, and

stimulation sites. We collected data with and without different combinations of stimulation parameters and analyzed tremor movement using the three output metrics: the dominant frequency, tremor power, and the frequency deviation.

4.3.1 Human Subjects

We recruited nine ET participants between the ages of 47 and 82 (five females and four males whose median age was 70) with kinetic tremor in at least one arm. We used our wearable tremor modulation system to collect tremor movement data with various combinations of stimulation parameter settings on peripheral electrical nerves. We asked the subjects to participate in several trials that took place on multiple days; the time gap between sessions was one to seven days. We provided electrical stimulation on only one nerve during one session on one day. To evaluate the effect of the stimulation parameters, we also collected the subjects' tremor movements without stimulation as their baseline tremor movement, which may have varied on the different days they were evaluated. To analyze the baseline tremor movement, we used the data from the wrist device and the subjective tremor measurement score from The Essential Tremor Rating Assessment Scale (TETRAS), which was evaluated by our research team.

We consistently followed the modified version of TETRAS definition while the participants performed a prescribed task (explained in *Section 4.3.4*), to measure the peak-to-peak distance of the tremor movements in Figure 3.4 (3), described as follows: TETRAS=0: no tremor; TETRAS=1: barely visible <1 cm; TETRAS=2: 1 to <5 cm; TETRAS=3: 5 to <20 cm; and TETRAS=4: >20 cm.

We obtained the required approval from the institutional review board (IRB) and written informed consent from each participating subject. We evaluated nine ET

Table 4.2 Number of sessions for each participant and each session for the three nerves.

Participants	Radial Nerve (RN)	Ulnar Nerve (UN)	Median Nerve (MN)
ET01	1 session	1 session	1 session
ET02	1 session	1 session	N/A
ET03	2 sessions	2 sessions	1 session
ET04	1 session	1 session	1 session
ET05	1 session	1 session	1 session
ET06	1 session	N/A	N/A
ET07	1 session	1 session	N/A
ET08	1 session	1 session	N/A
ET09	1 session	1 session	N/A
Sub Total	10 sessions	9 sessions	4 sessions
Total		23 sessions	

participants in 23 sessions: ten sessions on the radial nerve, nine on the ulnar nerve, and four on the median nerve. We only performed one session per a day to minimize the carry-over effect. We completed stimulation sessions for all three nerves on only four ET participants. A summary of the number of sessions for the three nerves appears in Table 4.2.

4.3.2 Tremor Output Metrics

We high-pass filtered (HPF) the root-mean squared three-axis accelerometer data from the wrist device with a cutoff frequency of 3 Hz and then analyzed the data to extract three tremor parameters: 1) the tremor frequency, 2) tremor power, and 3) the frequency deviation. We selected the tremor frequency as the peak frequency of the power spectral density (PSD) of the HPF RMS of the accelerometer data during the bean-transfer task. We

assigned an integral of the PSD between 4 and 12 Hz in the frequency domain as the tremor power (unit: g^2/Hz). The frequency deviation was the interquartile range of all tremor frequencies during the trial. The detailed analytical methods for the tremor output metrics appear in *Section 3.2.2.*

We defined the normalized tremor metrics as a ratio of the tremor output metrics of the control trial to those of the stimulation trial for each participant (tremor output metrics of $\frac{stimulation\ trial}{control\ trial}$). If the ratio was close to *1*, it equaled a control movement, and if smaller than *1*, it indicated a reduced effect of the metric by stimulation.

From one trial with a certain stimulation parameter setting, we collected tremor movement for ten seconds and analyzed these data in four 2.5-second segments. The averaged data from the four segments represented the tremor-output metric for the trial.

4.3.3 Stimulation Parameters and Combinations

From the preliminary data, we found that peripheral-nerve electrical stimulation decreased the frequency and the power (severity) of tremor with a constant stimulation setting. For this study, we attempted to expand the range of parameters with various combinations of stimulation to find an open-loop response model for a real-time optimization algorithm. We changed the combinations of stimulation parameters based on three stimulation amplitudes, three stimulation frequencies, five stimulation duty cycles, four stimulation phases, and random phase stimulation. To minimize the effects of bias, we selected combinations of stimulation parameters in random order, and to examine the effects of stimulation on three different nerves, we conducted the same experiment on various stimulation sites (Figure 4.3). An example of the parameters and the combinations

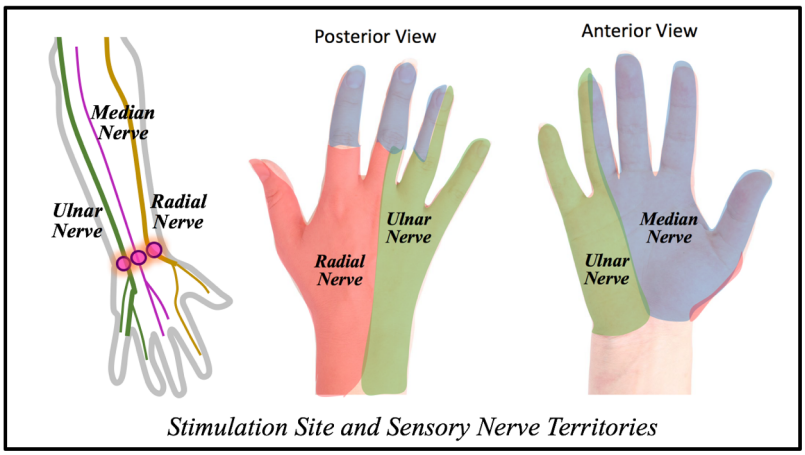

Figure 4.3 Stimulation sites: Radial, ulnar, and median nerves with their sensory nerve territories.

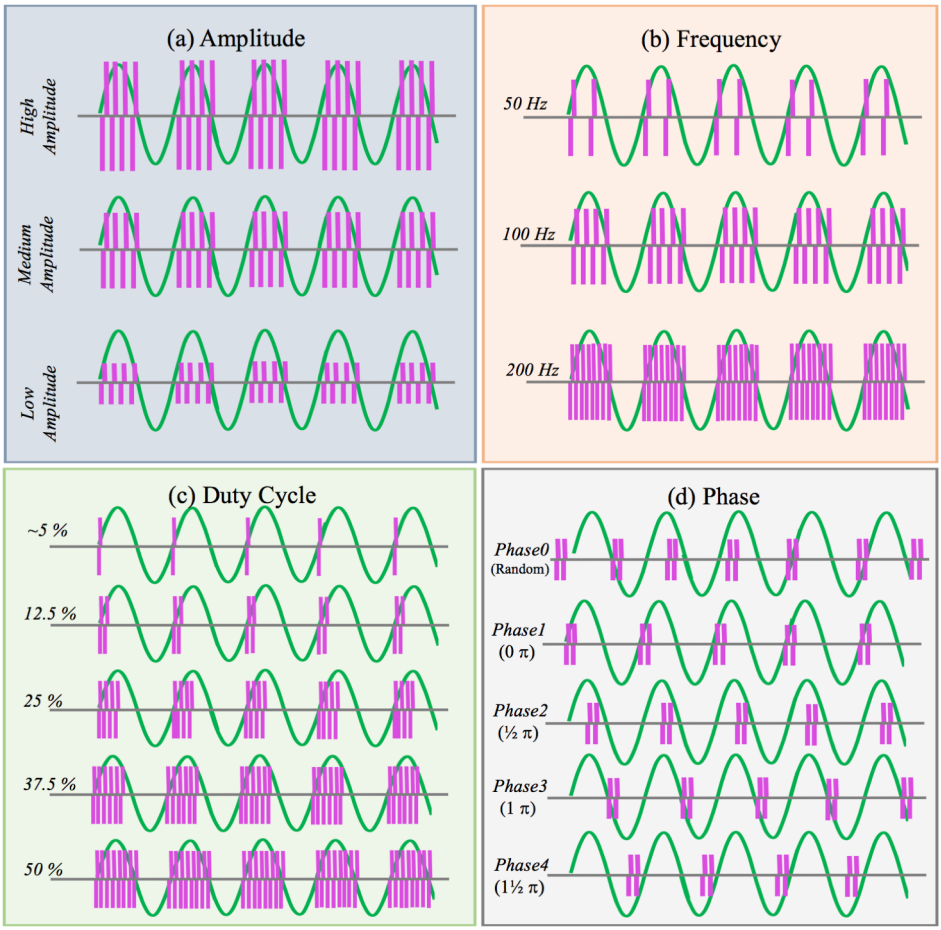

Figure 4.4 Stimulation parameters and their ranges: (a) amplitude, (b) frequency, (c) duty cycle, and (d) phase to the tremor cycle.

of stimulation are illustrated in Figures 4.2 and 4.4, and the stimulation parameters and their ranges are summarized in Table 4.1.

4.3.4 Experimental Procedure

The overall experimental procedure is plotted in Figure 4.5. We began by collecting the baseline tremor movement, *calibration*, to analyze the dominant frequency and the peak amplitude of the subjects' tremor without peripheral-nerve stimulation for ten seconds when they mimicked an eating task—the bean-transfer task. Although we could not strictly control the speed of their arm movements for the task, the participants were able to transfer four beans from one plate to another within ten seconds. Since ET participants mainly experience kinetic tremor, we asked them to perform a prescribed task—to transfer a small

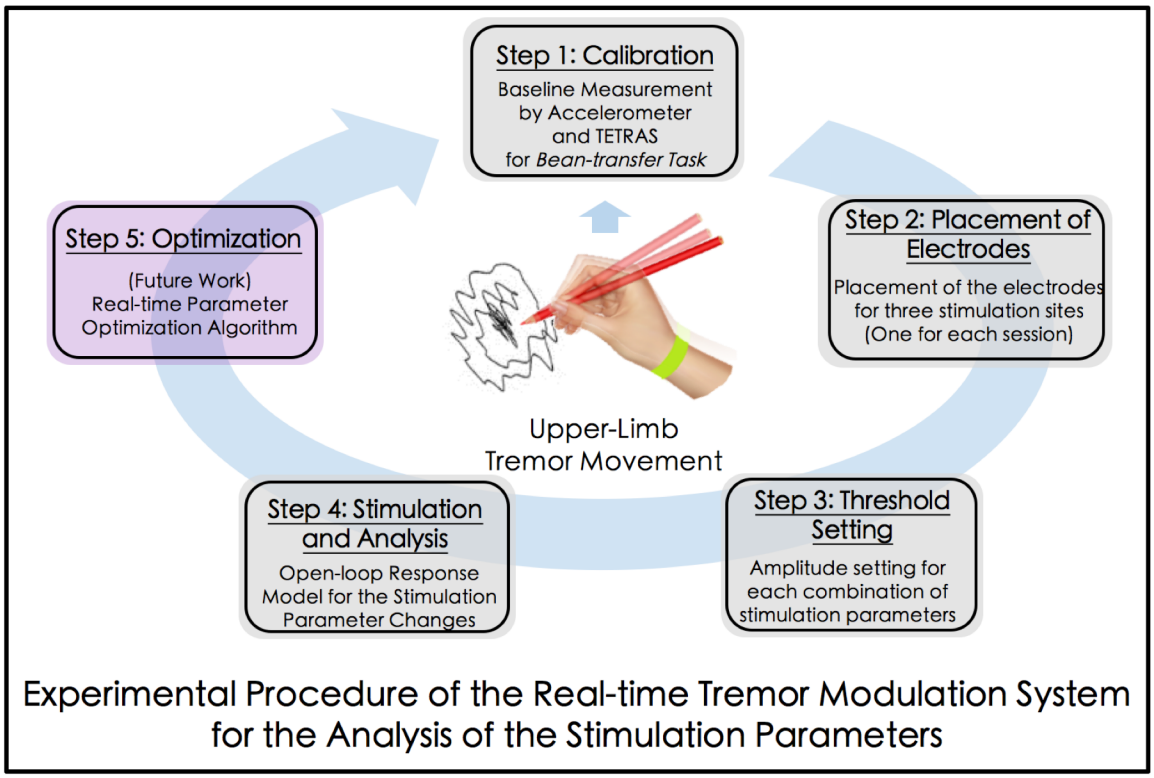

Figure 4.5 Experimental procedure for the analysis of the effects of the stimulation parameters using the tremor monitor and modulation system.

object (a medium-sized lima bean) from one plate to another using a spoon, shown in Figure 4.6—under the same condition. Then, we placed a pair of electrodes on a branch of the designated nerve near the wrist, shown in Figures 4.3 and 4.6. To confirm the desired nerve innervation, we asked the location of their sensing based on the highlighted area (Figure 4.3) of the hand while we provided electrical stimulation. Then we administered electrical stimulation under various parameter settings and minimum and maximum amplitudes of the stimulation. Since the frequency and the duty cycle generate distinct sensations, we set the threshold of the minimum sensible amplitude and the maximum amplitude under an uncomfortable range by different frequencies and duty cycles. The threshold amplitudes of the minimum and maximum range had different settings, but they only differed slightly under each condition. Even though we placed the electrodes near to the nerves, the electrical stimulation might activate muscle. The three amplitudes of stimulation (low, medium, and high) were lower than muscle activation levels, however, and we did not observe any direct motoric effects (muscle twitches).

After completing the calibration and threshold setting, the participants took at least a five-minute break. Although the threshold setting took less than three minutes, we wanted to minimize the effects of stimulation on tremor movement. Then, the GUI automatically generated different combinations of electrical stimulation parameters in random order, and the participants performed the *bean-transfer task* with stimulation. While we provided stimulation via the wrist device, we also collected motion sensor data to use in the tremor detection algorithm and evaluated changes in tremor performance in different stimulation settings.

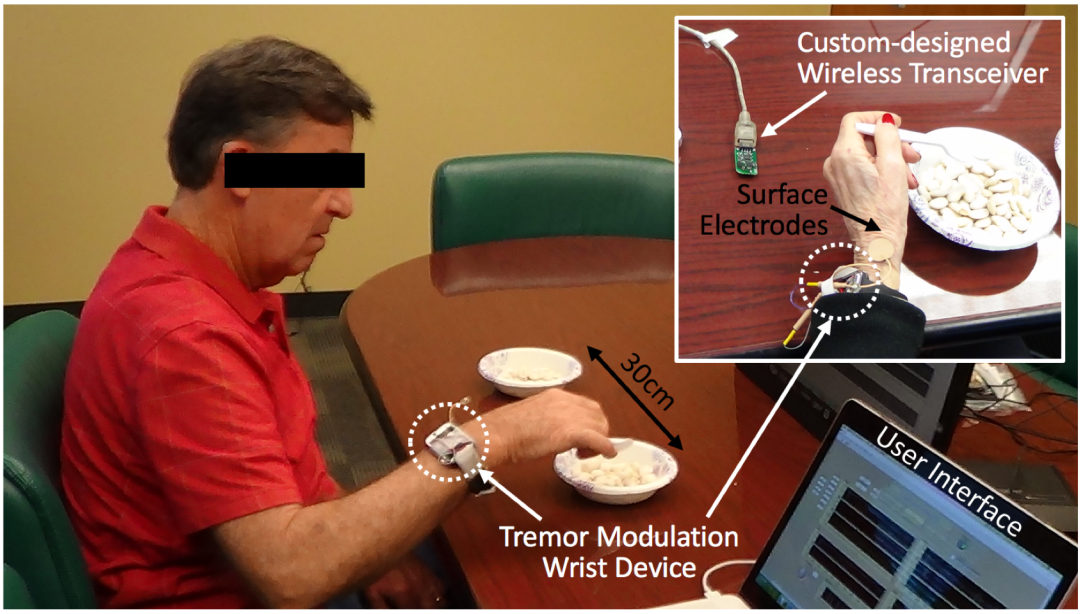

Figure 4.6 Experimental setup for peripheral-nerve electrical stimulation using the wrist device while one of the participants performed the bean-transfer task.

4.3.5 Statistical Analysis

To statistically analyze the effects of stimulation parameters on tremor movement, we conducted one-way ANOVA tests ($\alpha = 0.05$) to determine the differences with and without stimulation for various combinations of stimulation parameters across all subjects. We conducted a pairwise comparison with the least significant difference (LSD) method of the ANOVA test to analyze the ranges of parameters. We also conducted a linear regression analysis to determine the correlation between the three output metrics (frequency, power, deviation) and TETRAS score.

4.4 Results

To evaluate the effects of each stimulation parameter, we analyzed the tremor output metrics from the control trials and the stimulation trials with different subsets of data for each stimulation parameter, summarized in Table 4.3.

4.4.1 Baseline Tremor Movements

While the participants performed the *bean-transfer task,* we analyzed tremor movement without stimulation as the baseline tremor movement. Similar to our previous study in Chapter 3, we found that tremor power strongly correlated with the TETRAS score ($R^2 = 0.684$) (Figure 4.7 (b)), but the tremor frequency and the frequency deviation did not strongly correlated with the TETRAS score (R^2=0.026 (Figure 4.7 (a)), and $R^2 = 0.101$ (Figure 4.7 (c)), respectively). The power of the baseline tremor movement was between 4.47 ± 1.12 and 23.46 ± 1.73 g^2/Hz (mean: 8.98 ± 4.74 g^2/Hz). The baseline frequency was

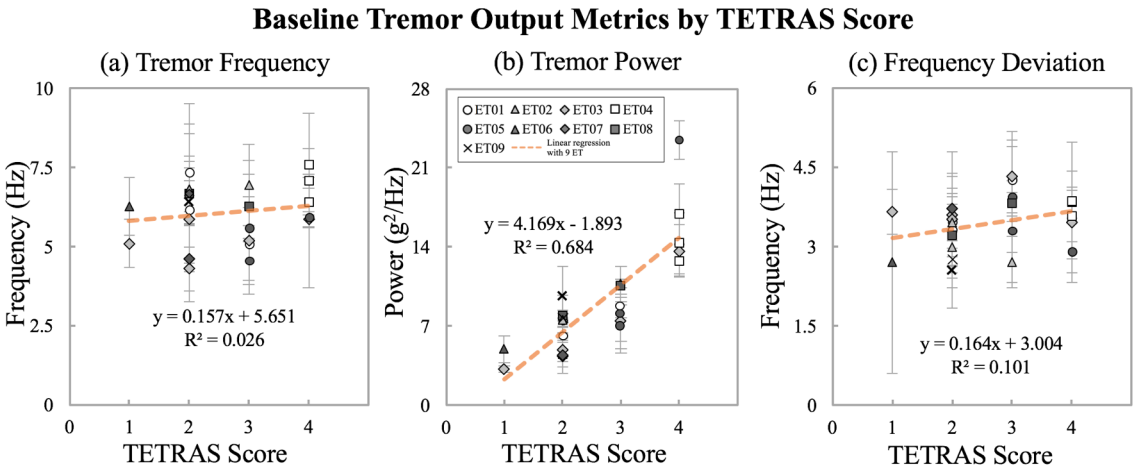

Figure 4.7 Baseline tremor output metrics from the TETRAS score for nine participants (from 23 sessions): (a) tremor frequency, (b) tremor power, and (c) frequency deviation.

Table 4.3 Subsets of the data for the analysis of the stimulation parameters.

Parameter Analysis	# of Sub. (Ses.)	Sites	Amp.	Freq. (Hz)	Duty Cycles (%)	Phases
Control Movement	9 (11)	N/A	N/A	N/A	N/A	N/A
Effect of Sites	4 (12)	R, U, M	L, M, H	50, 100, 200	12.5, 25, 37.5, 50	Phase 0 (Random)
Effect of Amplitudes	9 (10)	R	L, M, H	50, 100, 200	12.5	Phase 0 (Random)
Effect of Frequencies	9 (10)	R	L, M, H	50, 100, 200	12.5	Phase 0 (Random)
Effect of Duty Cycle	9 (10)	R	L, M, H	50, 100, 200	~5, 12.5, 25, 37.5, 50	Phase 0 (Random)
Effect of Phase	9 (10)	R	L, M, H	50, 100, 200	12.5	Phase 0 - 4

Sub.: Subjects; Ses.: Session; Amp.: Amplitudes; Freq.: Frequency.
R: Radial Nerve; U: Ulnar Nerve; M: Median Nerve.
L: Low Amplitude; M: Medium Amplitude; H: High Amplitude.

between 4.30 ± 0.68 and 7.33 ± 1.22 Hz (mean: 6.06 ± 0.92 Hz), and the frequency deviation was between 2.56 ± 0.72 and 4.32 ± 0.85 Hz (mean: 3.43 ± 0.49 Hz). We used these baseline tremor output metrics to evaluate the effects of the stimulation parameters, each of which we used to calculate the normalized tremor output metrics.

4.4.2 Effects of Stimulation Sites

Four of the nine subjects participated in this experiment, which entailed the stimulation of all three nerves on different days/sessions (Table 4.2). Figures 4.8 (a)-(f) summarize the tremor output metrics for the four participants from the three sessions. By comparing the baseline tremor frequency, we were able to analyze the RN ($P = 0.004$) and the MN ($P = 0.024$), both of which showed a statistically significant reduction in the

frequency of tremor (Figure 4.8 (a)). The normalized tremor frequencies for the RN (0.90 ± 0.03) and the MN (0.93 ± 0.03) did not statistically differ (P = 0.07), yet they did so for the UN (0.98 ± 0.02), the UN vs. the RN: P < 0.001, and the UN vs. the MN: P = 0.005 (Figure 4.8 (d)).

Stimulation most significantly affected tremor power when it was active in the RN (P < 0.001), yet it did not significantly reduce tremor power in the UN and the MN (P=0.984 and P=0.689, respectively) (Figure 4.8 (b)). Normalized tremor power in the RN showed that tremor decreased at 0.54 ± 0.04 from the baseline tremor power, which significantly differed in the UN and the MN (both for P < 0.001) (Figure 4.8 (e)). The frequency deviation (IQR) did not significantly increase in all three nerves (Figure 4.8 (c)); however, the normalized frequency deviation was 1.04 ± 0.04 in the RN and 1.03 ± 0.02 in the MN, which statistically differed from that in the MN (0.97 ± 0.02), (the UN vs. the RN: P = 0.003 and the UN vs. the MN: P = 0.011) (Figure 4.8 (f)). Overall, we conclude that stimulation most significantly affected the RN with respect to all three tremor output metrics, and it also statistically affected the MN with regard to the tremor frequency and the frequency deviation.

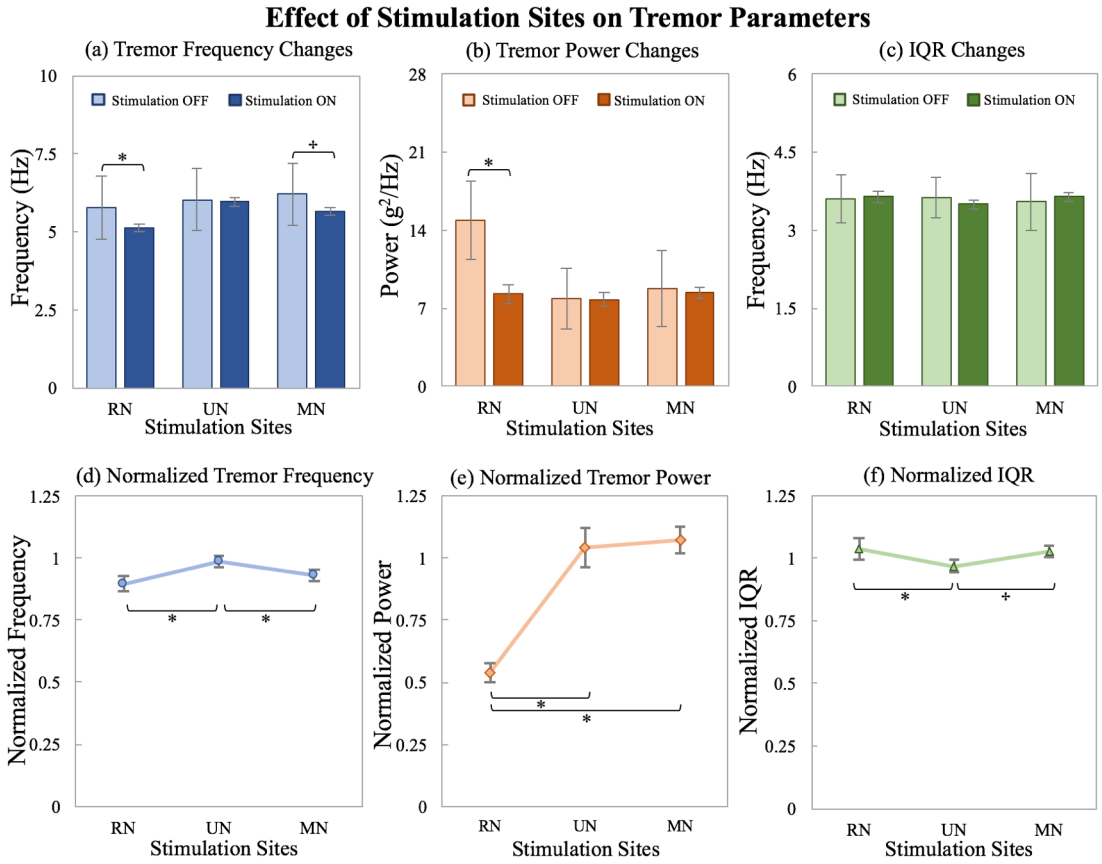

Figure 4.8 Effects of nerve stimulation on tremor output metrics: (a) tremor frequency, (b) tremor power, and (c) frequency deviation (IQR). The normalized tremor output metrics by nerve: (a) normalized tremor frequency, (b) normalized tremor power, and (c) normalized IQR. The error bar represents a 95% confidence interval; ∗: $P < 0.005$, ∔: $P < 0.05$.

4.4.3 Effects of Stimulation Amplitudes

To efficiently evaluate the effect of the amplitude of stimulation, we focused on tremor movement with combinations of the following parameters: three amplitudes, a 12.5% duty cycle, random phase stimulation of the RN for nine participants (ten sessions) (Table 4.3). We did not see a statistically significant reduction in frequency (Figure 4.9 (a)) ($P = 0.247$) or an increase between the IQR (Figure 4.9 (g)) ($P = 0.849$) with no stimulation

and that with three amplitudes of stimulation, but we did observe a reduction in tremor power (Figure 4.9 (d)) ($P < 0.001$). We were able to observe that a higher amplitude of stimulation resulted in a greater reduction in the effects of tremor power overall (Figure 4.9 (e)). When we analyzed the effects of the stimulation amplitude with regard to the subjects' baseline tremor movement (from TETRAS score group), we found that the greater baseline tremor movement exhibited a statistically significant power reduction ($P < 0.001$ for both TETRAS=3 and 4).

When we analyzed the normalized tremor frequency and the frequency deviation, we found no statistically significant differences between the stimulation amplitudes of TETRAS groups (Figures 4.9 (c) and (i)). We also analyzed the normalized tremor power by TETRAS scores and the amplitudes (Figure 4.9 (f)) and found no statistically significant power reduction in TETRAS=1 and 2 for three amplitudes; however, the normalized power for TETRAS=3 showed a higher amplitude until a medium level of stimulation led to a significant reduction in power, and the normalized power for TETRAS=4 showed that a higher amplitude led to a greater power reduction. From these findings, we can infer that the baseline tremor power of the subjects will be an important factor, indicating that closed-loop optimization will be useful to determining an optimal range of stimulation amplitudes based on the current tremor status.

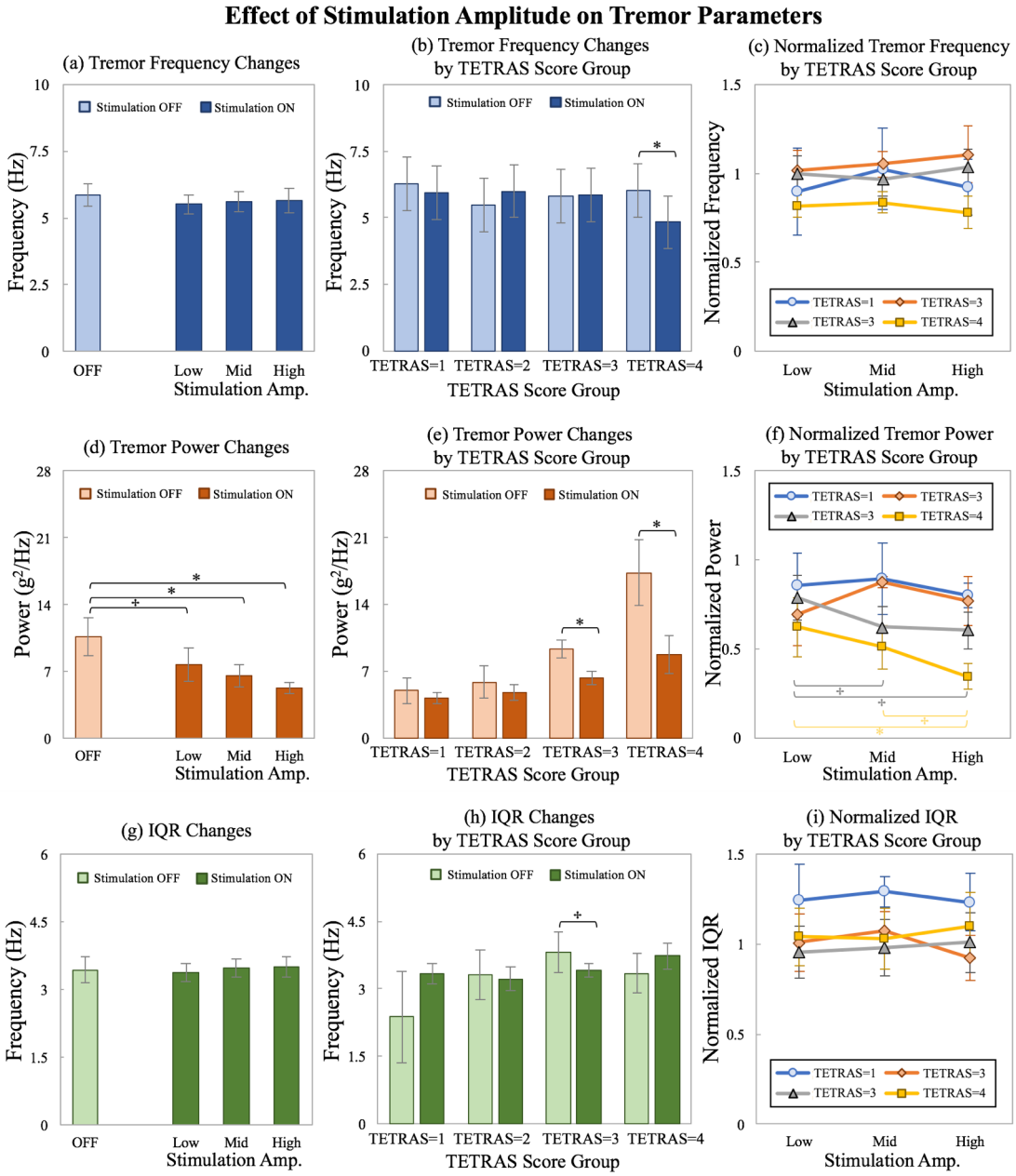

Figure 4.9 Effects of the amplitude of stimulation on tremor output metrics: (a) tremor frequency, (d) tremor power, and (g) IQR. The effect of stimulation on TETRAS score groups: (b) tremor frequency, (e) tremor power, and (h) IQR. The normalized tremor output metrics by stimulation amplitudes for the TETRAS score groups: (c) normalized tremor frequency, (f) normalized tremor power, and (i) normalized IQR. The error bar represents a 95% confidence interval; ∗: $P < 0.005$, ÷: $P < 0.05$.

4.4.4 Effects of Stimulation Frequencies

We analyzed the effects of stimulation frequencies on nine participants (ten sessions) (Table 4.3) with the following stimulation parameters: three amplitudes, a 12.5% duty cycle, three frequencies, and random-phase stimulation on RN. Results of the analysis showed no statistically significant reduction in frequency (Figure 4.10 (a)) (P = 0.719) or an increase in the IQR (Figure 4.10 (g)) (P = 0.511) from the combination of stimulation; however, we observed a statistically significant reduction in tremor power by stimulation (Figure 4.10 (c)) (P = 0.001). Although normalized tremor power was the lowest at 100 Hz stimulation, it was not statistically significant (Figure 4.10 (e)). When we analyzed the effect of the stimulation frequency on the TETRAS score group, we observed that the normalized power of TETRAS=3 showed a statistically significant difference among the frequencies (Figure 4.10 (f)).

Even though the normalized frequency (Figure 4.10 (b)) and the normalized frequency deviation (the gray line in Figure 4.10 (h)) exhibited no statistically significant differences, we were able to conclude that the subjects in the lowest TETRAS score group (TETRAS=1) showed a reduction in the normalized frequency and an increase in the normalized frequency deviation with a higher frequency of stimulation (the blue lines in Figures 4.10 (c) and (i)).

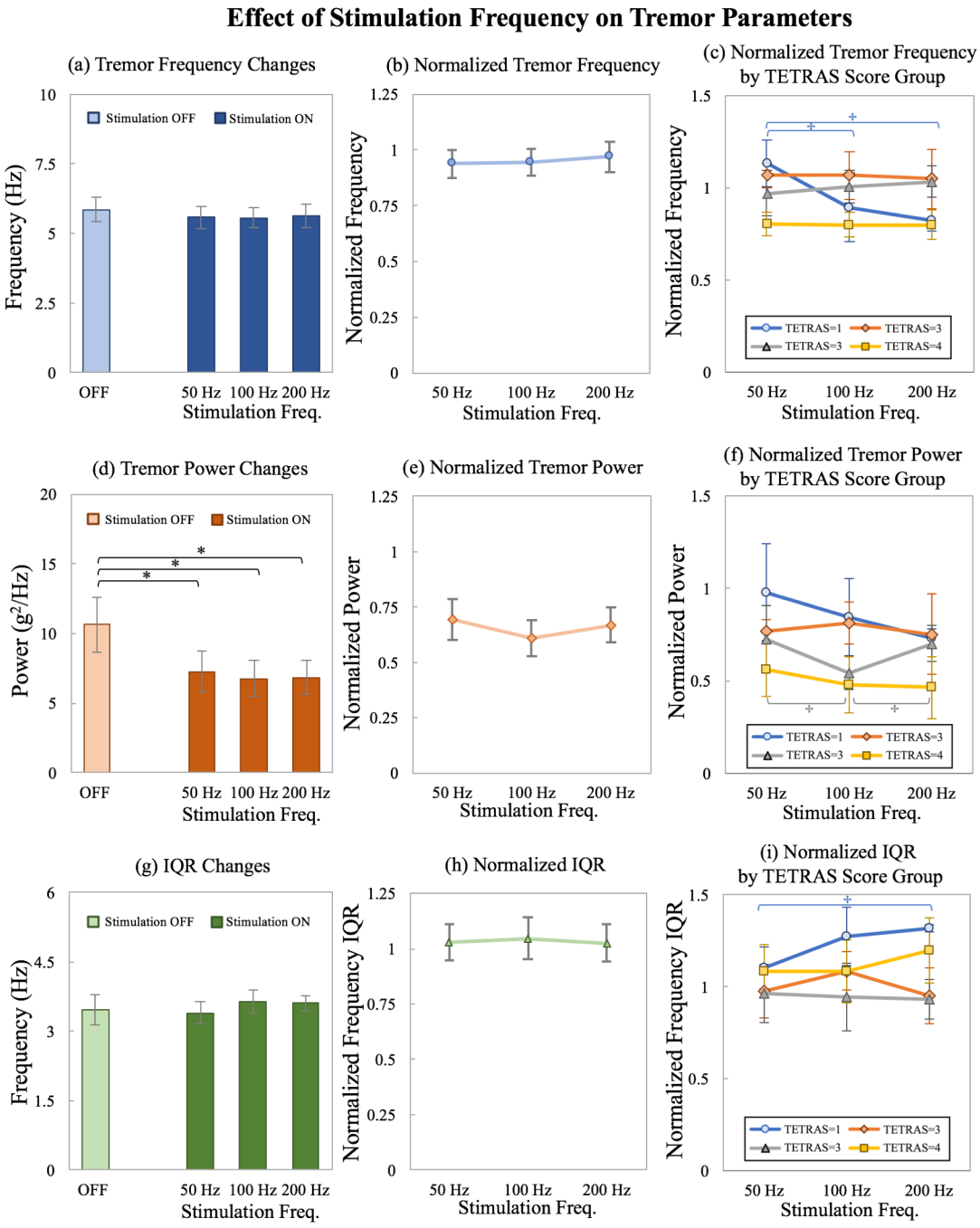

Figure 4.10 Effects of the frequencies of stimulation on the tremor output metrics: (a) tremor frequency, (d) tremor power, and (g) IQR. The overall normalized tremor output metrics by stimulation frequency: (b) normalized tremor frequency, (e) normalized tremor power, and (h) normalized IQR. The normalized tremor output metrics by stimulation frequency for the TETRAS score groups: (c) normalized tremor frequency, (f) normalized tremor power, and (i) normalized IQR. The error bar represents a 95% confidence interval; ∗: $P < 0.005$, ÷: $P < 0.05$.

4.4.5 Effects of Stimulation Duty Cycles

To analyze the effects of the stimulation duty cycle, we included data with combinations of the following stimulation parameters: three amplitudes, five duty cycles, three frequencies, random-phase stimulation of the RN in nine participants (ten sessions) (Table 4.3). We did not identify any significant differences among the duty cycles from the collected data, despite the significant reduction in tremor power by the stimulation with any duty cycle (see Figures 4.11 (a)-(i)). We found statistically significant increases in the normalized frequency deviation at only 12.5% and 25% of the duty cycle. When we analyzed the effect of the duty cycle on TETRAS score, we found that only the TETRAS=4 group had a statistically significant reduction in normalized tremor power (Figure 4.11 (f)) and an increase in the normalized frequency deviation of 50% of the duty cycle (Figure 4.11 (i)). In addition, the TETRAS=1 group showed an increase in the normalized IQR with duty cycles of 25% and 50% of stimulation (Figure 4.11 (i)).

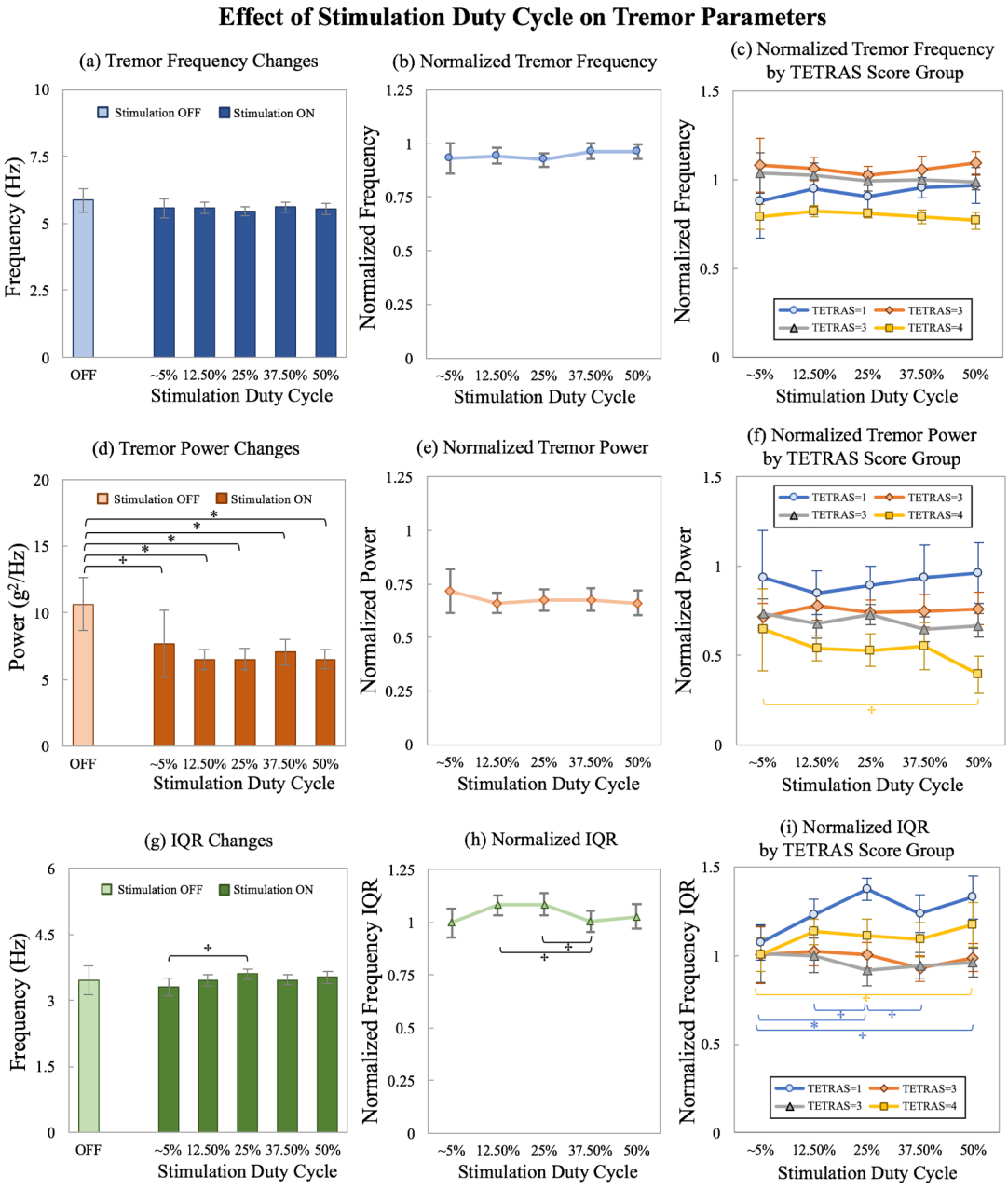

Figure 4.11 Effects of the duty cycles of stimulation on tremor output metrics: (a) tremor frequency, (d) tremor power, and (g) tremor frequency deviation. Overall normalized tremor output metrics by stimulation duty cycles: (b) normalized tremor frequency, (e) normalized tremor power, and (h) normalized IQR. The normalized tremor output metrics by stimulation duty cycles for the TETRAS score groups: (c) normalized tremor frequency, (f) normalized tremor power, and (i) normalized IQR. The error bar represents a 95% confidence interval; ∗: $P < 0.005$, ÷: $P < 0.05$.

4.4.6 Effects of Stimulation Phases

To analyze the effects of stimulation phases, we included data with combinations of the following stimulation parameters: three amplitudes, a 12.5% duty cycle, three frequencies, four-phase and random-phase stimulation on the RN for nine participants (ten sessions) (Table 4.3). Similar to the duty cycle, we found no significant effect on either phase-locked stimulation or random-phase stimulation, but overall, stimulation mostly affected tremor power (Figures 4.12 (a)-(i))). When we closely observed the effects of phases in the TETRAS groups, we found that the TETRAS=3 group exhibited the most significant reduction in tremor power in random-phase stimulation, and TETRAS=4 exhibited the most significant reduction in normalized power tremor: ½ π (Figure 4.12 (f)).

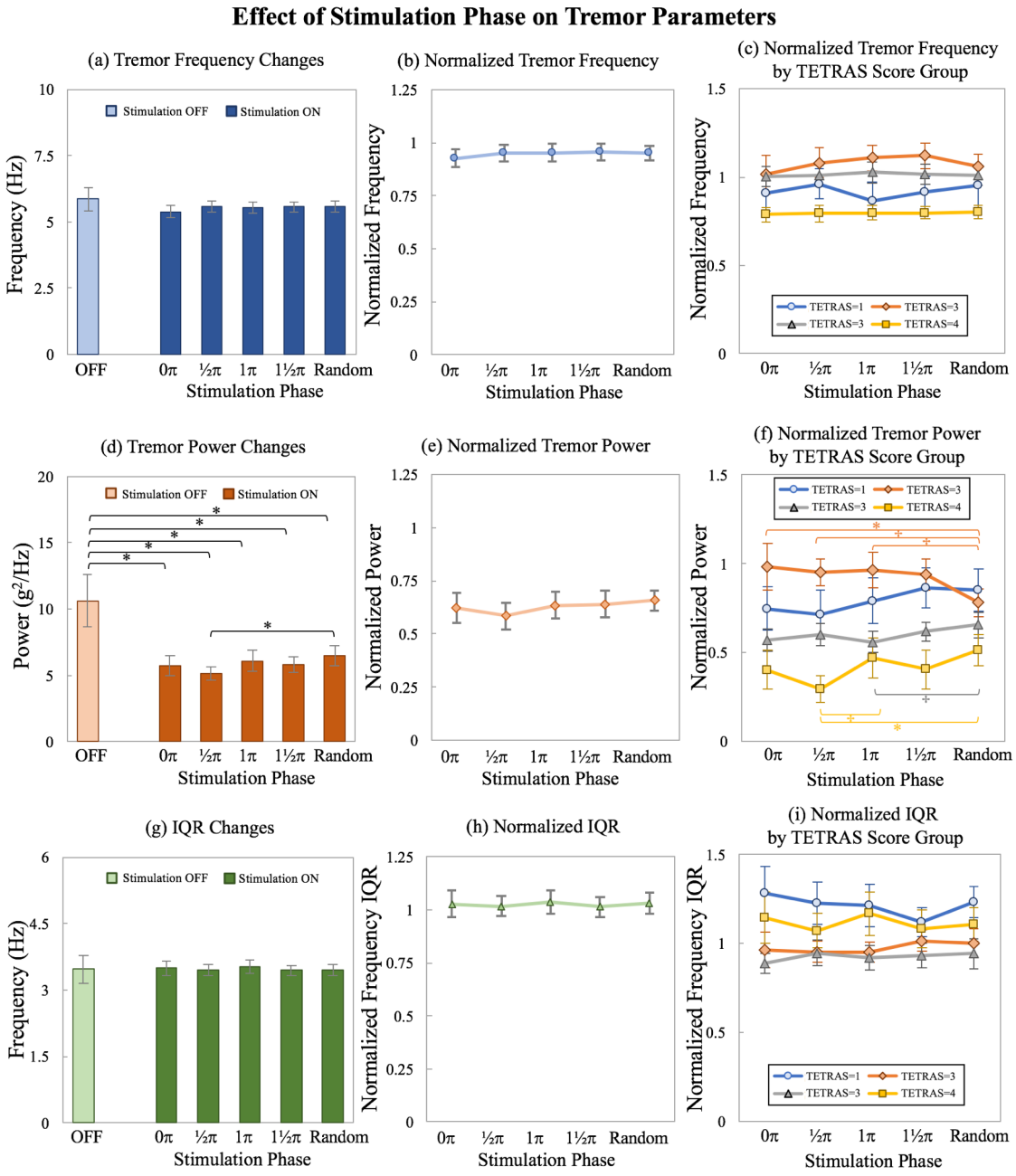

Figure 4.12 Effects of the phases of stimulation on tremor output metrics: (a) tremor frequency, (d) tremor power, and (g) IQR. Overall normalized tremor output metrics by stimulation phases: (b) normalized tremor frequency, (e) normalized tremor power, and (h) normalized IQR. The normalized tremor output metrics by stimulation phases for the TETRAS score groups: (c) normalized tremor frequency, (f) normalized tremor power, and (i) normalized IQR. The error bar represents a 95% confidence interval; ∗: $P < 0.005$, ∔: $P < 0.05$.

4.5 Discussion

From the effects on stimulation sites, we found the greatest reduction in tremor power on the RN; however, we collected data for all stimulation sites from only four participants on three different days/sessions (12 sessions). Moreover, the baseline tremor power during the three nerve stimulation sessions on different days fell into three ranges (RN: 14.67 ± 6.23, UN: 8.25 ± 4.60, and MN: 8.76 ± 5.53), and the corresponding average scores for the TETRAS groups also fell into three ranges (RN: 3.75 ± 0.50, UN: 2.50 ± 1.29, and MN: 2.75 ± 0.96). When we compared the effects of stimulation on only the RN vs. the UN in the eight subjects who participated in both RN and UN sessions (18 sessions), we still found that stimulation significantly reduced tremor power in the RN (normalized tremor power on the RN: 0.62 ± 0.28 and the UN: 0.94 ± 0.38; RN vs. UN: $P<0.001$). Although we attempted to evaluate the effect on stimulation sites in a larger number of participants, the baseline tremor power in the RN during the nine sessions was still higher than that in the UN (RN: 11.08 ± 5.44 and 7.43 ± 3.34), and the corresponding average scores for the TETRAS groups differed (RN: 3.11 ± 0.78 and UN: 2.22 ± 0.83). Since we found that stimulation resulted in a greater reduction in tremor power when the baseline tremor power was higher, we cannot definitively conclude that stimulation most significantly reduced tremor power in the RN. That is, we cannot infer that the greater reduction in tremor in the RN resulted from the greater effects of stimulation of the RN or from the greater baseline effects.

We attempted to compare the effects on the stimulation sites in a fair manner by analyzing stimulation data on the same subjects during the same number of sessions. This study, however, did not control for the regular medication of the subjects or the severity of

tremor, particularly tremor power, which differed from day-to-day and from time-to-time during their participation. Therefore, in a future study, we plan to regulate the pre-treatment conditions to obtain a more accurate evaluation of the stimulation effects under the same baseline conditions.

For the remaining effects of the stimulation parameters, we focused on data from the stimulation of the RN in nine participants (ten sessions) and analyzed the effects of stimulation parameters by baseline TETRAS score groups. The number of sessions for each group, however, was not the same (i.e., TETRAS=1: one session, TETRAS=2: two sessions, TETRAS=3: four sessions, and TETRAS=4: three sessions). Thus, in a future study, we plan to recruit more participants to obtain the same number of data points for each group and increase the confidence of the analysis. We also plan to include more sessions to find an individual model of stimulation effects and develop an optimization algorithm for individuals for use in further studies.

4.6 Conclusion

This study entailed the analysis of the effects of different ranges of stimulation parameters on three peripheral nerves. To evaluate the effect of stimulation parameters, we collected motion sensor data of tremor movement with and without combinations of stimulation parameters and analyzed changes in tremor movement according to three tremor output metrics: the dominant tremor frequency, tremor power, and the frequency deviation (IQR). Combinations of the stimulation parameters consist of the following range of parameters: stimulation sites (the radial nerve, the ulnar nerve, the median nerve), amplitude (low, medium, high), frequencies (50, 100, 200 Hz), duty cycles (~5, 12.5, 25,

37.5, and 50% of the tremor cycle), and phase (phase-locked at 0, ½, 1, 1½ π to tremor cycle, and continuous random-phase stimulation in the tremor cycle). We found that the radial nerve was the most efficient stimulation site for tremor power reduction, and the proper range of stimulation amplitudes differed according to the baseline tremor movement in the subjects. Although the other parameters had a relatively less significant effect on tremor reduction, we concluded that the stronger tremor group exhibited a greater reduction in tremor power and that the weaker tremor group showed a greater reduction in the frequency and a greater increase in the frequency deviation.

In future studies, we aim to develop an optimization algorithm based on the tremor characteristics of each participant to maximize the effect of stimulation in the modulation of tremor. The findings from this study were based on a limited number of participants and groups in TETRAS, and it did not regulate the pre-treatment condition of the human subjects with regard to their regular medications. Therefore, we will find a stronger model for an open-loop response model for an optimization algorithm and expect to use parameter changes in real time.

CHAPTER 5

CONCLUSION AND POTENTIAL APPLICATIONS

This doctoral thesis aimed to assess tremor movement quantitatively with computer-based standardized tasks, to develop a wearable wireless tremor monitor and modulation system that administers peripheral-nerve electrical stimulation that attenuates tremor movement, and to analyze the effects of stimulation parameters. The findings and the analysis of this thesis project demonstrate that the proposed method for quantitative tremor assessment and the tremor modulation system will have important clinical and commercial potentials for better symptom tracking and diagnosis and for a new method for tremor suppression.

Currently available diagnostic methods consist mostly of subjective measurements, and clinicians and researchers typically diagnose patients' symptoms with provocative maneuvers using such scoring methods as the Unified Parkinson's Disease Rating Scale (UPDRS), the Essential Tremor Rating Assessment Scale (TETRAS), and the Tremor Rating Scale with a 0-4 scale within a 1-point or 0.5-point range. The scoring methods focus only on the severity of tremor movement. Moreover, the methods are validated by the clinicians or researcher, and they are susceptible to inter- and intra-rater variability, particularly task-based evaluation such as drawing and writing. I designed the new methods of quantifying tremor movement with three computer-based tasks (spiral navigation, rectangular track navigation, and multi-directional tapping/clicking tasks) based on Fitts' Law using a 3D gyration mouse, and I analyzed the performance metrics (e.g., completion time, outside area, path efficiency, and throughput) that can represent the currently

available clinical scores and tremor metrics (i.e., frequency and severity). The analyzed results showed that the performance metrics of the proposed computer-based assessment tasks were highly correlated with the frequency and the power of tremor and that the linear regression model of the task performance demonstrated the feasibility of the quantitative tremor assessment of tremor frequency and severity without any additional devices by minimizing rater variability.

By using the proposed quantitative assessment method, tremor movements can be assessed at home on a daily basis. Information about changes in tremor characteristics, which can be tracked during tremor events and treatments, can provide a great reference for accurately diagnosing disease and determining the effects of current treatment regimens so that physicians can change medications or adjust dosages. Furthermore, by collecting additional physiological data, such as EMG and brain signals (EEGs), we will be able to determine the effects of peripheral nerve stimulation within tremor pathways. Although the origin of a tremor and its neurological pathways remain unclear, we will first examine the effects of stimulation on physiological phenomena for essential tremor (ET) and then expand our examination to other diseases (e.g., Parkinson's disease).

Conventional clinical treatments for tremor patients are medications, such as primidone or beta blockers, and deep-brain stimulation (DBS). However, many patients do not sufficiently respond to these treatments, or they experience intolerable side effects of the medication, and they are concerned about the procedure for implanting the electrode, which is costly and invasive. Even though the DBS has shown the effects of the tremor suppression, it does not guarantee effective tremor suppression for all patients. Several researchers tried to develop new techniques for treatment-resistant tremor using functional

electrical stimulation on muscles, a tremor cancelling robotic device, and mechanical or vibratory feedback to suppress tremor movements. Such techniques, however, have not been used extensively in patients because of the bulkiness of the systems or their lack of efficacy. Therefore, this non-invasive, wearable, tremor modulation system via peripheral-nerve stimulation for patients with treatment-resistant tremor has huge clinical and commercial potential by significantly suppressing the amplitude of the tremor.

We studied nine subjects diagnosed with essential tremor. Each subject was outfitted with a wearable system and a set of surface electrodes placed on the radial nerve of the forearms. We provided phase-locked electrical stimulation—200 μs bi-phasic stimulus, a sensory threshold (1T amplitude), a 100 Hz frequency, and a 12.5% duty cycle—while observing kinetic tremor in subjects performing prescribed dexterity tasks. We observed that peripheral nerve stimulation significantly affected the dominant frequency and tremor power. Participants who experienced stronger tremor power exhibited a greater reduction in tremor power. Given that the currently available clinical scoring technique, TETRAS, was highly correlated to the tremor power, we expected that the power decreases from the stimulation were clinically relevant effects that reduce the tremor.

We also examined the proper range of stimulation parameters with their combinations and the open-loop response model to identify their effects on tremor modulation. We evaluated the effects of the system on ET patients; we analyzed their tremor movement by changing the stimulation parameters (i.e., amplitude, frequency, duty cycle, phase, and stimulation sites) to find an open-loop response to their tremor movement according to the stimulation parameters. Based on the response model of each ET

participant and/or a group of ET participants, we expect to design a real-time tremor monitoring and parameter optimization algorithm that can play an important role in the long-term use of a tremor modulation system that uses peripheral-nerve electrical stimulation to minimize nerve fatigue and power consumption and that maximizes the efficacy of electrical peripheral nerve stimulation.

In a future study, we plan to develop an optimization algorithm based on tremor characteristics for each human subject to maximize the effect of stimulation on tremor modulation. Since we have findings from only a limited number of participants and TETRAS score groups, and since we did not regulate their pre-treatment conditions (i.e., medications), we plan to recruit more ET patients to analyze the stronger model for a better open-loop response. Despite these constraints, the results from the current experimental setup showed that the amplitude of stimulation is a useful parameter for optimization based on the current tremor status (i.e., tremor power) of each participant. Therefore, to maximize the effects on reductions in tremor power, we plan to implement a closed-loop algorithm that optimizes stimulation amplitudes based on their current tremor status. Then we will modify the optimization algorithm to expand the parameter space.

REFERENCES

[1] Bain PG, Findley LJ, Atchison P, Behari M, Vidailhet M, Gresty M, Rothwell J C, Thompson PD, and Marsden CD. Assessing tremor severity. *Journal of Neurology, Neurosurgery and Psychiatry,* 56(8), 868-873, 1993.

[2] Bain PG. Tremor. *Parkinsonism and Related Disorders*, 13, S369-S374, 2007.

[3] Bao L, and Stephen IS. Activity recognition from user-annotated acceleration data. Pervasive computing. Springer Berlin Heidelberg, 1-17. 2004.

[4] Bhidayasiri R. Differential diagnosis of common tremor syndromes. *Postgraduate Medical Journal*, 81(962), 756-762, Jan. 2005.

[5] Bland JM, Altman D. Statistical methods for assessing agreement between two methods of clinical measurement. *The Lancet,* 327(8476), 307-310, 1986.

[6] Britton TC, Thompson PD, Day BL, Rothwell JC, Findley LJ, and Marsden CD. "Resetting" of postural tremors at the wrist with mechanical stretches in Parkinson's disease, essential tremor, and normal subjects mimicking tremor. *Annals of Neurology*, 31(5), 507-514, 1992.

[7] Charles PD, Esper GJ, Davis TL, Maciunas RJ, and Robertson D. Classification of tremor and update on treatment. *American Family Physician*, 59(6), 1565-1572, 1999.

[8] Dai H, Zhang P, and Lueth TC. Quantitative assessment of parkinsonian tremor based on an inertial measurement unit. *Sensors*, 15(10), 25055-25071, 2015.

[9] Deuschl G, Raethjen J, Lindemann M, and Krack P. The pathophysiology of tremor. *Muscle Nerve,* 24(6), 716-735, 2001.

[10] Elble R, Higgins C, Leftler K, and Hughes L. Factors influencing the amplitude and frequency of essential tremor. *Movement Disorders*, 9(6), 589-596, 1994.

[11] Elble RJ, Brilliant M, Leffler K, and Higgins C. Quantification of essential tremor in writing and drawing. *Movement Disorders*, 11(1), 70-78, 1996.

[12] Elble RJ. Essential tremor frequency decreases with time. *Neurology*, 55(10), 1547-1551, 2000.

[13] Elble RJ, Pullman SL, Matsumoto JY, Günther Deuschl JR, and Tintner R. Tremor amplitude is logarithmically related to 4-and 5-point tremor rating scales. *Brain,* 129(10), 2660-2666, 2006.

[14] Elble R, Comella C, Fahn S, Hallett M, Jankovic J, Juncos J, Louis E, Lyons K, Ondo W, Pahwa R, Sethi K, Stern M, Tanner C, Tarsy D, Tintner R, Watts R. The essential tremor rating assessment scale (TETRAS). *Movement Disorders*, 23(1), S357-S357, 2008.

[15] Elble R, Comella C, Fahn S, Hallett M, Jankovic J, Juncos JL, LeWitt P, Lyons K, Ondo W, Pahwa R and Sethi K, Reliability of a new scale for essential tremor. *Movement Disorders*, 27(12), 1567-1569, 2012.

[16] Elias WJ and Shah BB. Tremor. JAMA, 311(9), 948-954, 2014.

[17] Ergonomic Requirements for Office Work with Visual Display Terminals (VDTS)—Part 9: Requirements for Non-Keyboard Input Devices, **ISO 9241-9:2000 (E)**, Feb. 2002.

[18] Gillard DM, Cameron T, Prochazka A, and Gauthier MJ. Tremor suppression using functional electrical stimulation: a comparison between digital and analog controllers, *IEEE Transactions on Rehabilitation Engineering*, *7*(3), 385-388, 1999.

[19] Giuffrida JP, Riley DE, Maddux BN, and Heldman DA. Clinically deployable Kinesia™ technology for automated tremor assessment. *Movement Disorders*, 24(5), 723-730, Apr. 2009.

[20] Goetz CG, Tilley BC, Shaftman SR, Stebbins GT, Fahn S, Martinez-Martin P, Poewe W, Sampaio C, Stern MB, Dodel R, and Dubois B. Movement Disorder Society-sponsored revision of the Unified Parkinson's Disease Rating Scale (MDS-UPDRS): Scale presentation and clinimetric testing results. *Movement Disorders*, 23(15), 2129-2170, Nov. 2008.

[21] González R, Barrientos A, del Cerro J, and Coca B. DIMETER: A Haptic Master Device for Tremor Diagnosis in Neurodegenerative Diseases. *Sensors,* 14(3), 4536-4559, Jan. 2014.

[22] Growdon JH, Shahani BT, and Young RR. The effect of alcohol on essential tremor. *Neurology*, 25(3), 259-259, 1975.

[23] Halliday DM, Conway BA, Farmer SF, Shahani U, Russell AJC, and Rosenberg JR. Coherence between low-frequency activation of the motor cortex and tremor in patients with essential tremor. *The Lancet*, 355(9210), 1149-1153, 2000.

[24] Hao MZ, He X, Kipke DR, and Lan N. Effects of electrical stimulation of cutaneous afferents on corticospinal transmission of tremor signals in patients with Parkinson's disease. *Intl. IEEE/EMBS Conference on Neural Engineering (NER)*, 355-358, Nov. 2013.

[25] Hellwig B, Häußler S, Schelter B, Lauk M, Guschlbauer B, Timmer J, and Lücking CH. Tremor-correlated cortical activity in essential tremor. *The Lancet*, 357(9255), 519-523, 2001.

[26] Hellwig B, Mund P, Schelter B, Guschlbauer B, Timmer J, and Lücking CH. A longitudinal study of tremor frequencies in Parkinson's disease and essential tremor. *Clinical Neurophysiology*, 120(2), 431-435, Feb. 2009.

[27] Hess CW and Pullman SL. Tremor: Clinical Phenomenology and Assessment Techniques. *Tremor and Other Hyperkinetic Movements*, 2, 1-15, June 2012.

[28] Hubble JP, Busenbark KL, Wilkinson S, Penn RD, Lyons K, and Koller WC. Deep brain stimulation for essential tremor. *Neurology*, 46(4), 1150-1153, Apr. 1996.

[29] IETF. Essential Tremor (ET) Common Medications. [Online]. Available: http://www.essentialtremor.org/treatments/medication/ [Oct. 17, 2017].

[30] IETF: Treatment Options: Assistive Devices. [Online]. Available: http://www.essentialtremor.org/treatments/assistive-devices/ [Oct. 17, 2017].

[31] IETF: Treatment Options: Surgical Treatment. [Online]. Available: http://www.essentialtremor.org/treatments/surgical-treatments/ [Oct. 17, 2017].

[32] IETF: 12-Month Annual Report**,** Hope through research, awareness and support. 2006 [online]. Available: http://www.essentialtremor.org/wp-content/uploads/2013/07/2006-IETF-An-Rep-for-WEB.pdf [Oct. 17, 2017].

[33] Jankovic J, and Schwartz K. Botulinum toxin treatment of tremors. *Neurology*, 41(8), 1185-1185, 1991.

[34] Javidan M, Elek J, and Prochazka A. Attenuation of pathological tremors by functional electrical stimulation II: clinical evaluation. *Annals of Biomedical Engineering,* 20(2), 225-236, Mar. 1992.

[35] Jöbges EM, Elek J, Rollnik JD, Dengler R, and Wolf W. Vibratory proprioceptive stimulation affects Parkinsonian tremor. *Parkinsonism and Related Disorders*, 8(3), 171-176, Jan. 2002.

[36] Joyce GC, Rank PMH. The effects of load and force on tremor at the normal human elbow joint. *The Journal of Physiology*, 240(2), 375-396, 1974.

[37] Kim J, Parnell C, Wichmann T, and DeWeerth SP. Quantitative assessment of arm tremor in people with neurological disorders. *Proc. IEEE Conf. Eng. Med. Biol. Soc. (EMBC)*, 2299-2302. Aug. 2016.

[38] Kumar R, Lozano AM, Kim YJ, Hutchison WD, Sime E, Halket E, and Lang AE. Double-blind evaluation of subthalamic nucleus deep brain stimulation in advanced Parkinson's disease. *Neurology*, 51(3), 850-855, Sept. 1998.

[39] Lee RG, Stein RB. Resetting of tremor by mechanical perturbations: a comparison of essential tremor and parkinsonian tremor. *Annals of Neurology*, 10(6), 523-531, 1981.

[40] Liftware. [Online]. Available: https://www.liftware.com/ [Oct. 17, 2017].

[41] Logan B, Healey J, Philipose M, Tapia EM, and Intille S. A long-term evaluation of sensing modalities for activity recognition. Springer Berlin Heidelberg, 483-500, 2007.

[42] Lyons KE, and Pahwa R. Deep brain stimulation and tremor. *Neurotherapeutics*, 5(2), 331-338, 2008.

[43] Marsden CD. The mechanisms of physiological tremor and their significance for pathological tremors. In: J.E. Desmedt, editor. Physiological tremor, pathological tremors and clonus. *Progress in Clinical Neurophysiology*, vol. 5. Basel: Karger; 1-16, 1978.

[44] Matthews PB. Interaction between short- and long-latency components of the human stretch reflex during sinusoidal stretching. *Journal of Physiology,* 462, 503-527, 1993.

[45] Mayo Clinic. Essential Tremor: Treatment. [Online]. Available: http://www.mayoclinic.org/diseases-conditions/essential-tremor/basics/treatment/con-20034509 [Oct. 17, 2017].

[46] McAuley JH, Rothwell JC, and Marsden CD. Frequency peaks of tremor, muscle vibration and electromyographic activity at 10 Hz, 20 Hz and 40 Hz during human finger muscle contraction may reflect rhythmicities of central neural firing. **Experimental Brain Research, 114(3), 525-541, May 1997.**

[47] McAuley JH, and Marsden CD. Physiological and pathological tremors and rhythmic central motor control. *Brain*, 123(8), 1545-1567, 2000.

[48] Miralles F, Tarongi S, and Espino A. Quantification of the drawing of an Archimedes spiral through the analysis of its digitized picture. *Journal of Neuroscience Methods*, 152(1), 18-31, 2006.

[49] Mostile G, Giuffrida JP, Adam OR, Davidson A, and Jankovic J. Correlation between Kinesia system assessments and clinical tremor scores in patients with essential tremor. *Movement Disorders*, 25(12), 1938-1943, 2010.

[50] Natapov D, Castellucci SJ, and MacKenzie IS. ISO 9241-9 evaluation of video game controllers. *Proc. of Graphics Interface*, 223-230, 2009.

[51] Norman KE, D'amboise SN, Pari G, and Héroux ME. Tremor during movement correlates well with disability in people with essential tremor. *Movement Disorders*, 26(11), 2088-2094, 2011.

[52] Pahwa R, Busenbark K, Swanson-Hyland EF, Dubinsky RM, Hubble JP, Gray C, and Koller WC. Botulinum toxin treatment of essential head tremor. *Neurology*, 45(4), 822-824, 1995.

[53] Pathak A, Redmond JA, Allen M, and Chou KL. A noninvasive handheld assistive device to accommodate essential tremor: a pilot study. *Movement Disorders*, 29(6), 838-842, 2014.

[54] Pledgie S, Barner KE, Agrawal SK, and Rahman T. Tremor suppression through impedance control. *IEEE Trans. on Rehabilitation Engineering*, 8(1), 53-59, 2000.

[55] Prochazka A, Elek J, and Javidan M. Attenuation of pathological tremors by functional electrical stimulation I: Method, *Annals of Biomedical Engineering*, 20(2), 205-224, Mar. 1992.

[56] Pulliam CL, Eichenseer SR, Goetz CG, Waln O, Hunter CB, Jankovic J, Vaillancourt DE, Giuffrida JP, and Heldman DA. Continuous in-home monitoring of essential tremor. *Parkinsonism and Related Disorders*, 20(1), 37-40. Jan. 2014.

[57] Raethjen J, Govindan RB, Kopper F, Muthuraman M, and Deuschl G. Cortical involvement in the generation of essential tremor. *Journal of Neurophysiology*, 97(5), 3219-3228, 2007.

[58] Raethjen J, and Deuschl G. The oscillating central network of essential tremor. *Clinical Neurophysiology*, 123(1), 61-64, 2012.

[59] Rigas G, Tzallas AT, Tsipouras MG, Bougia P, Tripoliti EE, Baga D, Fotiadis DI, Tsouli SG, and Konitsiotis S. Assessment of tremor activity in the Parkinson's disease using a set of wearable sensors. *IEEE Trans. Inf. Technol. Biomed.*, 16(3), 478-487, May 2012.

[60] Rocon E, Belda-Lois JM, Ruiz AF, Manto M, Moreno JC, and Pons JL. Design and validation of a rehabilitation robotic exoskeleton for tremor assessment and suppression. *IEEE Trans. on Neural Systems and Rehabilitation Engineering*, *5*(3), 367-378, 2007.

[61] Schnitzler A, Münks C, Butz M, Timmermann L, and Gross J. Synchronized brain network associated with essential tremor as revealed by magnetoencephalography. *Movement Disorders*, 24(11), 1629-1635, 2009.

[62] Soukoreff RW and MacKenzie IS. Towards a standard for pointing device evaluation, perspectives on 27 years of Fitts' law research in HCI. *International Journal of Human-Computer Studies,* 6, 751-789, Dec. 2004.

[63] Stacy MA, Elble RJ, Ondo WG, Wu SC, and Hulihan J. Assessment of interrater and intrarater reliability of the Fahn–Tolosa–Marin Tremor Rating Scale in essential tremor. *Movement Disorders*, 22(6), 833-838, 2007.

[64] Stein RB, Lee RG. Tremor and Clonus. Handbook of Physiology, Section 1, Volume II: Motor Control. Baltimore, Williams & Wilkins, 325-343, 1981.

[65] Stiles RN, Randall JE. Mechanical factors in human tremor frequency. *Journal of Applied Physiology,* 23, 324-30, 1967.

[66] Tintner R. The tremor rating scale (TRS). *Movement Disorders*, 19(9), 1131-1132, 2004.

[67] Uhríková Z, Šprdlík O, Hoskovcová M, Komárek A, Ulmanová O, Hlaváč V, Nugent CD, and Růžička E. Validation of a new tool for automatic assessment of tremor frequency from video recordings. *Journal of Neuroscience Methods*, 198(1), 110-113, 2011.

[68] Walsh EG. Muscles, masses and motion. London: Mac Keith Press; 67-77, 1992.

[69] Yousefi B, Huo X, Kim J, Veledar E, and Ghovanloo M. Quantitative and comparative assessment of learning in a tongue-operated computer input device–Part II: navigation tasks. *IEEE Trans. Inf. Technol. Biomed.,* 16(4), 633-643, July 2012.

[70] Zeuner K, Shoge R, Goldstein S, Dambrosia J, Hallet M. Accelerometry to distinguish psychogenic from essential or parkinsonian tremor. *Neurology,* 6, 548-550, 2003.

VITA

Jeonghee Kim

Jeonghee Kim was born in Daegu, South Korea. She received her B.S. degrees in electrical engineering from Kyungpook National University in Daegu, Korea, and the University of Texas at Dallas in Richardson in 2007 and 2008, respectively, and an M.S. degree in electrical engineering and computer science at the University of Michigan in Ann Arbor in 2009. In 2010, she joined the Georgia Institute of Technology, where she is currently pursuing her Ph.D. degree. Her research interests are system design for biomedical and rehabilitation systems in real-time closed-loop and embedded mobile applications, human computer interaction, and assistive technologies. She received the Best Demonstration Award at the 2012 IEEE Biomedical Circuits and Systems Conference, the 2014 Samsung Human-Tech Paper Honorable Mention Award, Poster Competition Awards from the Office of the Executive Vice President for Research at the Career, Research, Innovation and Development Conference 2016 at Georgia Tech, the NSF Young Professional Award at EMBC 2016, and the Outstanding Research Award for Predoctoral Students: Association of Korean Neuroscientists (AKN), 2016.